QATAR UNIVERSITY

COLLEGE OF ENGINEERING

BOND DURABILITY OF BASALT FIBER REINFORCED POLYMER BARS EMBEDDED IN FIBER REINFORCED CONCRETE UNDER THE EFFECT OF SALINE ENVIRONMENT AND ELEVATED TEMPERATURES.

BY

ALAA HASAN TAHA

A Thesis Submitted to

the Faculty of the College of Engineering

in Partial Fulfillment of the Requirements for the Degree of

Masters of Science in Civil Engineering

June 2019

COMMITTEE PAGE

The members of the Committee approve the Thesis of
Alaa Hasan Taha defended on 15/04/2019.

Dr.Wael Alnahhal
Thesis/Dissertation Supervisor

Dr.Usama Ebead
Committee Member

Dr.Khaireldin Abdulla
Committee Member

Dr.Mohammed Elshafie
Committee Member

Approved:

Abdel Magid Hamouda , Dean, College of Engineering

ABSTRACT

TAHA, ALAA, H, Masters : June : 2019, Masters of Science in Civil Engineering

Title: Bond Durability of Basalt Fiber Reinforced Polymer Bars Embedded in Fiber Reinforced Concrete under the Effect of Saline Environment and Elevated Temperatures

Supervisor of Thesis: Dr.Wael Al nahhal.

Fiber-reinforced polymer (FRP) is promising to be an alternative solution for conventional steel to prevent the fast infrastructures' deterioration. Moreover, FRPs are utilized by the construction industry to improve the structural performance of concrete structures. FRPs have many advantages over the conventional steel reinforcements as FRPs exhibit better durability and higher resistance to aggressive environments, particularly, when exposed to high possibility of corrosion. The high strength-to-weight ratio of FRPs make them superior over the traditionally used materials when considering seismic loads as an increase in the dead load of a structure yields to a higher seismic force. One of the major parameters that significantly influence the structural performance is the bond behavior between the concrete and the reinforcement, since bond controls the concrete structures' capacity, serviceability and durability. Although FRPs exhibit high resistance to corrosion, chemical, and sever weather conditions, however unlike steel reinforcement, FRPs are anisotropic, linear elastic, and are mainly affected by their mechanical properties, manufacturing process, materials used, etc. Therefore, this will lead to a highly variable force transfer mechanism between the concrete and the FRP reinforcements. Therefore, investigating their bond performance and possible solutions to improve their bond with concrete is of a crucial importance.

This thesis is done for the purpose of investigating the influence of fiber reinforced concrete (FRC) on the bond durability of helically wrapped Basalt Fiber Reinforced Polymers (HWBFRP) bars subjected to harsh saline environmental conditioning. A total of 105 Pullout specimens were tested. The parameters investigated were: (1) the fiber type: steel and basalt fiber; (2) conditioning duration: 30,60, and 90 days; (3) conditioning temperature: 35 ^{o}C and 60 ^{o}C; and (4) the fiber volume fractions: 0.5% and 1%. Moreover, 105 concrete cylinders, with similar parameters used for studying the bond mechanism, were tested for tracking the compressive strength when subjected to harsh saline environmental conditioning. The results of this study revealed that the addition of non-corrosive macro fibers such as basalt macro fibers (BMF) to normal strength concrete improved the bond durability performance of HWBFRP bars and showed higher retentions in the bond strength compared to plain concrete and steel FRC after 90 days of immersion in saline solution. Whereas the addition of steel fibers to normal strength concrete especially at low contents suggests that steel macro fibers are to be utilized in offshore applications rather than marine structures. Moreover, the durability test indicated that the bond performance of HWBFRP bars is significantly influenced at high temperature with the presence of large contents of BMF in normal strength concrete. the pullout specimens with 1 % steel fiber volume fraction showed higher bond durability performance compared to specimens with 0.5% steel fiber volume fraction and is more pronounced at the high temperature. The results of the study suggest that the bond durability test of FRP bars embedded in steel FRC in saline solution is to be carried at relatively low temperatures to avoid the influence of early stages of steel fiber corrosion on the bond performance. Based on the results of this study, the optimum fiber volume fractions are 1% in case of steel fiber and 0.5% in case

of BMF.

DEDICATION

“To my grandparents, parents and my dear sisters”

ACKNOWLEDGMENTS

First, I sincerely would like to thank almighty Allah for the grants He blessed me with.

Also, I would like to thank, my supervisor, Dr.Wael Alnahhal for his continuous support throughout the two years of my master degree. As without his support, this work would have never been carried out.

The deepest gratitude after all to my dear parents for their continuous encouragement and efforts in meeting all my needs in order to finish this work.

TABLE OF CONTENTS

LIST OF TABLES

LIST OF FIGURES

CHAPTER ONE: INTRODUCTION

The application of FRP composites for strengthening and retrofitting of civil engineering structures is increasingly growing and gaining its popularity in the civil engineering field. Easy application, lower occupants' disturbance, and construction time and costs savings are some of the significant advantages of FRP composites. In addition, the developed mechanical properties of FRP composites allow them to be more durable and have reasonable fatigue resistance. They exhibit extraordinary strength to weight ratio and can be almost manufactured to any structure's size and shape [1-4]. Consequently, FRP composites have high corrosion, weather, and chemical resistance [5]. Also, some of the advantages of FRP composites are their light weight and their relatively low cost of manufacturing [6]. The ratio of the fiber and matrix material, the constituent mechanical properties of the material, orientation of the fiber's matrix, and the methods of processing and manufacturing are the factors that determine the mechanical properties of the FRP composites [7, 8]. Some of the fibers' types are Carbon Fiber Reinforced Polymer(CFRP), Glass Fiber Reinforced Polymer (GFRP), Aramid Fiber Reinforced Polymer(AFRP), and one of the latest and growing types of FRPs are the Basalt Fiber Reinforced Polymer(BFRP).

1.1. Research Significance

The application of FRP as an alternative for the conventional steel rebar, particularly in corrosive environments, has always encouraged researchers to investigate the bond mechanism of different FRP bars in the construction field for the last few decades. Glass Fiber-Reinforced Polymer (GFRP) bars have been one of the most widely studied type of FRPs due to their advantages over conventional steel. However, the application of GFRP bars until now remains limited due to their durability concerns for some of their mechanical properties. Therefore, an alternative FRP made

of basalt (BFRP) has been introduced to overcome the durability concerns of GFRP bars. BFRP bars are getting widely accepted in the construction industry. Therefore, to ensure a suitable performance in civil engineering applications, it is necessary to investigate the mechanical and structural behavior of BFRP bars. One of the major factors that significantly influence the structural performance is the bond behavior between the concrete and the reinforcement, because bond controls the concrete structures' capacity, serviceability and durability. Moreover, the addition of fibers to the concrete mix has shown to improve the shear and flexural strength but its effect on improving the bond strength of FRP bars requires more investigations as studies have shown to be contradictory. Consequently, the bond durability of FRP bars to concrete is of crucial importance to maintain the structural integrity of any structure. Up to the writer's knowledge, no study has been done on the bond durability of BFRP bars embedded in fiber reinforced concrete. Therefore, this thesis presents an experimental and analytical investigation of the bond durability of BFRP bars embedded in steel and basalt macro FRC.

1.2. Aim of this Study

This study presented in this thesis aims at achieving several crucial objectives which are summarized in the following points:

(1) Examine the bond strength of helically wrapped BFRP bars with no sand coating by pullout testing to evaluate their suitability in meeting the international specifications.

(2) Investigate the effect of adding structural fibers such as the conventionally used steel fibers and the recently introduced basalt macro fiber on the bond strength of HWBFRP bars with no sand coating.

(3) Evaluate the bond durability of BFRP bars under the combined effect of saline environment and elevated temperatures of 35 ^{o}C and 60 ^{o}C and the influence of

structural fibers addition to concrete in improving the bond of BFRP bars in terms of strength and durability.

(4) Obtain the optimum fiber volume fraction that can be safely used along with BFRP reinforcements in marine structures.

(5) Analytically model all the tested pullout specimens using the available analytical models in the literature and calibrate their coefficients and present design values that take into consideration the BFRP bars used, saline environment, exposure temperatures, exposure duration, type of structural fibers, and structural fibers' volume fraction.

(6) Provide a model that predicts the bond strength retention after 50 years of service life and the effect of structural fibers in maintaining equivalent or higher retention values compared to plain concrete.

(7) Investigate the effect of high temperature-immersion in saline solution on the moisture and chloride diffusion in the polymeric resin of the BFRP bars along the embedment length using scanned electron microscopy (SEM).

1.3. Thesis Organization

The study presented in this thesis is divided into seven chapter and are described briefly as follows:

Chapter One: Provides a brief introduction about the topic presented in this study along with the research significance and aim of the study.

Chapter Two: Conducts a literature review that covers topics about: (1) the bond behavior of FRP bars and available analytical models; (2) the most widely used standard tests methods (3) experimental investigations on the bond strength of FRP bars; (4) Bond Durability of FRP bars; and (5) Effect of structural fibers on bond strength and bond durability to severe environmental conditions.

Chapter Three: Describe in details the experimental procedures followed and materials

used along with their mechanical properties.

Chapter Four: Provides a detailed discussion of the obtained results during the durability test.

Chapter Five: Applies the available proposed analytical models on the experimental data to examine the most effective model in representing the actual experimental data and calibrate the models' coefficients to take into consideration the BFRP bars used, structural fibers' addition, and environmental conditioning to provide design values that can be used in the absence of experimental data.

Chapter Six: Introduces a model that predicts the retention values of the bond strength of BFRP bars after 50 years of service life.

Chapter Seven: Discusses the influence of immersion temperature on the BFRP bar's surface using scanned electron microscopy (SEM).

CHAPTER TWO: LITERATURE REVIEW

The performance of FRP composites heavily depends on the bonding performance between concrete and FRP bars [9,10]. Some of the factors that affect the bond behavior are the loading type [11-13], the bonding material that the FRP composites bars are supposed to go through, the base material [14], the adhesive material and its thickness [15], and the environmental conditions [16,17]. The different test methods for conducting the FRP-concrete characterization do in fact affect the loading type to some extent, however in this thesis, the main focus will be evaluating the bond performance by pull-out testing. A comprehensive review about the effect of the test method is done by Mukhtar and Faysal [18].

The preparation of the concrete specimens that is responsible for the concrete strength properties plays a crucial role in bond performance between FRP bars with concrete. Pan and Leung [19] mentioned that the bond strength is related more to the tensile strength of specimen's surface and the coarse aggregate content in the concrete mix rather than the strength properties of concrete. It is widely known that the roughness of the concrete surface that is direct contact with the FRP composite exhibits mechanically higher interlocking at the interface between concrete and FRP composites. Santos and Julio presented a comprehensive review about this effect [20].

Additionally, concrete is a highly alkaline material with a pH level that ranges from 12.7 to 13.6 [21,22], therefore, multiple past studies indicated that FRP bars such as GFRP bars that are embedded in concrete experience reduction in the bond and tensile strength [23-27]. Consequently, test results indicated that the elevations in temperature can accelerate the process of strength degradation [28]. The modelling and prediction for the retention of tensile strength degradation based on the Arrhenius concept has been successfully proposed and validated [21, 27]. The bond degradation

of FRP bars due to sever environmental conditions such as severe cycles of temperature, alkaline, and attacks of chemical solutions attacks are often complicated whereas, the existing studies about the prediction and mechanism of degradation is found to be with contradictory opinions based on the available literature [29-31]. Therefore, it of crucial importance to more effectively understand the bond behavior and performance of FRP composite for wider implementation of FRP bars in the concrete structures.

In order to optimize the gained knowledge and experience of the existing available literature, the literature review in this thesis is conducted for several objectives: (1) to summarize two of the most widely used pull-out testing methods for the bond strength which are: ASTM D7913 and CSA S806 [32,33]; (2) to discuss the bond performance and mechanism in terms of bond strength and type of failure modes; (3) to investigate the bond stress/slip relationship models, meanwhile a comparison between the different standards in design for prediction of bonding strength is discussed in the present review; (4) To discuss several factors that could have an effect on FRP bars' bond strength with concrete; (5) to discuss the bond durability of FRP composites under severe environmental conditioning such as alkaline solutions, acidic solutions, saline solutions, and high temperature; and (6) to conduct a general overview about the addition of structural fibers

2.1. Standard Tests for Bond Strength by Pull-out Testing

2.1.1. ASTM D7913

The test setup for examining bond strength of FRP composites bars in accordance to ASTM D7913/D7913M-14 [37] is shown in figure 1. The FRP composite bars shall be embedded in 200×200×200 mm concrete cubes. The bonded length in concrete prism shall be 5 times the FRP bar's diameter. The remaining embedded length of the bar in the concrete shall be covered with PVC tube to prevent bonding with concrete, this length is called debonding length. The FRP bars shall be protruded

outside the concrete slightly from the free-end so that LVDT can take the measured slippage of the bar at the free end. A steel frame can be manufactured for hydraulic testing machines with no cross head. The steel frame is to be composed of 2 steel plates of at least 200 mm × 200 mm with at least 20 mm thickness and 4 steel rods. The optional loaded end LVDTs can be used to determine elongation that may occur to the bar due to the loading. The length and the diameter of the steel tube at the anchorage side are tabulated in Table 1 according to ASTM D7205/D7205M-06 [38] and depends mainly on the diameter of the FRP composite bar. The steel tube is to be filled with an expansive Cementous grout or polymeric resin. The grout thickness shall be not less than 4mm between the inner surface of the steel tube and the outer surface of the FRP bar. The wall thickness of the steel tube should be not less than 4.8mm. The testing machine must be set to apply a load at a rate no more than 1.3mm/min. The data acquisition rate must be set for recording the slippage that will occur at the free end at an increment of no more than 0.01 mm. The specimens can be constructed with any concrete mix but for this test method it is recommended that the concrete mix should be a standard mixture with a compressive strength at 28 days equals to 30 MPa± 3. The specimen for bond strength is shown in Figure 2. The average bond strength of the tested specimen should be calculated using Eq. (1) and reported with three significant digits of precision for each for force reading in the test

$$\tau = \frac{F}{C_b l} \qquad (1)$$

Where:

$\tau =$ the average bond stress in MPa.

F = the machine tensile force in N.

C_b= the effective circumference of the FRP bar calculated as $\pi \times d_b$ where d_b is the effective diameter of the FRP composite bar.

l= bonded length of concrete, according to this test method l is calculated 5 d_b.

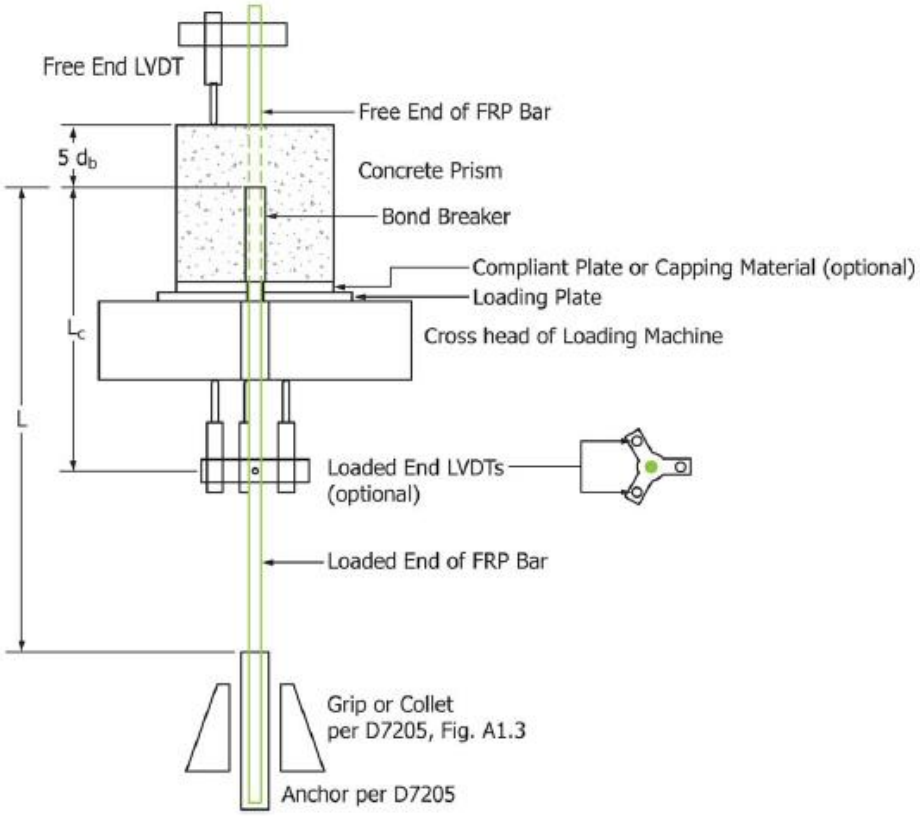

Figure 1:ASTM D7913 Test Setup for Bond Strength.

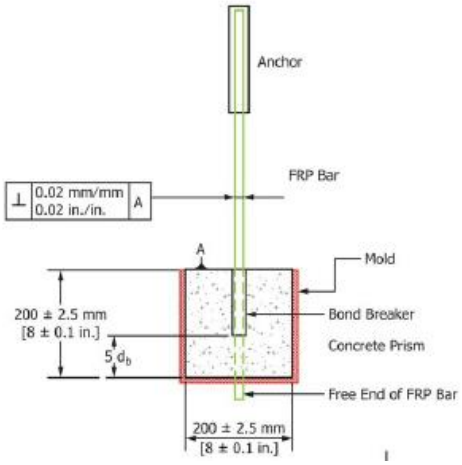

Figure 2: ASTM D7913 Pullout Specimen.

Table 1: Anchorage Steel Tube Specifications [37]

FRP Bar Type	Diameter of the FRP bar,d (mm)	Outside Diameter of the Steel Tube (mm)	Minimal Length of the Steel Tube, L_a (mm)
GFRP	6.4	35	300
GFRP	9.5	35	300
GFRP	13	42	380
GFRP	16	42	380
GFRP	19	48	460
GFRP	22	48	460
GFRP	25	48	460
GFRP	29	48	460
GFRP	32	75	800
CFRP	9.5	35	460

2.1.2. CSA S806

The test specimen and the test setup for examining bonding strength of FRP composites bars in accordance to CSA S806 [39] are shown in Figures 3 and 4. The FRP composite bars shall be embedded in 150×150×150 mm concrete cubes. The bonded length in concrete prism shall be 4 times the FRP bar's diameter. The remaining embedded length of the bar in the concrete shall be covered with PVC tube to prevent bonding with concrete, this length is called debonding length. The FRP bars shall be

protruded outside the concrete slightly from the free-end so that LVDT can take the measured slippage of the bar at the specimen's free end. Three LVDTs at loaded end are to be used to determine elongation that may occur to the bar due to the loading as well as three LVDTs to be used at the free end. The length of the steel anchoring tube is equal to $f_uA/350$ but not less than 250. The steel tube is to be filled with resin and clean sand or with non-shrink cement grout. The wall thickness of the steel tube should be not less than 5 mm. The testing machine must be set to apply a load at a rate no more than 1.27mm/min. The specimens can be constructed with any concrete mix but for this test method it is recommended that the concrete mix should be a standard mixture with a compressive strength at 28 days equals to 30 MPa± 3. The loading must be continued until (a) rupturing of FRP composite bar, (b) splitting of concrete, or (c) at least 2.5 mm of slippage has occurred at the loaded end of the length embedded in concrete.

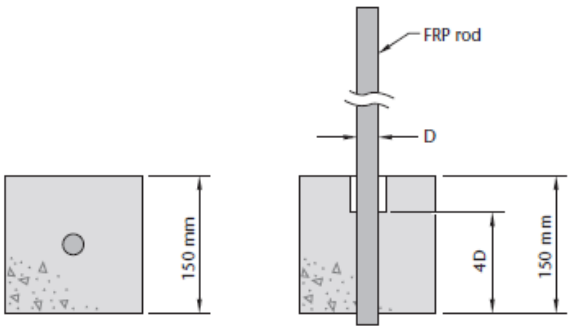

Figure 3: CSA Test Specimen [39].

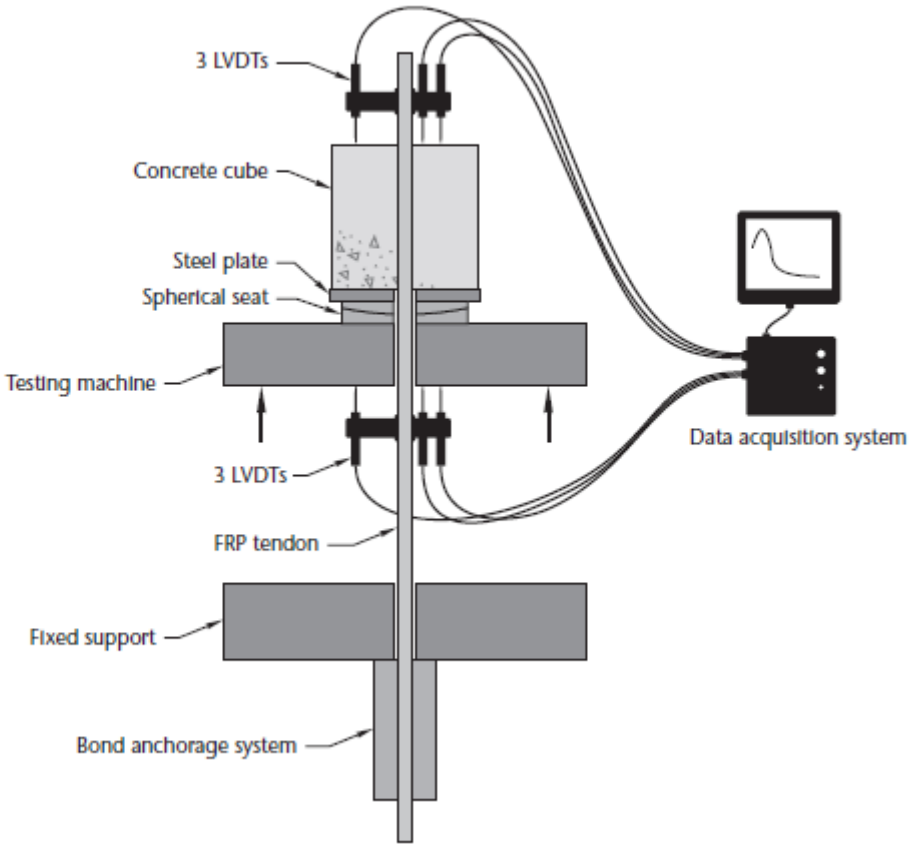

Figure 4: CSA Test Setup for Bond Strength.

2.2. Bond Behavior and Modelling of FRP composite Bars.

Bond performance between the FRP composite bars and concrete is expressed in terms of a bond-slip curve in Figure 5 where the area under the curve is called the mode fracture energy (a property of FRP composites) [40]. The mode fracture energy property is used to investigate the debonding at the interface between concrete and FRP composite. In general, the bond between the embedded bar and concrete depends on (a) The chemical bond which is the resistance of adhesion at FRP composite bars' interface with concrete; (b) The resistance of friction due to the occurring slippage; (c) The mechanical interlock that occurs due to the surface irregularity [41]. The material properties and the texture of the surface of FRP bars make their bond behavior different from that of steel which leads to a different mechanism of force transfer and toughness

of surface between concrete and reinforcement bars [42]. FRP bars behave in a linear elastic way until failure which is different from traditional steel reinforcements which have plastic behaviour when subjected to large deformations. FRP bars have different surface treatments such as sand coated, ribbed, and helically wrapped surfaces which yields lower mechanical interlock and thus to a lower bearing force than that of conventional steel. Achillides and Pilakoutas [43] indicated that the bond strength of GFRP bars mainly depends on the mechanical interlock of the surface treatments to concrete matrix whereas Pepe et al. [44] mentioned that the chemical adhesion is the major contributor to the bond strength while the mechanical interlock is the minor contributor in the bond strength of FRP bars. Using the explicit mathematical formula, multiple analytical models that describe the bond stress-slip relations for FRP bars to concrete have been developed such as: BPE and modified BPE.

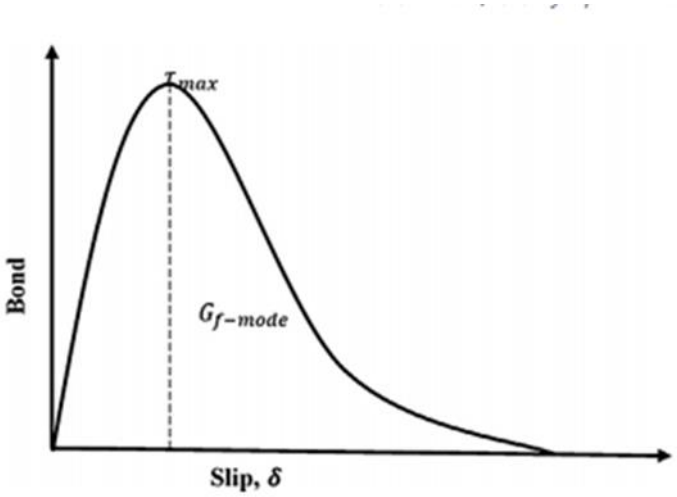

Figure 5: Bond-Slip Curve.

2.2.1.BPE and Modified BPE Bond-slip Analytical Models:

The BPE model is used to describe the bond performance of steel reinforcement with concrete [45] and is shown in Figure 6. Consequently, the BPE model was modified to account for bonding behavior of FRP composite bars when embedded in concrete [46] and is shown in Figure 7. The modified BPE model is divided into three stages. The first stage shows an increase in the bond stress which is due to the chemical adhesion and the bearing force between the FRP composite bar and concrete. And after that bonding stress increases to a particular value and the FRP bar slides on the lug area. In the second stage, cracks start to develop, sometimes concrete crushing, and the bearing force caused by the mechanical interlocking reduces causing a rapid reduction in the bonding stress with an obvious slippage. In the third stage, large concrete cracks are formed and the FRP bars continues to slide at a constant bonding stress of a particular value caused by friction. Therefore, the modified BPE (mBPE) model can be expressed in a piecewise function in Eqns 2-4

$$\frac{\tau}{\tau_b} = (\frac{s}{s_b})^{\alpha} \; for \; 0 \leq s \leq s_b, \qquad (2)$$

$$\frac{\tau}{\tau_b} = 1 - p(\frac{s}{s_b} - 1) \quad for \; s_b \leq s \leq s_3, \qquad (3)$$

$$\tau = \tau_3 \; for \; s \geq s_3, \qquad (4)$$

Where τ and s are the bond stress and the slippage, τ_b and s_b are the maximum bond stress and its corresponding slippage; α and p are parameters obtained from curve fittings of the experimental data. The mBPE was found to be conservative when compared to experimental data at the ascending branch [47]. The mBPE takes into account the surface treatment [48] but does not take into account the bar diameter and the fiber type.

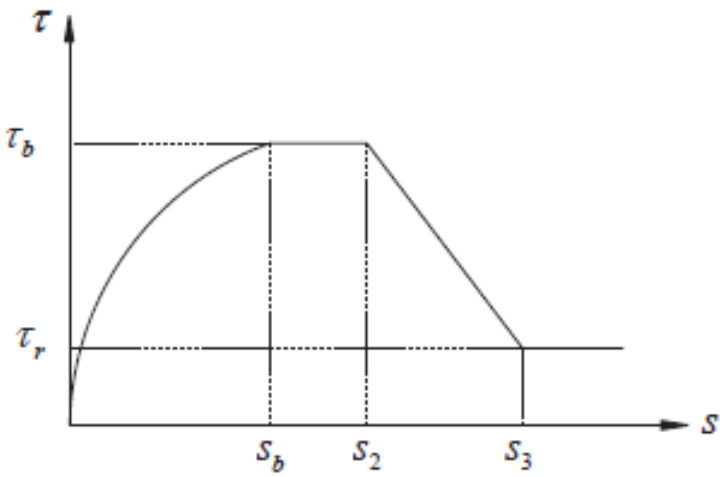

Figure 6: BPE Model for Steel Bar.

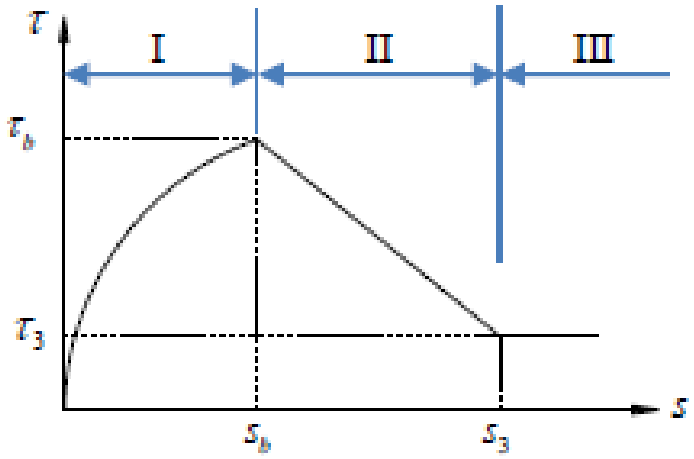

Figure 7: mBPE Model.

2.2.2.CMR Model

Cosenza et al. [49] proposed the CMR mode for better presentation of the ascending function at the first stage in the FRP bar's bonding stress-slip. This model may account for the chemical adhesion since the slope is infinite at the initial stage. This model agreed with the experimental data of Masmoudi et al. [47]. Analytical Modelling is furtherly discussed in the Analytical Modelling chapter.

2.3. Experimental Investigations on Bond Behavior of FRP Bars.

2.3.1 Bond Performance of Unconditioned FRP Bars Embedded in Concrete

Rolland et al. [50] investigated the bond behavior of different types of FRP bars such as glass FRP (GFRP), carbon FRP (CFRP), and aramid FRP (AFRP) by pull-out testing and studied the influence of the FRP type, bar diameter, and the surface treatment. The study also investigated the bond behavior of steel deformed bars. In their study, they studied the different surface treatments of FRP bars such as: sand coated GFRP bars, non-sand coated GFRP bars, sand coated CFRP bars, non-sand coated CFRP bars, and sand coated AFRP bars shown in Figure 8. The bond behavior was determined by pullout testing of bars embedded in concrete cylinders. They concluded that the surface treatment especially, the sand coated, played an important role in the mechanism of the load transfer at the interface between concrete and FRP bars surface. The summary of the bond strength results is shown in Figure 9. It was found that sand coated GFRP bars exhibited the highest bond performance among the studied types of FRP bars and even a higher bond strength than that of the deformed steel bars. Moreover, it is interesting to note that in their study, the larger diameter of GFRP bars exhibited higher bond strength which is contradictory to what is reported in the literature. The summary of the bond-slip experimental curves is shown in Figure 9.

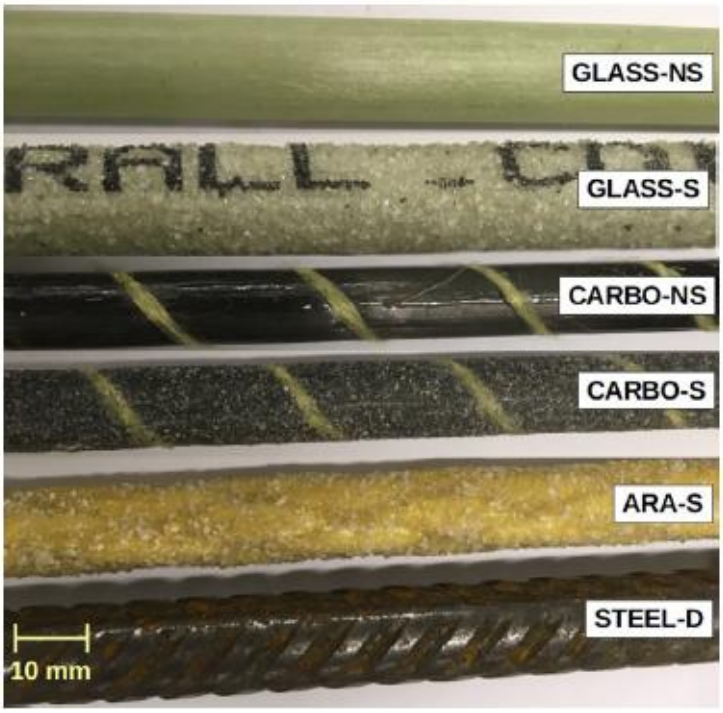

Figure 8: FRP Bars Studied in [50].

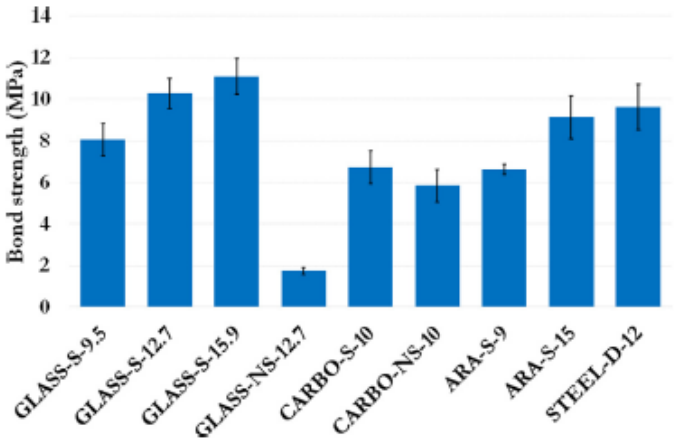

Figure 9: Bond Strength Summary of Results [50].

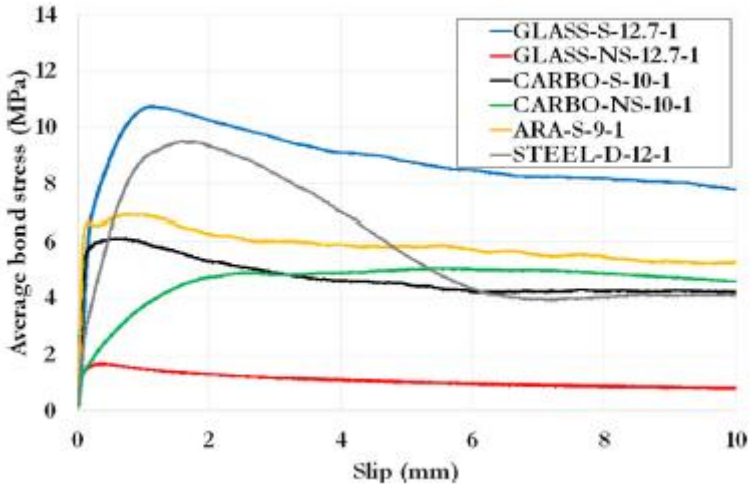

Figure 10: Typical Bond-Slip Curved Obtained in [50].

Baena et al. [51] tested 88 pullout specimens to examine the bond performance of CFRP and GFRP bars with different surface treatments and diameters. In their contribution to the database of the bond behavior of FRP bars with concrete, they mentioned that the bond performance of FRP bars is influenced by the concrete compressive strength, FRP bar diameter, and the surface treatment of the bars. In their experiment they noticed that the impact of the surface treatment is lower in concrete with low compressive strength, whereas in high compressive strength concrete the effect of the surface treatment was noticeable. The results of their study confirm with the existing literature that the larger diameter of FRP bars have lower bond strength than that of smaller diameter bars. The slippage in GFRP bars was higher than that of CFRP bars.

El Rifai et al[52] tested thirty-six pullout specimens of Basalt FRP (BFRP) and twelve pullout specimens of GFRP bars in concrete cylinders. The test parameters in their study were the embedment length, the FRP bar diameter, and the material of FRP (basalt and glass). According to their study, the BFRP bars exhibited a bond strength

that is 75% of that of GFRP bars. The results' comparison between the bond strength of BFRP bars and GFRP bars is shown in Figure 11 The summary of the BFRP bars bond strength results is shown in Figure 12. They concluded that small diameters of FRP bars have better adhesion performance than that of larger diameter FRP bars. The residual stress of BFRP bars was higher than that of GFRP bars. Moreover, increasing the embedment length decreased the bond strength of FRP bars with concrete. The mBPE analytical model was used to represent the bond slip behavior of the studied bars.

Figure 11:Average bond strength results' comparison between BFRP and GFRP bars[52]

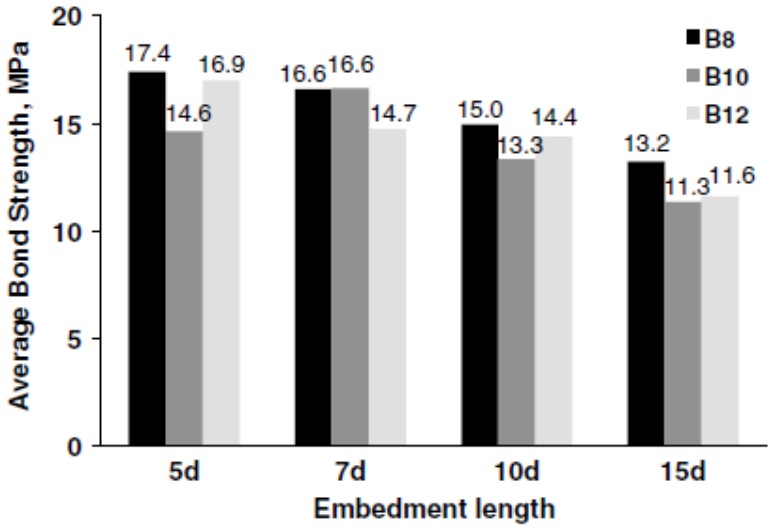

Figure 12: Average bond strength of BFRP bars with different diameters at different embedment lengths [52].

2.3.2. Effect of Fiber Reinforced Concrete on Bond Behavior of FRP Bars.

Ding et al. [53] studied the effect of fiber reinforced concrete on the bond behavior of GFRP bars embedded in concrete. In their study, they used two types of fibers which are steel fibers (SF) and macro-polypropylene fibers (PPA) and compared the results with the obtained results for GFRP bars embedded in plain concrete (PC). They indicated that the usage of SF and PPA in concrete improved the bond performance of GFRP bars to a level equivalent or even better than the bond performance of steel rebar embedded in plain concrete. Figure 13 shows a comparison between the bond strength of GFRP bars embedded in a cocktail of SF and PPA fiber reinforced concrete and the bond strength of steel rebar embedded in plain concrete. Table 2 shows a summary of the observations found in their study. The hybrid usage of fibers in the concrete mix showed a better bond performance than the summation of improvement provided by SF and PPA reinforced concrete. It was concluded that the usage of fiber reinforced concrete not only improves the bond capacity but also reduces the slippage at the

maximum bond stress.

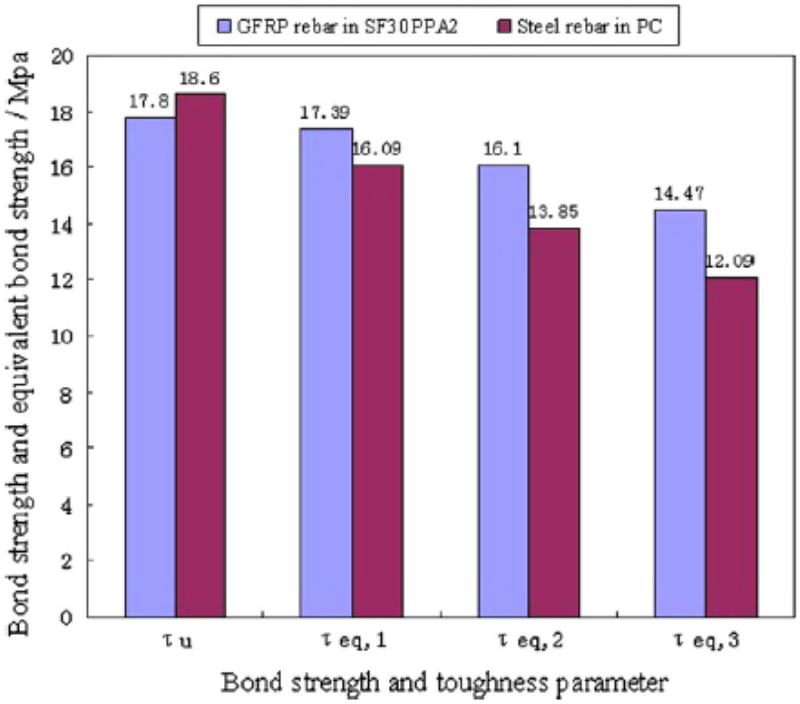

Figure 13:Comparison between bond strength of GFRP bars embedded in cocktail of SD and PPA fiber reinforced concrete and bond strength of steel rebar embedded in plain concrete[53]

Table 2: Bond strength increase rate and slippage decrease rate of fiber reinforced concrete[53]

Samples	τ_u (MPa)	Increase rate of τ_u (%)	S_0 (mm)	Decrease rate of S_0 (%)
GFRP in PC	12.6	-	2.64	-
GFRP in PPA2	15.0	19.0	2.33	11.7
GFRP in PPA4	15.5	23.0	1.92	27.3
GFRP in SF30	14.3	13.5	2.43	8.0
GFRP in SF50	16.3	29.4	2.38	9.8
GFRP in SF30PPA2	17.8	41.3	1.77	33.0
Steel in PC	18.6	47.6	1.45	45.1

Bi and Wang [54] investigated the effect of high strength concrete reinforced with basalt fiber on the bond performance of BFRP bars by testing 108 pullout specimens. They tested three diameters of BFRP bars, three volume fractions of basalt fiber in high strength concrete (0.1%, 0.15%, and 0.2%), and three different embedment lengths (40mm, 70mm, and 100mm). They concluded that larger diameters that yield larger embedment length reduced the BFRP bars' bonding strength with concrete. The most noticeable enhancement in BFRP bars' bond strength was obtained at 0.2% volume content of fiber. Consequently, Solyom and Balazs [55] tested 144 pullout specimens with three different types of fibers which are SF, synthetic micro-fiber, and synthetic macro fibers. They used four types of concrete, three of which are conventional concrete of different grades and one is self-compacting concrete. Three different types of FRP bars (CFRP, GFRP, and BFRP) were used in their study. They concluded that the addition of short fibers to the concrete mix enhanced the bond behavior in almost all cases.

On the contrary, Liu et al. [56] took a further step and studied the influence of fiber reinforced concrete made with recycled aggregate. They tested 54 pullout specimens and 162 mechanical properties specimens. The parameters of their study were the volume fraction of basalt fiber (0%, 0.2%, 0.3%, and 0.4%), the aspect ratio of the fiber, and recycled aggregate concrete(RAC) grade. It was noted that the RAC grade had a larger effect on the mechanical properties and the bonding performance of BFRP bars. Also, the effect of the aspect ratio of the basalt fiber on the bond performance was found to be weak when compared to the other parameters. [56] proposed the following non-linear regression model to predict the bond strength of BFRP bars embedded in RAC:

$$Y=6.9098+0.1316X_1-75.6202X_2-23353.3X_3^2+0.239X_3-0.00315X_3^2-66.727X_2X_3 \quad (5)$$

Where X_1 is the RAC grade, X_2 is the volume fraction, and X_3 is the length of the fiber. They found that increasing the RAC content increased the bond strength, but when it came to increasing the volume fraction of basalt fiber, the bond strength reduced which is contradictory to [55]. Additionally, Kim et al.[57] investigated the effect of structural fibers on bonding behavior of GFRP bars. The study mentioned that it is more appropriate to investigate the effect of fibers addition on delaying the bond failure and improving the ductility rather than enhancing the bond strength. The study investigated three types of fibers: polypropylene (PP) fiber, polyvinyl alcohol (PVA) fiber, and hooked-end steel fiber. It was concluded that the addition of the fibers to the concrete matrix maintained high residual loads and toughness and thus delayed the pull-out failure of the bars. Moreover, Belarbi and Wang[58] studied the bond-slip response of FRP bars in FRC. The study investigated two types of bars: GFRP and CFRP bars. It was reported that the addition of fibers had no contribution on improving the bond strength and the enhancement of the fibers' addition on the ductility response of the bars was moderate.

2.4 Bond Durability of FRP Bars Embedded in Concrete under Severe Environmental Conditions.

2.4.1. Effect of High Temperature

Li et al.[59] studied the impact of high temperature on the bond behavior of BFRP and GFRP bars embedded in concrete. Seven parameters were investigated, temperature, bar diameter, bonding length, FRP type, thickness of concrete cover, and coating material. It was noted that both GFRP and BFRP bars exhibited similar bond slip curves at high and room temperature, however the peak bond strength decreased when the temperature increased. The bond strength of GFRP bars showed more severe

decrease than BFRP bars when subjected to high temperature. The bond performance was reduced by 2.45%-14.24% at 70^{o}C-220^{o}C.

2.4.2. Effect of Saline Solution

Altamas et al. [60] investigated the bond degradation of BFRP and GFRP bars when subjected to conditions of accelerated aging. The specimens were subjected to three environmental conditioning which are acidic, ocean water, and alkaline solutions for 30, 60, and 90 days. The summary of the bond strength results is shown in Figure 14. It was concluded that BFRP bars experienced a 25 % reduction when immersed in oceanic water, whereas GFRP bars experienced a 17% bond strength reduction. Dong et al. [61] studied the bond durability of BFRP bars embedded in concrete conditioned in seawater. In their study, 114 pull-out specimens were tested, 99 out of the tested specimens were submerged in seawater for at different temperatures and for different durations. The parameters investigated in their study were: (1) the conditioning duration: 15, 30, 45, and 60 days; (2)The bar type: BFRP, GFRP, CFRP, and steel bars; (3) the resin type: vinyl ester and epoxy; (4) conditioning temperature: 25 °C, 40 °C, and 55 °C. The surface configuration of the bars tested in their study are shown in Figure 15. The results of their study revealed that: (1) basalt vinyl ester (BV) and glass vinyl ester (GV) bars had bond degradations of 9.1% and 7.1% respectively compared to control specimens; (2) the basalt epoxy (BE) bars showed better alkali resistance than BV bars; (3) the sand coated ribbed BFRP (RBFRP) bars had lower short term bond strength than their long term bond strength; (4) the bond strengths of steel bars did not decrease along the durability test because of the passivation layer that was formed on the surface of the bar due to the high alkali environment in concrete (this layer is usually destroyed because of the carbonization and chloride penetration inside the concrete which causes rapid corrosion of the steel bar); and (5) The retentions of

bond strength after 50 years of service life was found to be 93%, 78%, and 47% for dry, moist, and moisture saturated environments respectively. El Refai et al. [62] investigated the bond durability of BFRP bars by direct pullout conditions for fifty-six pullout cubic specimens with a side length of 200mm. The parameters of their study were: (1)the bar type : GFRP and BFRP; and (2) the conditioning environment : Water-conditioning, Seawater-conditioning, Temperature conditioning, temperature then water immersion, and temperature then seawater immersion. It was concluded that the response of bond-slip was attributed mainly to the bar's surface treatment and the bar's quality of manufacturing. Consequently, the results of their study revealed that the bond strength was slightly affected by exposure to elevated temperatures up to 80 ^{o}C. Last but not least it was found that the immersion of FRP bars in aqueous solution improved the adhesion stresses but affected the bond strengths, this reduction of bond strength was mainly attributed to the moisture absorption of the bar and its quality of manufacturing regardless what the type of fiber is.

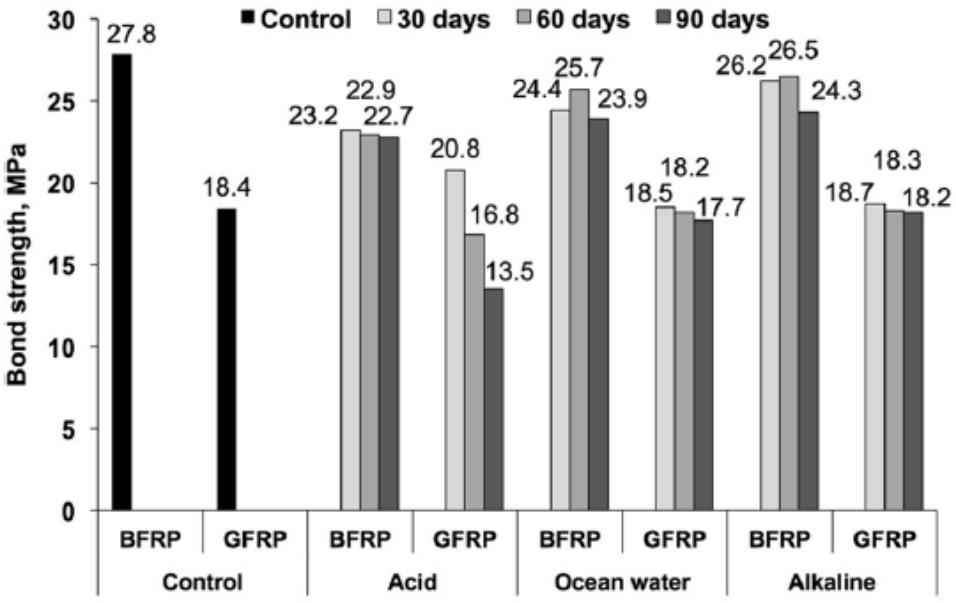

Figure 14:Comparison for Bond Strength at Different Conditions[60].

Figure 15:FRP Bars Tested in [61]

2.4.3. Acidic Solution.

According to [60], the bond strength of BFRP bars reduced by 14% when subjected to acidic environment whereas, GFRP bars experienced a reduction of 25% when subjected to an acidic solution for 90 days. It is interesting to note that most of the bond failures for GFRP specimens were governed by concrete splitting rather than pullout. Likewise, Zhou et al. [63] the bond degradation of GFRP and steel bars embedded in concrete and subjected to tap water and acidic environments of different PH levels. The study was performed on 120 pullout specimens for an exposure duration of 30,45,60, and 75 days at 20 ^{o}C. The results of the study are summarized in the column chart shown in Figure 16. Even though the study showed an increasing trend of the bond strength with exposure time for specimens conditioned in tap water, however the increase in the bond strength was not enough to retain the bond strength of the control specimens. The average bond strength reductions for the GFRP bars after 75 days of exposure are: 11%. 22%. 17.2% and 14% for specimens immersed in tap water, pH=2, pH= 3, and pH=4 solution respectively.

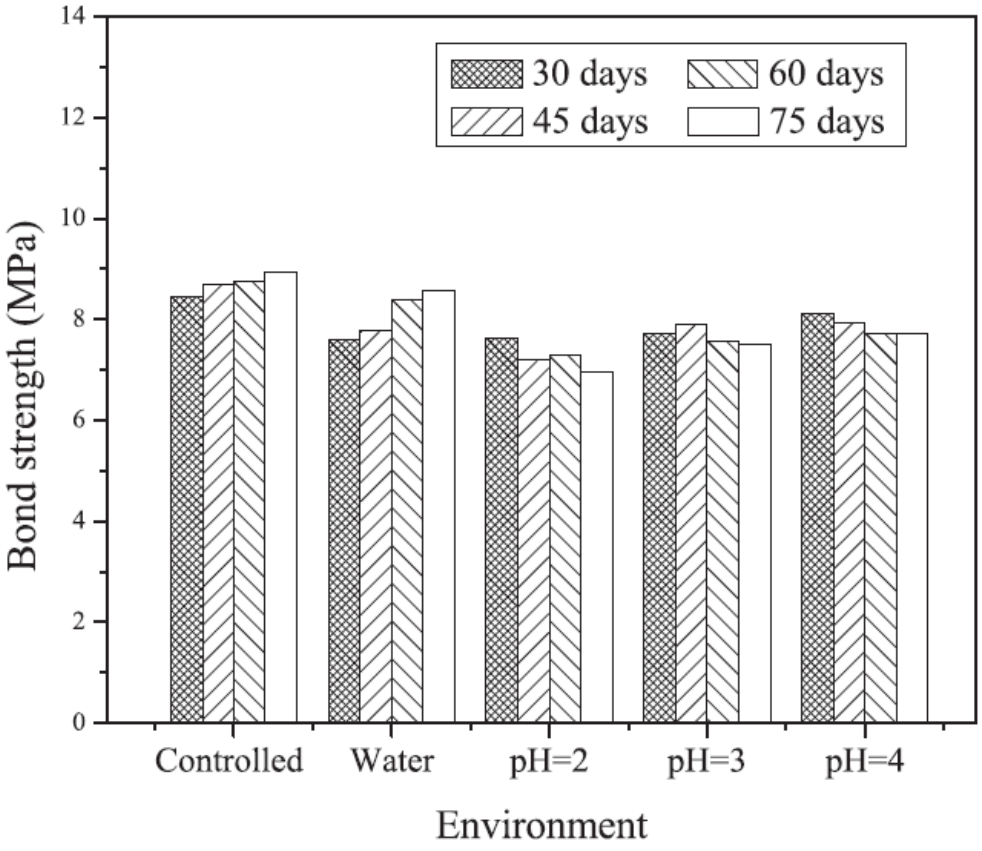

Figure 16: Bond Strength Changes with Exposure Time [63].

2.4.4. Alkaline Solution:

Referring to [60], The bond strength of GFRP bars suffered a reduction of 17% when subjected to alkaline solution for 90 days whereas the bond strength of BFRP bars was reduced by 25%. Likewise, El hassan et al. [64] observed the long term durability of BFRP bars embedded in concrete exposed to a highly alkaline solution of (pH=12.9) for 1.5,3, and 6 months at 40 ^{o}C, 50 ^{o}C, and 60 ^{o}C. The study revealed the highest bond strength loss of (14%) was at 40 ^{o}C after 6 months of exposure followed by 50 ^{o}C, and 60 ^{o}C with a loss of 7% and 5% respectively when compared to specimens exposed for 1.5 months. No reductions in the bond strength were observed for specimens exposed to 50 ^{o}C and 60 ^{o}C when compared to the unconditioned (control) specimens The results of the study are summarized in figure 17.

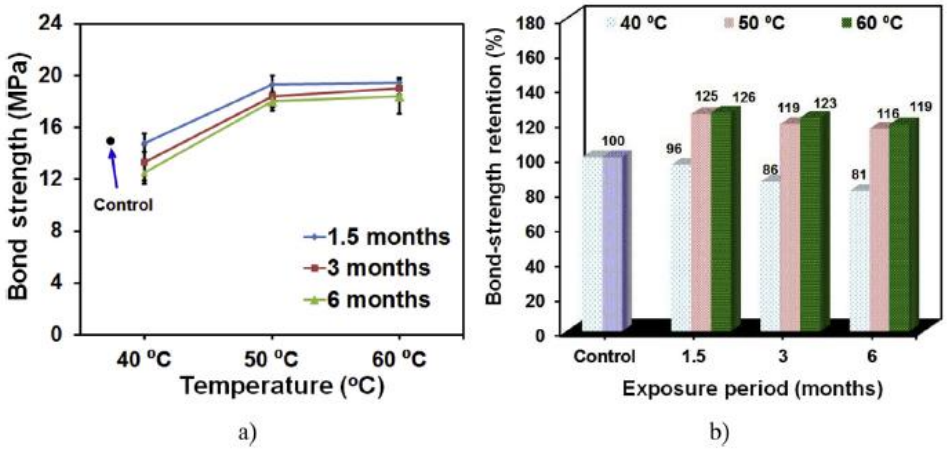

Figure 17: Bond Strength Retentions with Exposure Time.

2.4.5: Effect of fiber reinforced concrete on the bond degradation of FRP bars:

Very few studied were performed on the effect of fiber reinforced concrete on the bond degradation of FRP bars. One study [65] was found that investigates the bond durability of GFRP bars subjected to saline solution. They tested 105 pullout specimens with polyvinyl alcohol (PVA) fibers and steel fibers(0.5% and 1%) at high temperatures of 50^{o}C and 70^{o}C for 30,45, and 60 days. SF specimens with 1% volume content enhanced the bond strength of unconditioned specimens by 44% and experienced a reduction of 10% at 60 days. Whereas plain concrete bond strength was reduced by 12% at 60 days. The summary of the results is shown in figure 18. On the other hand, Belarabi and Wang [27] tested the bond durability of FRP bars embedded in polypropylene FRC subjected to combined environmental conditioning such as: (1) high temperature of 60 ^{o}C; (2) cycles of freeze and thaw; and (3) and deicing saline solution. The results revealed a reduction in the bond strength of unconditioned specimens with the addition of polypropylene fibers but an improvement in the bond

durability by exhibiting higher tolerance to severe environmental conditions when compared to plain concrete.

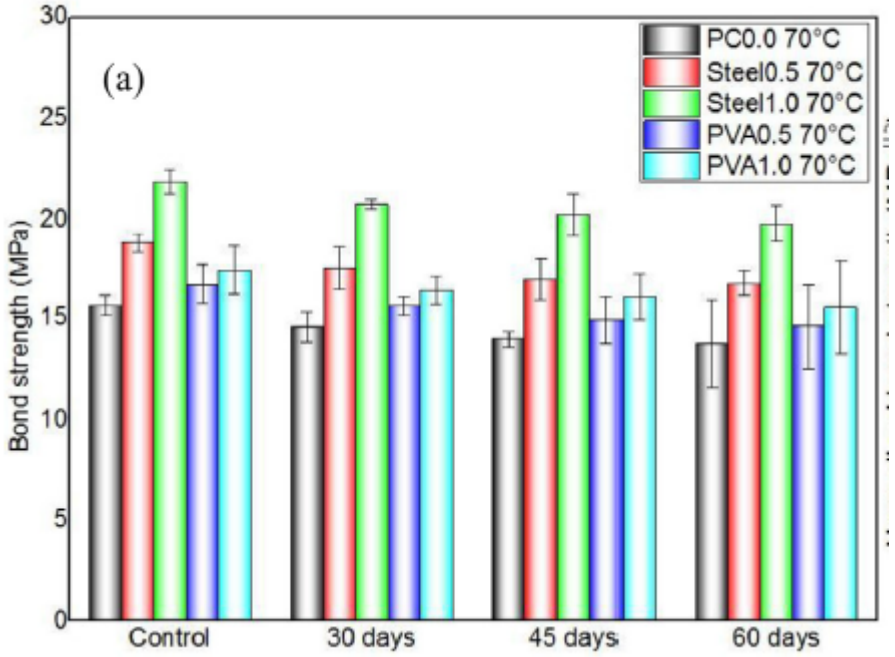

Figure 18: Summary of Bond Strength Reductions with Exposure Time[65].

2.5 Structural Fibers Overview

The chopped discrete fibers are usually made in two arrangements: monofilament and multifilament shown in Figure 19. When fibers are separated from one another, it is often called a monofilament configuration whereas when the fibers are bundled together in the form of helical wrappings, this is referred to as a multifilament configuration. Moreover, the discrete chopped fibers are available in a variety of lengths and diameters ranging from few millimeters up to 80 millimeters in length, and from a tenth of a millimeter up to 2 millimeters in diameter [66]. Furthermore, the fibers are classified as micro or macro fibers depending on their length and diameter when compared to the maximum aggregate size and cement grain size

used in the concrete mix. When the length and the diameter of the added fibers are greater than the maximum aggregate size and cement grain size, they are often classified as macro fibers whereas they are classified as micro-fibers when their length and diameter are less than the maximum aggregate size and cement grain size [67]. The fibers used in this study are classified as macro fibers.

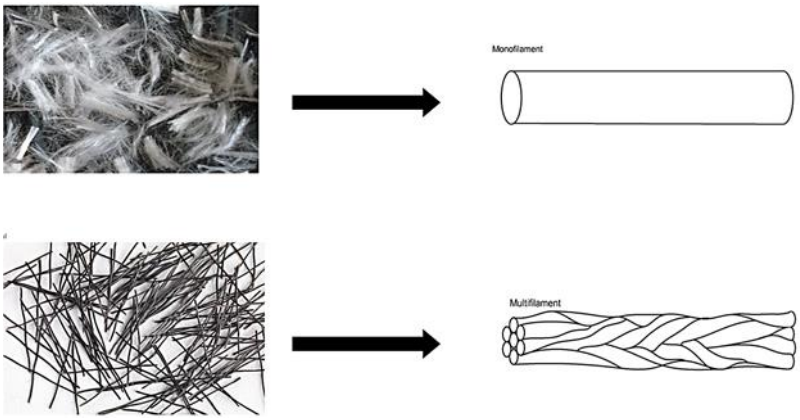

Figure 19: Monofilament and Multifilament Configurations.

The structural enhancement of concrete by adding discrete fibers is mainly governed by the interfacial interactions of the fiber and surrounding concrete which the chemical adhesion and the frictional bond due to the mechanical interlock developed due to the surface treatment of the fiber [68]. When using conventional smooth and straight fibers to be added to concrete, insufficient interfacial interaction might be induced with surrounding concrete resulting in an ineffective utilization of the added fibers. Therefore, surface treatments have been performed by deforming the fiber's surface in multiple complex geometries and forms to increase the mechanical interlock of the fiber with the surrounding concrete [68]. Some of these complex forms and geometries are depicted in Figure 20.

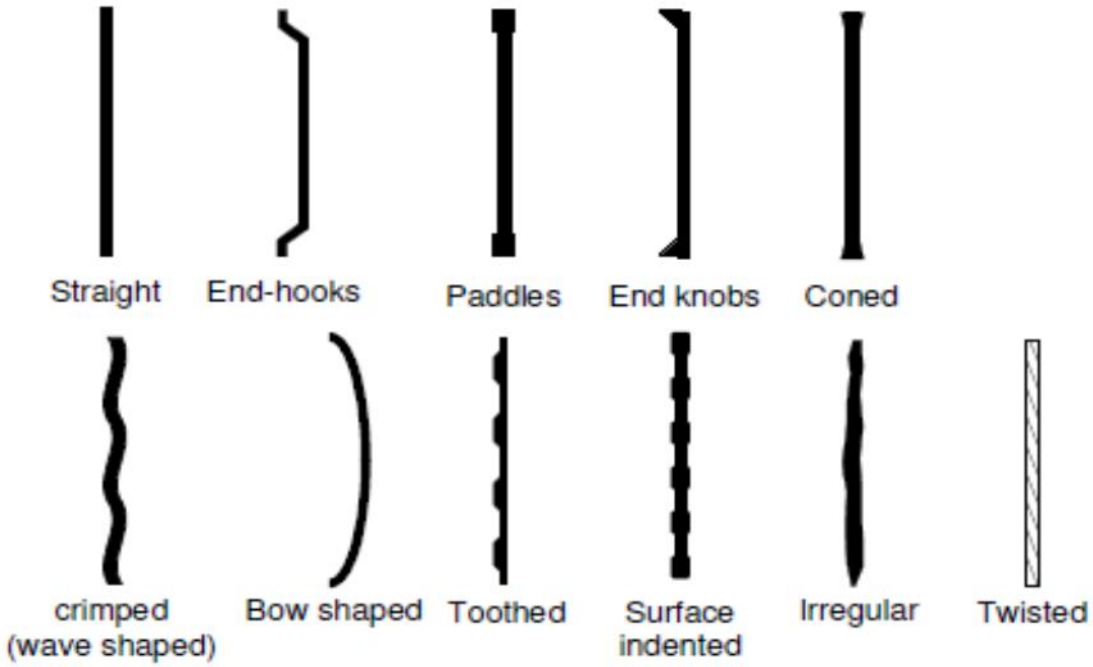

Figure 20:Various geometries of the commercial discrete fibers [66].

Based on the presented studies in this review, the following conclusion can be drawn

- FRP composite bars are promising to be an excellent alternative to conventional steel due to their excellent corrosion and chemical resistance.
- The most widely used test methods for determining the bond strength of FRP bars by direct pull-out testing are the ASTM D7913 and CSA S806.
- The most widely used analytical model used to represent the bond-slip experimental curves are the mBPE, and CMR models.
- The surface treatment of the FRP composite bars plays a significant role in the bond performance.
- Increasing the embedment length of FRP bars in concrete cubes decreases the bond strength

- Larger diameters of FRP bars exhibit a reduction in the bond strength between FRP bars and concrete.
- The concrete compressive strength affects the bond strength between the FRP bars and concrete.
- The addition of fibers to normal concrete mixes may enhance the bond strength of FRP bars with concrete however, this requires more investigation because the studies concerning this matter are few and contradicting.
- Durability of FRP bars under different environmental conditions such as high temperature, saline, acidic, and alkaline solution was discussed. It was found out that the FRP bars experience severe reductions in these solutions especially when they are accompanied by high temperatures.

Very few studies were performed on the influence of FRC on the FRP composite bars bond degradation, but based on the discussed studies in this review, the effect of FRC on the bond strength remains unclear whereas its influence on the durability of the FRP bars seems to be more pronounced. However, up to the author's knowledge, only one study was performed on the effect of FRC on the durability of FRP bars immersed in seawater which indicated an improvement on the bond durability of GFRP bars specimens in saline solution when subjected to extremely high temperatures of 50^{o}C and 70^{o}C. The addition of metallic and highly conductive fibers susceptible to corrosion in a highly corrosive solution such as a saline solution requires more investigations to confirm their suitability along with the noncorrosive FRP composite bars in marine structures. That is why, to furtherly investigate the effect of steel FRC in improving the bond durability of FRP bars, longer exposure duration and lower temperatures are required to investigate the addition of corrosive mild steel fibers the concrete mix in improving the bond durability of the newly developed BFRP composite bars.

Therefore, this study is conducted to effectively evaluate the durability of BFRP bars embedded in corrosive and noncorrosive FRC subjected to oceanic water at elevated temperature due to the need of fulfilling the gap and enriching the literature.

CHAPTER THREE: EXPERIMENTAL PROGRAM

3.1. Materials

3.1.1. Basalt Fiber Reinforced Polymers Bars

One type of basalt FRP (BFRP) bars was used in this study and is denoted as HWBFRP referring to its surface shape of helical wraps which consists of indentations distanced at 3 cm. These indentations are used to increase the mechanical interlock at the interface between concrete and BFRP bar's surface and thus increases the bond strength of the bar. The BFRP bars used in this study are obtained from a Norwegian company called Reforcetch. Figure 21 shows the BFRP bars investigated in this study. The mechanical properties of the HWBFRP bar investigated in this study are shown in Table 3. All bars have a nominal diameter of 10 mm which includes the size of the polymeric resin used in manufacturing the BFRP bars. The process followed for producing the BFRP bars is wet ley-up which basically consists of laying up the basalt fibers and soaking them with the polymeric resin such that it forms a usable BFRP composite bar when cured. The fibers in the BFRP bars used in this study are extracted from basaltic igneous rocks which primarily compose of numerous forms of oxides, where silica oxides being the most abundant with a composition percentage of 51.6 to 57.5 %. In general, silica oxide content above 46% is the acceptable composition for basalt fiber production. The polymeric resin used in manufacturing the BFRP bars is vinyl ester. The tensile strength of the BFRP bar provided by the manufacturer is 1100 MPa with an elastic modulus of 44 GPa. The density of the used bars is 1.9 g/cm^3

Figure 21: BFRP Bar Used in the Study.

Table 3: Material Properties for the Used BFRP Bars in this Study

Material Properties	Basalt Fibers w/o resin	HWBFRP bars
Tensile Strength (MPa)	2900	1100
Elastic Modulus GPa	88	44
Density g/cm^3	2.9	1.9

3.1.2 Structural Fibers Added to the Concrete Mix

Two types of fibers were used in this study: basalt macro fiber (BMF) and steel macro fiber (SMF). The basalt fibers investigated in this study are manufactured by a Norwegian company called (ReforceTech AS). The trademark name of the used basalt fibers is (MiniBar^{TM}ReforceTech). According to the datasheet provided by the manufacturer, these fibers can be mixed with concrete up to 4% volume fraction without affecting the workability of concrete. The basalt fiber content of the minibars is 46% with Vinyl ester being the polymeric resin in the production process which is similar to the manufacturing process of the BFRP bars. Vinyl ester resin is produced by combining an unsaturated polyester resin with an epoxy resin. The outer surface of the minibars used in this study is treated to form helical windings along the fiber's length to effectively improve the mechanical interlock with the surrounding concrete.

Hence, it can be clearly noticed that the minibars are just a small-scale prototype of the HWBFRP bars used in this study

On the other hand, the steel fibers used in this study are obtained from a manufacturer, located in the Republic of Serbia, called Spajic. The commercial name of the steel fibers used in this study is Hook Ended steel fibers referring to their shape. Figure 22 shows the two types of fibers investigated in this study. The material properties of both types of fibers investigated in this study are shown in Table 4.

Figure 22: Steel and Basalt Fibers Used in this Study.

Table 4: Properties of Structural Fibers Used in this Study

Type	Length (mm)	Diameter (mm)	Aspect Ratio	Tensile Strength (MPa)	Density (g/cm^3)
Basalt Fibers	43	0.72	59	900	2.1
Steel Fibers	50	0.9	55	1100	7.85

3.1.3 Concrete Mix

The concrete mix used in this study was chosen so that the cylindrical compressive strength of most of the specimens would be within 30 MPa. The normal strength concrete was chosen in accordance to ASTM D7913 and CSA S806[37,39] Moreover, most of the studies that investigated the bond durability of FRP bars have chosen a relatively high strength concrete which might not reflect the practical mix design used in the Arabian Gulf. The use of normal strength concrete exhibits higher permeability than the high strength concrete which will accelerate the water penetration in the concrete matrix during the conditioning. The concrete mix designs are shown in table 5. Two fiber volume fractions of 0.5% and 1% were used in the mix design of the fiber reinforced concrete. Trial mixes were performed to achieve the proper mix design with satisfactory concrete workability and fiber distribution. All specimens were prepared in the same conditions including the control specimens. Each batch was mixed using a mixer that has a capacity of 0.1 m^3. The coarse aggregate, washed sand, and two thirds of the water were added to the mixer and mixed for 1 min. Then the cement and remaining water were added and mixed for 1 min. Finally, the fibers and superplasticizers were added slowly to the mix and mixing was continued for an additional 3 min to ensure uniform dispersion of fibers and to minimize fiber balling. A confirmation of good fiber distribution was done via visual inspection.

Table 5: Concrete Mix Designs Used in this Study.

Mix Type	Fiber Type	Cement (kg/m^3)	Water (kg/m^3)	Sand (kg/m^3)	Coarse Aggregate (kg/m^3)	Fiber Volume Fraction (%)	Super-plasticizer (kg/m^3)
PC	Plain concrete	350	204	714	1082	0	0
Steel-0.5%	Hook ended steel	350	204	714	1082	0.5	0.27
Steel-1%	Hook ended Steel	350	204	714	1082	1	0.35
BMF-0.5%	Basalt MiniBars	350	204	714	1082	0.5	0.27
BMF-0.1%	Basalt MiniBars	350	204	714	1082	1	0.44

3.2. Specimens Preparation

In this research, numerous pull-out tests were done in order to investigate the bond strength between the BFRP rebar and concrete. The pullout specimens composed of a BFRP bar embedded in the center of a concrete cube with side length of 200mm. The BFRP bars has a length of 1050mm with part of it being embedded in concrete. The pullout specimens are shown in Figure 23. The surface of the bar that is in direct contact with concrete (bonded length) is 5 times the diameter of the bar which is equivalent to 50 mm according to [37]. A polypropylene (PP-R) tube with outer diameter of 20 mm and inner diameter of 16 mm was used to separate the bond between the BFRP bar and concrete in the remaining 150 mm of the concrete cube (debonded length) to minimize the bottom plate restraining effect on the BFRP bars used in this study. The spacing between the bar and the tube was filled with silicone before casting to prevent concrete from penetrating inside the tube along the debonded length. The specimens were cast horizontally in molds made of plywood with a thickness of 18mm. Two holes were opened in the center of the plywood molds using a drill at both ends of the cubic mold. One of them was of 20 mm diameter to fit the PP-R tube and the other was of 11 mm to fit the BFRP bars because the bar was protruded for a length of 50

mm to measure the free end slippage of the bar. Figure 24 shows the pullout specimens' mold. Since BFRP bars are weak in the traverse direction (perpendicular to the fibers' direction), the bars had to be inserted in carbon steel tubes with a diameter of 42.6 mm and thickness of 4.85 mm filled with Cementous grout before testing to prevent crushing of the BFRP bars by the machine jaws. The steel tubes were cut so that their length is equal to 400 mm according to [38] to ensure enough bonding stress provided by the Cementous grout between the steel tube the BFRP bar and to successfully transmit the load from the machine to the bar surface. The Cementous grout used in this study was obtained from a local supplier with a brand name of SIKA GROUT 214 shown in figure 25. According to the datasheet provided by the manufacturer, 3.3 Liters of water are needed to be mixed with 25 kg of the grout to achieve a fluid paste. The procedure used for preparing the grout was as follows: (1) 2/3 of the needed water was poured in a bucket (2) the grout was added gradually to prevent lumps formation while slowly mixing using a drill mixer; and (3) the remaining water was added, and mixing was kept for 3 minutes after the remaining water was added. To centralize the bar inside the steel tube two aluminium washers with a hole in their center of a size sufficient to fit the bar’s diameter were fabricated for each specimen and were installed at the end of the steel tube. These washers are shown Figure 26. The bars were embedded in the grout filled steel tubes before casting the pullout specimens as shown in figure 27. After the specimens were casted, the specimens were left for one day before being removed from the molds and then were immersed along with 105 concrete cylinders in tap water for 28 days of curing before the environmental conditioning.

Figure 23: Pullout Specimens after Curing.

Figure 24: Plywood Molds Used for Casting Pullouts Specimens.

Figure 25: The Cementous Grout Used in this Study to Anchor the Bars.

Figure 26: Washers Fabricated to Centralize the Bar inside the Streel Tube.

Figure 27: Bar Preparation before Casting.

3.3 Test Setup

The pullout tests were conducted at Qatar University laboratory using Universal Testing Machine (UTM) with a capacity of 1500 kN as shown in figure 28. Since the machine was not capable of performing the pullout test, a special steel frame setup, shown in figure 29, had to be designed and fabricated to hold the pullout specimens in order to perform the pullout test. The steel frame consisted of a top and bottom plate with a thickness of 20mm and a surface area sufficient to cover the surface area of the pullout specimens in addition to the six threaded steel rods with a diameter of 16mm. The bottom steel plate was cut in the center for a length of 3 cm for easier placement of the pullout specimens. A 32 mm steel rod was welded at the center of the top plate to be held with the upper jaws of the UTM. The six threaded rods served as reaction rods to prevent the bottom plate from moving down due to the load applied by the specimen during the test. Two LVDTs, shown in figure 30, with capacity to measure a displacement of 25 mm were used to measure the linear displacements. The top LVDT

was used to measure the free end slippage whereas the bottom LVDT was used to measure the loaded end slippage. The top LVDT was fixed using a magnet to the upper plate and was placed on the cross-section of the BFRP bar's protruded length. A steel bracket, shown in figure 31, was fabricated to hold the bottom LVDT. The steel bracket was held at a fixed length of 21 cm to measure the net displacement by subtracting the bar's elongation from the loaded end measured displacement at each force reading. The two LVDTs were connected to the data logger that can measure the displacement at a rate of 1 reading per second. The pullout specimens were pulled at a rate of 1.2 mm/min in accordance to [37]. A detailed schematic of the pullout specimen and the fabricated steel frame is shown in Figure 32.

Figure 28: Universal Testing Machine Used in the Study.

Figure 29:Fabricated Pullout Steel Frame Setup.

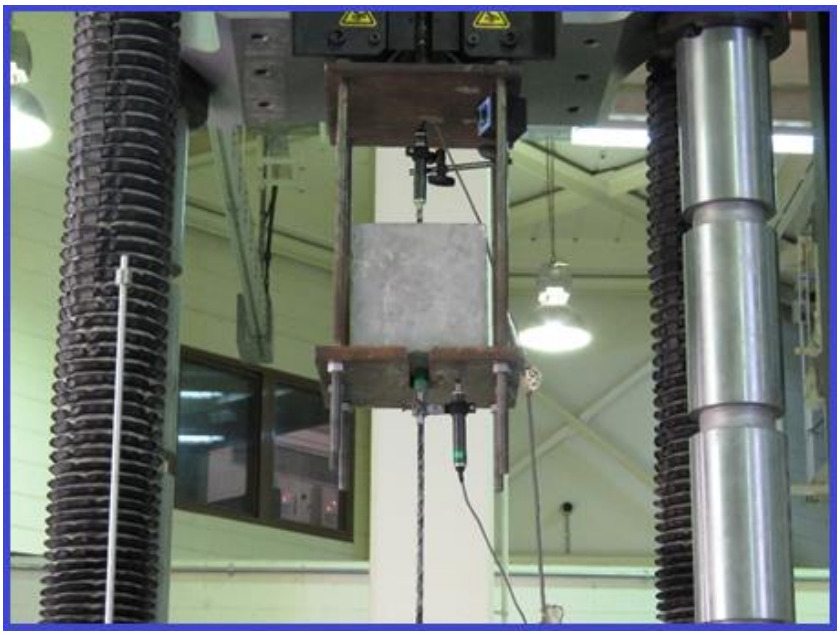

Figure 30: The Two LVDTs Used in the Study.

Figure 31: Fabricated Steel Bracket Used to Hold the Bottom LVDT.

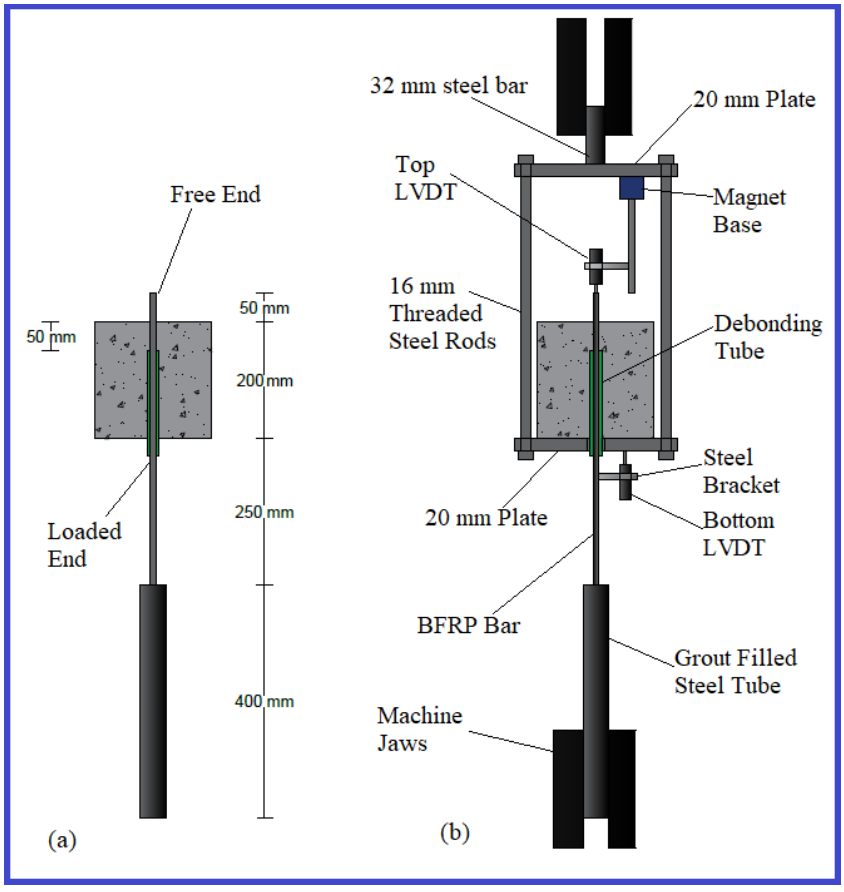

Figure 32: Detailed Schematic of the (a) Pullout Specimen; (b) Test Setup.

3.4 Environmental Conditioning

Two steel tanks of size 2.46 m × 1.23m ×1.23 m, shown in Figure 33, were fabricated from 3 mm thick galvanized steel sheets to prevent corrosion of the tanks due to the existence of NaCl. A GRP cover was fabricated to fit the steel tanks. The GRP cover was then cut to fit the shape of the heaters and the pumps' wires. After 28 days of curing, the specimens were left for three days and were immersed in a saline solution of 3.9% NaCl concentration. The solution was prepared so that the saline solution level reaches 71.5 cm height inside the tank. This was done by marking the required level of solution inside the tank and adding 81.9 kg of NaCl in each tank, then filling the tanks with tap water until the marked level, this was accompanied with thorough mixing until the NaCl was completely dissolved in the solution. This was ensured via visual inspection. Consequently, the total dissolved solids (TDS) test, shown in Figure 34, was carried out to insure the salinity of the solution. The TDS was found to be 4.3 g per 100 ml of solution which is close to the required NaCl concentration of 3.9%. The tanks were then insulated using 2.5 cm thick rockwool sheets shown in Figure 35 to prevent heat loss and save energy because the heaters required 8 amperes of energy consumption and the test was done during the winter time which could damage the heaters if the tanks were left uninsulated (since heaters are equipped with thermostat to maintain the temperature and are designed to turn on and off accordingly). The insulation was done by adding glue to the external tank sheets and sticking the sheets to the tanks immediately. Each tank contained a total of 90 specimens including 45 pullout specimens and 45 cylinders. A total of 5 heaters and 6 pumps were used for the conditioning. 4 heaters and 4 pumps were used to maintain 60 ^{o}C temperature in one tank whereas only 1 heater and 2 pumps were needed to maintain

the 35 ^{o}C in the other tank. After the specimens were immersed in the solution, the GRP cover was placed along with required heaters and pumps. All gaps were then filled with polyfoam shown in Figure 36 to prevent excessive evaporation of water in order to maintain the desired salinity. Additional salt was added to compensate the volume of the specimens that is removed from the tanks each month to maintain the same solution level and same salt concentration.

Figure 33:Fabricated Steel Tanks.

Figure 34: Total Dissolved Solids Test.

Figure 35: Steel Tanks Insulated with 2.5 cm Rockwool Sheets.

Figure 36: Polyfoam Used to Fill the Gaps and Openings.

3.5 Testing Matrix

A total of 105 pullout specimens were prepared in an attempt to investigate the bond strength and bond durability of BFRP bars embedded in different types of fiber reinforced concrete (FRC). The parameters studied in this research program are: (1) The type of FRC: basalt FRC and steel FRC; (2) The fiber volume fractions in the concrete matrix: 0.5% and 1%; (3) the elevated temperatures of 35 ^{o}C and 60 ^{o}C; and (4) the conditioning duration of 30, 60, and 90 days. The specimens were immersed in a saline solution with NaCl concentration of 3.9% simulating the average salinity of the Arabian Gulf seawater. The 35 ^{o}C temperature was chosen since it represented the annual average temperature of the Arabian Gulf. and the 60 ^{o}C temperature was chosen to simulate accelerated environmental conditioning. The specimens were grouped into 35 groups. Each group consisted of three identical specimens. Table 6 presents some details of all the specimens used in this experimental program. The labelling system was chosen so that it is easy to identify the fiber volume fraction of (0.5% for 0.5% fiber volume fraction and 1% fiber volume fraction), the FRC type (SF for steel FRC and BF for basalt FRC), the duration of (30,60, and 90 for 30 days, 60 days, and 90 days respectively) , conditioning temperature (35 for 35 ^{o}C temperature and 60 for 60 ^{o}C temperature) , and specimen number (1,2, and 3 for first, second, and third identical specimen of the same group) . For example, 0.5%SF-30-60-2 refers to the second specimen of 0.5% volume fraction of steel FRC conditioned for 30 days at 60 ^{o}C. 15 control specimens were prepared and were left at room temperature. The control specimens were tested with the 90 days conditioned specimens.

Table 6: Testing Matrix.

No. of Specimens	Fiber Type	Volume Fraction (%)	Temperature (ºC)	Name
Unconditioned Specimens (Control Specimens)				
3	Plain Concrete	0	23	PC-Control
3	Steel FRC	0.5	23	0.5%SF-Control
3	Steel FRC	1	23	1%SF-Control
3	Basalt FRC	0.5	23	0.5%BF-Control
3	Basalt FRC	1	23	1%BF-Control
Conditioned Specimens for 30 days				
3	Plain Concrete	0	35	PC-30-35
3	Steel FRC	0.5	35	0.5%SF-30-35
3	Steel FRC	1	35	1%SF-30-35
3	Basalt FRC	0.5	35	0.5%BF-30-35
3	Basalt FRC	1	35	1%BF-30-35
3	Plain Concrete	0	60	PC-30-60
3	Steel FRC	0.5	60	0.5%SF-30-60
3	Steel FRC	1	60	1%SF-30-60
3	Basalt FRC	0.5	60	0.5%BF-30-60
3	Basalt FRC	1	60	1%BF-30-60
Conditioned Specimens for 60 days				
3	Plain Concrete	0	35	PC-60-35
3	Steel FRC	0.5	35	0.5%SF-60-35
3	Steel FRC	1	35	1%SF-60-35
3	Basalt FRC	0.5	35	0.5%BF-60-35
3	Basalt FRC	1	35	1%BF-60-35
3	Plain Concrete	0	60	PC-60-60
3	Steel FRC	0.5	60	0.5%SF-60-60
3	Steel FRC	1	60	1%SF-60-60
3	Basalt FRC	0.5	60	0.5%BF-60-60
3	Basalt FRC	1	60	1%BF-60-60
Conditioned Specimens for 90 days				
3	Plain Concrete	0	35	PC-90-35
3	Steel FRC	0.5	35	0.5%SF-90-35
3	Steel FRC	1	35	1%SF-90-35
3	Basalt FRC	0.5	35	0.5%BF-90-35
3	Basalt FRC	1	35	1%BF-90-35
3	Plain Concrete	0	60	PC-90-60
3	Steel FRC	0.5	60	0.5%SF-90-60
3	Steel FRC	1	60	1%SF-90-60
3	Basalt FRC	0.5	60	0.5%BF-90-60
3	Basalt FRC	1	60	1%BF-90-60

CHAPTER FOUR: TEST RESULTS AND DISCUSSION.

4.1. Introduction

In this chapter, the test results of the control (Unconditioned) specimens and conditioned specimens are presented and discussed. As discussed earlier, 105 pullout specimens were tested to evaluate the effect of temperature, exposure duration, fiber type and fiber volume fraction on the bond durability of BFRP bars under saline environment. 105 concrete cylinders were tested to monitor the compressive strength during immersion. In general, the concrete compressive strength showed an increasing trend during the at early stages of immersion until 60 days regardless of the mix type. After 60 days, the concrete compressive strength showed minor changes. The immersed specimens are labeled in the following order: test type, mix type of concrete, duration of exposure, temperature of exposure, and specimen number. For instance, specimen PO-1%BF-30-35-2 indicates a pullout specimen with 1% basalt fiber volume fraction conditioned for 30 days at 35 ^{o}C. The digit (2) refers to the second specimen of the three identical specimens. In pullout testing, the bond stress is not uniformly distributed along the embedment length of the bar in concrete, therefore the average bond stress can be approximated using the following equation:

$$\boldsymbol{\tau} = \frac{\boldsymbol{P}}{\boldsymbol{\pi d_b L_d}} \qquad (6)$$

Where $\boldsymbol{\tau}$ is the bond stress, P is the maximum pullout load, d_b is the diameter of the bar, and L_d is bar's embedment length in concrete and was fixed at 50 mm equivalent to $5d_b$. The slippage of the bar at the free end (unloaded end) is measured using an LVDT that was attached at the top plate of the steel frame using a magnet and was placed directly on the bar's cross-section. The slippage of the bar at the loaded end

was measured by subtracting the bar's elongation from the total deformation measured using an LVDT that was attached to the bar using a fabricated steel bracket as follows:

$$\text{Loaded end slippage of the bar= Bottom LVDT reading - } \frac{PL}{AE} \quad (7)$$

Where L is the distance between the location of the steel bracket and the start of the embedment length of the bar, which was kept at 210 mm, E is the bar's young's modulus, (E=44 GPa), A is the cross-sectional area of the bar. Table 8 shows the obtained experimental results from the pullout test.

4.2. Bond Failure Mechanism

The test results are shown in Table 7, All unconditioned (control) specimens failed under typical pullout failure mechanism by exhibiting slippage at the free end without any signs of cracks appearing the specimen's surface that indicates a splitting failure, however it is worth to note that specimen 1%BF-control-3 exhibited a pullout failure followed by a rebar fracture after a large amount of slippage after reaching the peak load which gives an indication that basalt fiber reinforced concrete with high volume fraction does have an effect on the mode of failure. For the conditioned specimens, all specimens conditioned at 35 ^{o}C exhibited a typical pullout mode of failure regardless of the mix type, fiber volume fraction, or exposure duration, however, this was not the case for the specimens conditioned at 60 ^{o}C. At the early time of exposure, the mode of failure was mainly dominated by pullout mode of failure. After 60 and 90 days of exposure, one specimen out of the three identical specimens of the BFRP bars embedded in 0.5% and 1% basalt FRC changed the mode of failure from pullout to rebar fracture where bar's layers seemed to be sheared off as shown in Figure

37 indicating the faster deterioration due to the higher immersion temperature and the accelerated chloride ions penetration inside the concrete to reach the bar's resin at higher temperatures therefore, weakening the resin surrounding the basalt fibers of the rebar which lead to rebar fracture. Similar behavior was observed for PC-90-60-3 indicating the more predominant influence of the temperature on changing the mode of failure rather than the presence of the fibers. It is important to note that the quality of manufacturing and the random deterioration of the specimens play an important role for not causing the same type of failure for all the three identical specimens. In general, specimens that experienced rebar fracturing displayed a relatively higher bond strength than those failed at a typical pullout mode of failure. No concrete splitting failure was observed due to the sufficient concrete cover provided as well as the presence of fibers in concrete that provide additional confining pressure to the concrete. Some of the specimens were split using a grinder equipped with concrete cutting disc for closer inspection on the surface of concrete along the BFRP bar's embedment length as shown in figures 38, 39, and 40 for control, 90 days at 35 ^{o}C, and 90 days at 60 ^{o}C plain concrete specimens respectively. The visual inspections revealed a whitish color at the concrete surface along the embedment length was for the conditioned specimens regardless of the conditioning temperature indicating the presence of NaCL along the embedment length, the more severe condition of the bar surface of the immersed specimens indicates the bond degradation when compared to the control specimens. Moreover, examination of the BFRP bar's surface indicated concrete residue between the bar ribs along with some small scratches on the bar's ribs at the bar-concrete interface, this behavior was observed for both conditioned and unconditioned specimens, however the wearing of the conditioned specimens was more obvious. No noticeable difference could be visually inspected between the different durations of the

immersed specimens. All steel FRC specimens failed under pullout mode of failure regardless of the significant increase in the concrete compressive strength which implies that the bond strength relies more on the performance of the FRP bar than the increase in the compressive strength of surrounding concrete. The mode of failure was governed by interlaminar shearing between the successive layers of the BFRP bar, rather than concrete shearing at the interface between the bar and surrounding concrete, for all the tested specimens that failed by pullout mode failure. This is explained by the delamination of the BFRP bar's outer surface layer that can be easily observed by visual inspections when the concrete cubes were split with the presence of chopped fibers and bar's crushed resin at the concrete surface along the embedment length. This agrees with the findings of [43] that the governing factor of the failure mode of FRP bars depends mainly on the shear strength between the fibers and the surrounding resin, rather than the shear strength of the surrounding concrete, when the compressive strength is greater than 30 MPa.

.

Table 7: Test Results

Specimen	f'c (MPa)	τ_{max} (Mpa)	τ^*_{max} (MPa)	τ^*n (MPa)	δ_{LE} (mm)	δ_{FE} (mm)	τ_{ons} (MPa)	τ_r (MPa)	Failure Mode	Retention (%)
Unconditioned (Control) Specimens										
PC-C-1		11.78			6.2	6.21	1.49	9.58	PO	
PC-C-2	32.5	13.14	13.14	2.3	7.18	8.65	0.39	12.51	PO	100
PC-C-3		14.49			4.81	6.44	2.58	12.47	PO	
0.5%SF-C-1		15.97			7.31	9.22	0.11	14.23	PO	
0.5%SF-C-2	33.1	16.58	15.7	2.73	5.14	N. A	0.04	13.55	PO	100
0.5%SF-C-3		14.55			4.59	6.47	0.12	10.22	PO	
1%SF-C-1		13.11			6.24	7.19	0.22	11.93	PO	
1%SF-C-2	31.1	14.34	13.34	2.39	6.23	6.76	0.16	12.44	PO	100
1%SF-C-3		12.56			6.23	6.66	0.31	10.17	PO	
0.5%BF-C-1		13.25			5.77	5.84	0.45	11.18	PO	
0.5%BF-C-2	30	12.64	13.27	2.42	4.46	6.18	0.98	11.51	PO	100
0.5%BF-C-3		13.91			6.8	7.54	0.32	10.19	PO	
1%BF-C-1		13.6			6.95	8.37	0.12	12.85	PO	
1%BF-C-2	30.6	16.33	16.01	2.89	5.66	N. A	0.13	13.06	PO	100
1%BF-C-3		18.09			6.32	7.43	0.24	13.58	PO/R	
30 Days Conditioned Specimens at 35 ºC										
PC-30-35-1		11.4			4.08	5.18	0.23	9.98	PO	
PC-30-35-2	30.4	8.96	9.547	1.73	4.63	4.72	0.35	6.51	PO	73
PC-30-35-3		8.28			7.82	8.61	0.29	7	PO	
0.5%SF-30-35-1		12.25			5.53	5.97	0.54	10.83	PO	
0.5%SF-30-35-2	33.3	11.72	10.97	1.9	4.78	5.29	0.34	8.69	PO	70
0.5%SF-30-35-3		8.93			4.98	5.54	0.29	5.52	PO	
1%SF-30-35-1		11.2			7.37	7.82	0.37	10.18	PO	
1%SF-30-35-2	30.3	NA	12.49	2.27	N. A	N. A	N. A	N. A	N.A	94
1%SF-30-35-3		13.77			6.11	6.01	0.49	12.12	PO	
0.5%BF-30-35-1		10.63			2.68	3.59	0.27	9.67	PO	
0.5%BF-30-35-2	27.9	8.09	10.7	2.03	5.75	5.59	0.5	6.13	PO	81
0.5%BF-30-35-3		13.37			6.33	6.78	0.5	11.19	PO	
1%BF-30-35-1		12			5.65	6.57	0.21	9.27	PO	
1%BF-30-35-2	30.3	7.71	10.29	1.87	6.18	6.43	0.31	6.34	PO	64
1%BF-30-35-3		11.15			5.88	7.8	0.14	9.06	PO	

Table 7 (Continued)

Specimen	f'c (MPa)	τ_{max} (Mpa)	τ^*_{max} (MPa)	τ^*n (MPa)	δ_{LE} (mm)	δ_{FE} (mm)	τ_{ons} (MPa)	τ_r (MPa)	Failure Mode	Retention (%)
30 Days Conditioned Specimens at 60 ºC										
PC-30-60-1		12.14			6.26	6.59	0.12	10.45	PO	
PC-30-60-2	29.3	13.38	13.4	2.48	6.54	7.01	0.42	10.46	PO	102
PC-30-60-3		14.69			4.24	5.51	0.48	10.93	PO	
0.5%SF-30-60-1		11.81			4.19	4.83	0.51	9.52	PO	
0.5%SF-30-60-2	31.1	8.01	10.54	1.89	5.51	5.13	0.54	6.45	PO	67
0.5%SF-30-60-3		11.81			6.03	5.75	0.13	9.11	PO	
1%SF-30-60-1		13.48			4.8	5.82	0.17	10.63	PO	
1%SF-30-60-2	35.5	14.92	14.15	2.37	5.92	6.36	0.19	12.4	PO	106
1%SF-30-60-3		14.05			5.55	6.75	0.46	11.12	PO	
0.5%BF-30-60-1		17.2			7.22	7.76	0.71	14.24	PO	
0.5%BF-30-60-2	31.2	12.32	15.18	2.72	4.62	4.45	0.59	11.39	PO	114
0.5%BF-30-60-3		16.02			5.74	5.77	0.33	13.25	PO	
1%BF-30-60-1		11.3			5.39	6.16	0.51	9.02	PO	
1%BF-30-60-2	33.4	9.78	11.55	2	3.81	4.84	0.16	7.5	PO	72
1%BF-30-60-3		13.56			5.19	6.62	0.19	9.28	PO/R	
60 Days Conditioned Specimens at 35 ºC										
PC-60-35-1		12.14			7.35	7.01	0.64	11.11	PO	
PC-60-35-2	34.2	10.26	10.9	1.86	4.8	5.59	0.56	8.46	PO	83
PC-60-35-3		10.31			3.64	4.09	0.51	6.63	PO	
0.5%SF-60-35-1		14.04			5.6	6.18	0.46	11.22	PO	
0.5%SF-60-35-2	34.5	10.93	12.21	2.08	7.52	8.54	0.51	8.65	PO	78
0.5%SF-60-35-3		11.66			8.03	8.36	0.63	10.77	PO	
1%SF-60-35-1		11.33			6.3	6.41	0.39	10.48	PO	
1%SF-60-35-2	30.4	10.93	10.69	1.94	6.82	7.44	0.54	8.39	PO	80
1%SF-60-35-3		9.81			7.86	8.16	0.28	8.97	PO	
0.5%BF-60-35-1		12.07			4.89	5.16	0.63	9.45	PO	
0.5%BF-60-35-2	30.3	12.94	13.22	2.4	5.23	5.42	0.37	8.87	PO	100
0.5%BF-60-35-3		14.65			6.51	7.23	0.64	13.33	PO	
1%BF-60-35-1		14.76			5.3	5.39	1.17	12.61	PO	
1%BF-60-35-2	33.2	13.93	14.97	2.6	7.75	7.29	0.34	12.23	PO/R	94
1%BF-60-35-3		16.21			4.38	5.26	0.24	11.31	PO	

Table 7 (Continued)

Specimen	f'c (MPa)	τ_{max} (Mpa)	τ^*_{max} (MPa)	τ^*n (MPa)	δ_{LE} (mm)	δ_{FE} (mm)	τ_{ons} (MPa)	τ_r (MPa)	Failure Mode	Retention (%)
60 Days Conditioned Specimens at 60 C										
PC-60-60-1		16.34			3.9	3.97	0.09	11.74	PO /R	
PC-60-60-2	34.4	11.65	12.17	2.07	6.81	7.07	0.11	10.44	PO	93
PC-60-60-3		8.52			5	5.49	0.22	7.51	PO	
0.5%SF-60-60-1		11.95			6.01	5.93	0.35	8.78	PO	
0.5%SF-60-60-2	31.8	9.56	10.12	1.79	6.08	6.02	0.62	6.98	PO	64
0.5%SF-60-60-3		8.85			5.33	5.54	0.36	7.29	PO	
1%SF-60-60-1		14.41			4.53	6.03	0.29	10.71	PO	
1%SF-60-60-2	37.1	NA	13.72	2.25	NA	NA	NA	NA	NA	103
1%SF-60-60-3		13.02			3.28	4.25	0.25	11.75	PO	
0.5%BF-60-60-1		12.28			9.02	9.07	0.28	11.09	PO	
0.5%BF-60-60-2	33.1	16.83	14.72	2.56	2.84	3.37	0.3	NA	R	111
0.5%BF-60-60-3		15.05			7.53	8.2	0.41	13.33	PO	
1%BF-60-60-1		15.95			1.91	6.66	0.07	NA	R	
1%BF-60-60-2	33.8	15.81	13.97	2.4	6.605	6.99	0.7	NA	PO/R	87
1%BF-60-60-3		10.15			5.97	6.45	0.21	7.74	PO	
90 Days Conditioned Specimens at 35 C										
PC-90-35-1		14.22			4.52	5.2	0.3	11.14	PO	
PC-90-35-2	35	9.96	12.14	2.05	5.7	5.85	0.15	8.3	PO	92
PC-90-35-3		12.25			5.25	5.28	0.28	9.18	PO	
0.5%SF-90-35-1		10.37			4.4	4.48	0.89	8.57	PO	
0.5%SF-90-35-2	34	9.95	9.157	1.57	4.93	5.54	0.28	8.84	PO	58
0.5%SF-90-35-3		7.15			10.92	10.75	1.01	6.52	PO	
1%SF-90-35-1		10.32			4.49	4.87	0.41	8.49	PO	
1%SF-90-35-2	31.2	11.95	10.53	1.89	4.44	4.62	0.21	8.09	PO	79
1%SF-90-35-3		9.33			3.86	5.02	0.03	8.12	PO	
0.5%BF-90-35-1		11.51			6.21	7.23	0.31	8.89	PO	
0.5%BF-90-35-2	34.1	12.52	14.16	2.42	7.23	7.91	0.15	11.65	PO	107
0.5%BF-90-35-3		18.45			6.74	6.92	1.19	13.99	PO	
1%BF-90-35-1		13.96			7.36	NA	0.16	11.87	PO	
1%BF-90-35-2	31.1	15.72	15.03	2.7	6.21	7.33	0.36	12.41	PO	94
1%BF-90-35-3		15.42			6.57	7.09	0.35	11.77	PO	

Table 7 (Continued)

Specimen	f'c (MPa)	τ_{max} (Mpa)	τ^*_{max} (MPa)	τ^*n (MPa)	δ_{LE} (mm)	δ_{FE} (mm)	τ_{ons} (MPa)	τ_r (MPa)	Failure Mode	Retention (%)
90 Days Conditioned Specimens at 60 ºC										
PC-90-60-1		11.6			8.35	8.68	0.76	10.34	PO/R	
PC-90-60-2	35.6	10.56	11.77	1.97	4.43	5.2	0.39	7.29	PO	90
PC-90-60-3		13.15			5.57	4.824	1.74	NA	R	
0.5%SF-90-60-1		9.48			5.69	7.23	0.14	7.69	PO	
0.5%SF-90-60-2	33.6	10.15	10.37	1.79	5.5	6.14	0.23	8.4	PO	66
0.5%SF-90-60-3		11.48			4.94	7.15	0.04	8.44	PO	
1%SF-90-60-1		14.05			4.04	NA	0.05	11.79	PO	
1%SF-90-60-2	38	13.14	13.76	2.23	3.58	4.29	0.24	8.38	PO	103
1%SF-90-60-3		14.1			6.59	7.07[a]	1.19	13.17	PO	
0.5%BF-90-60-1		12.24			6.77	5.78	6.16	10.64	PO	
0.5%BF-90-60-2	34.2	14.05	14.03	2.4	5.13	4.5	1.94	10.63	PO	106
0.5%BF-90-60-3		15.81			5.65	4.87	3.81	NA	R	
1%BF-90-60-1		11.63			3.22	3.42	1.15	9.3	PO	
1%BF-90-60-2	34.5	12.31	12.73	2.17	3.16	3.45	0.47	7.55	PO	80
1%BF-90-60-3		14.25			3.93	4.49	0.24	NA	PO/R	

**f'c: Concrete Compressive Strength; $\tau_{max:}$ Bond Strength; $\tau^*_{max:}$ Average Bond Strength; $\tau^*n = \tau^*_{max}/\sqrt{fc'}$; δ_{LE}= Loaded End Slippage; δ_{FE}: Free End Slippage; τ_{ons}: Adhesion Stress τ_r: Residual Bond Strength; PO: Pullout Failure; R: Rebar Fracture; PO/R: Pullout Followed by Rebar Fracture; a: Data Test Not Adopted in the Analysis.

Figure 37: Complete Interlaminar Shear Failure between the Layers of the Bar.

Figure 38: Closer Examination of Unconditioned Plain Concrete Specimens.

Figure 39: Closer Examination of conditioned Plain Concrete after 90 Days at 35 ^{o}C .

Figure 40: Closer Examination of conditioned Plain Concrete after 90 Days at 60 ºC.

4.3. Bond-Slip Response

Figures 41, 42, and 43 show representative bond-slip curves that describe the bond behaviors of the HWBFRP bars embedded in plain concrete, steel FRC, and basalt FRC at 0.5% and 1% fiber volume fractions subjected to elevated temperatures of 35 °C and 60 °C at 30, 60, and 90 days of exposure periods. The bond-slip curves corresponding to the loaded end have been calibrated by subtracting the elongation of the bar at each force reading from the bottom LVDT reading as according to [37]. All the tested pullout specimens showed a bond-slip curve with an initial ascending branch up to a point where the formation of cracks start to develop on the surrounding concrete and the bearing friction force due to the mechanical interlock between the bar and concrete reduces causing a gradual decay in the slope of the ascending branch in which the rate of increase in the bond stress decreases whereas the rate of slippage increases, this continues to a point where the maximum sustainable pullout stress, $\tau_{max,}$ is reached

followed by a gradual decrease in the bond stress due to the residual action of wedging done by the BFRP bar's deformations on the surrounding concrete which governs the post-peak behavior of the BFRP bar and is often called the descending branch.

In general, the bond-slip curves at the free end of most of the specimens are similar to those at the loaded end slippage indicating comparable values of slippage between the loaded and free end slippage. This is attributed to the usage of normal strength concrete rather than high strength concrete, similar behavior was reported by Okelo and Yuan [69], whereas, when high strength concrete is used, the free end slippage tends to be lower than the loaded end slippage [60,62]. It should be noted that the loaded end slippage corresponding to the maximum stress tabulated in Table 7 is the effective loaded end slippage that does not consider the elongation of the bar since it is calibrated by subtracting the deformation of the BFRP bar using equation (7). It can be noted from the bond-slip curves of Figure 41 that the chemical adhesion of the used bars in this study is relatively low since the bars began to slip at relatively low applied loads, therefore, the mechanical interlock between the bar's helical wraps surface and surrounding concrete is accounted for the majority of the bond stress developed by the applied pullout force which agrees with what Achillides and Pilakoutas [43] have mentioned in their study.

From the test results shown in table 7, the enhancements of adding structural fibers to concrete compared to plain concrete are 19.5% and 1.5% for 0.5% and 1% steel fiber volume fractions respectively, whereas the improvements due to the addition of basalt fibers to concrete are 1% and 21.9% for 0.5% and 1% basalt fibers volume fractions respectively. Thus, it can be said that 0.5% volume fraction of basalt FRC and 1% volume fraction of steel FRC did not show a noticeable improvement on the bond strength of helically wrapped BFRP bars with a relatively smooth surface. Therefore,

this implies that the steel fiber volume fraction has no effect on the bond strength of HWBFRP bars whereas the relationship is vice versa for the effect of basalt fiber volume fraction. The effect of steel fiber volume fraction found in this study agrees with what have been mentioned in [57]. The results reveal that FRC enhances the bond strength of BFRP bars compared to plain concrete. The improvement of bond capacity in FRC is explained in the bridging effect of the fibers which transmit the tensile stresses induced in concrete due to the bond stress developed between the BFRP bars and concrete during the loading. In plain concrete, these large tensile stresses induced by the pullout forces lead to cracking of concrete surrounding the bar due to the brittle nature of plain concrete in tension. Therefore, the fibers addition improves the concrete matrix bond strength to the bar by transmitting the large tensile stresses induced during the loading along the fiber slippage at the onset of cracking which provide additional resistance to the tensile stresses and prevent further cracks' openings in the FRC which is not the case for plain concrete. It is worth to note that the lack of sand coating in the studied bar in this research may cause insufficient triggering of the additional confinement provided by FRC which might explain the observed effect of increasing the steel fiber volume fraction in the insignificant improvement on the bond strength of HWBFRP bars with no sand coating. However, this research aims at evaluating the overall durability performance of HWBFRP bars embedded in FRC at marine structures under aggressive environmental conditions rather than studying the FRC effect on bond strength at ideal environmental conditions. It should be noted that the lowest bond strength for the unconditioned specimens found in this study was 13.1 MPa dedicated for BFRP bars embedded in plain concrete which meets the minimum requirements provided by the CSA S807[70] (>8 MPa) and ACI 440.6 M [71] (>9.6 MPa).

Consequently, the effect of structural fiber reinforced concrete on delaying the

bond failure seems to depend on the type of FRC and type of bar used rather than the volume fractions, since for unconditioned specimens, the low steel fiber volume fraction showed higher slippage at peak bond strength whereas the effect of basalt fiber volume fraction was the opposite as the high content of basalt macro fibers delayed the bond failure by exhibiting higher slippage at failure. In other words, for unconditioned specimens, the fiber volume fraction of each type that showed a significant improvement in the bond strength possessed higher slippage at failure. On the other hand, the effect of fibers' addition on the bar's slippage at failure was more pronounced. Figure 44 shows the average free end slippage of the bars taking into consideration the temperature and exposure duration. It can be indicated that at a temperature of 60 °C, all specimens show a decrease in slippage after 90 days of exposure compared to their control specimens with 1% basalt FRC showing the highest decrease in slippage by retaining 48% of the average free end slippage exhibited by the unconditioned specimens which indicates a clear influence of temperature on the increased amount of basalt macro fiber in the concrete mix. For plain concrete specimens, a clear reduction after 90 days of exposure can be noticed at both temperatures with a higher decrease in slippage at 60 °C than 35 °C. For steel FRC, the rate of decrease in slippage at failure in both volume fractions used in this study indicates that the reduction in slippage of HWBFRP embedded in steel FRC is mainly affected by immersion rather than the increase in temperature whereas for basalt FRC specimens, the reduction is influenced mainly by temperature rather than immersion since 0.5% basalt fiber volume fraction at 35 °C exhibited an increase in slippage compared to control specimens.

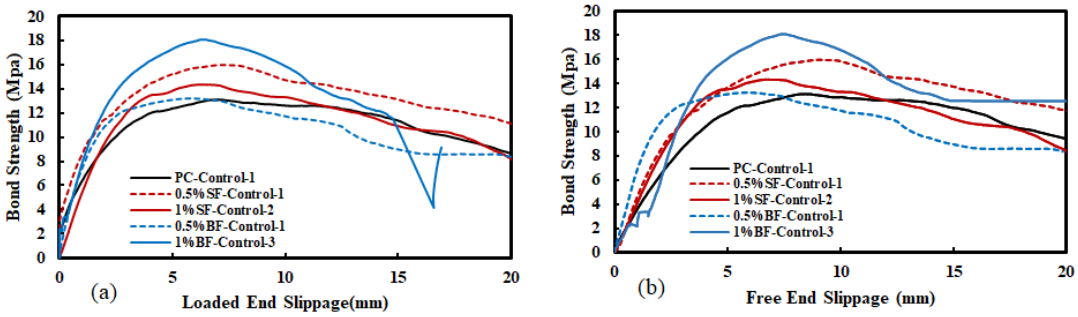

Figure 41:Bond-Slip Cuves for Control Specimens: (a) Loaded End; (b) Free End Slippage

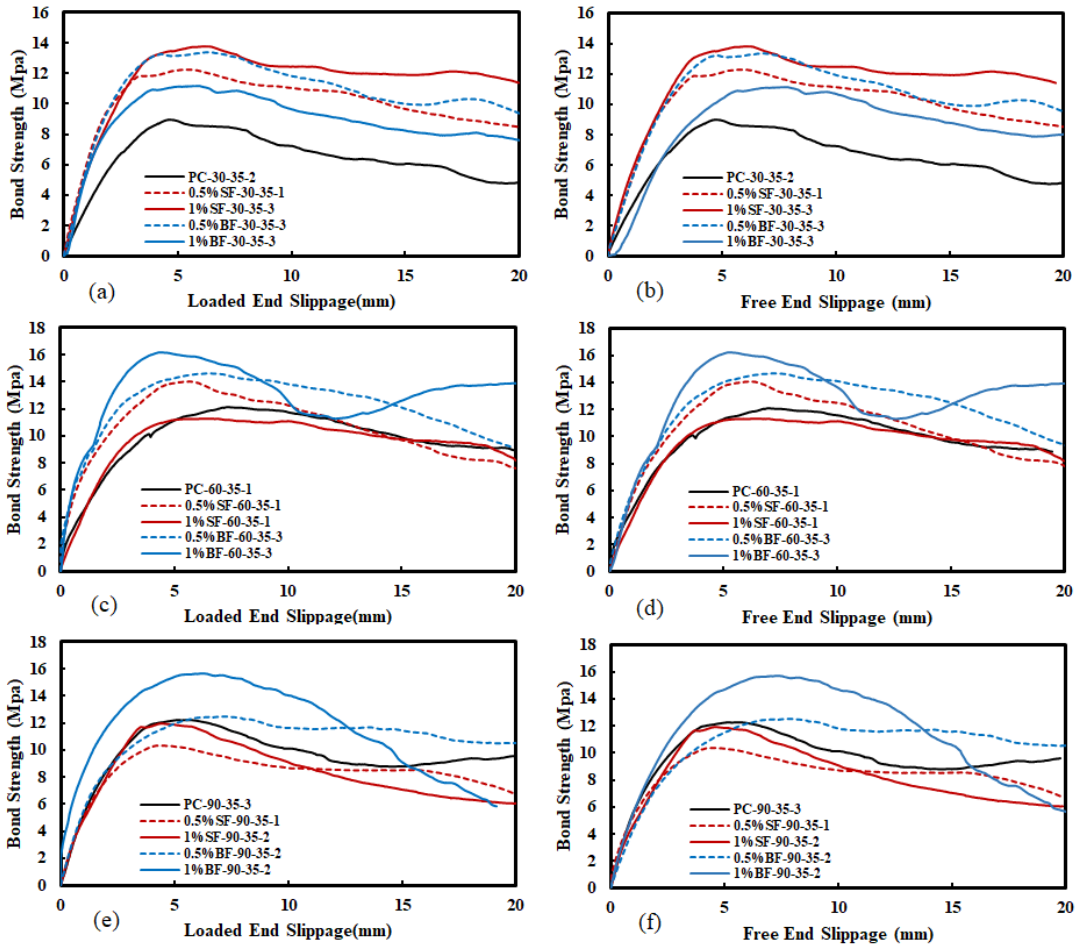

Figure 42:Bond-Slip Curves for 35 °C Conditioned Specimens at Loaded and Free Ends: (a) 30 Days; (b) 30 Days; (c) 60 Days; (d) 60 Days; (e) 90 Days; (f) 90 Days.

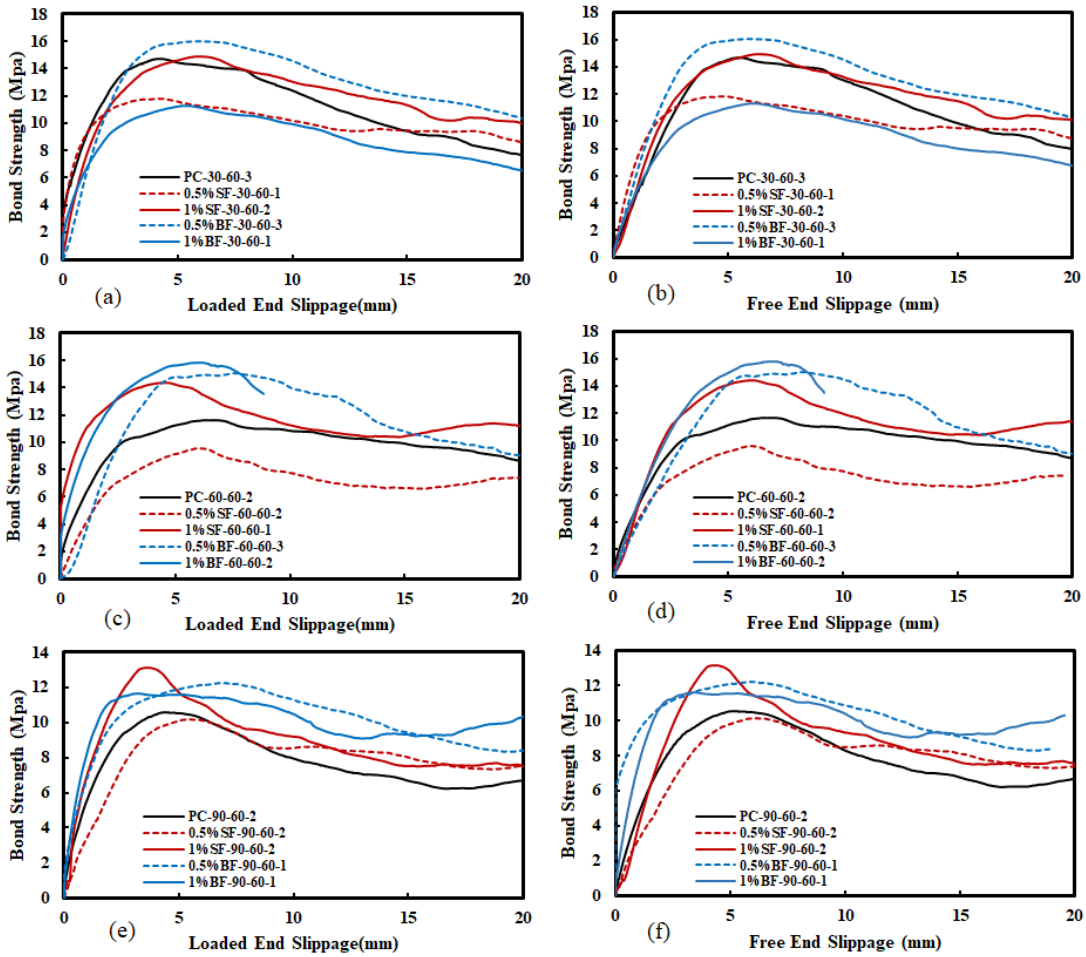

Figure 43: Bond-Slip Curves for 60 °C Conditioned Specimens at Loaded and Free Ends: (a) 30 Days; (b) 30 Days; (c) 60 Days; (d) 60 Days; (e) 90 Days; (f) 90 Days.

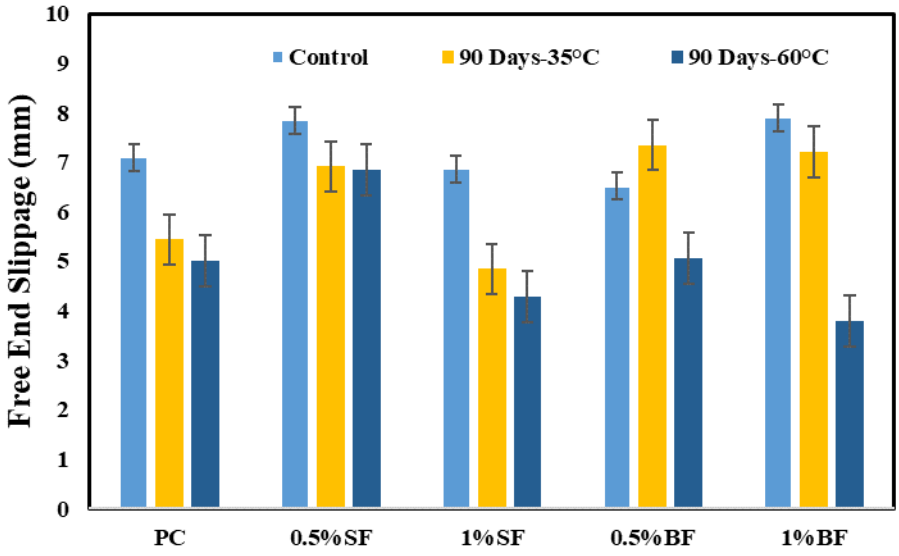

Figure 44: Effect of Immersion-Temperature on Slippage after 90 Days of Exposure Time.

4.3. Bond Strength Degradation

Bond strength is one of the most important parameters that govern the performance of FRP reinforced concrete structures. Based on the conducted literature review on the experimental investigations that have been done on bond strength of BFRP, it can be said that the used bars in this study are susceptible to reductions in the interfacial bond between the bar and surrounding concrete with the presence of chlorides, moisture, and elevated temperatures which are the typical conditions for marine structures in the Arabian Gulf. Since, the studies on bond durability of BFRP bars are very limited, understanding the degradation mechanism of FRP bars constituents, would be a useful tool to explain the obtained experimental results in this study since most of the bond degradation is attributed to the degradation of the polymeric resin rather than the fiber itself and the surrounding concrete. When the durability of FRP bars' mechanical properties is concerned, much of the reductions in

the mechanical properties of FRP rods are attributed to the degradation of interfacial bond between the fiber and the polymeric resin used [72]. Many studies [73-75] have revealed that the type of resin used dramatically influenced the degradation of glass FRP bars exposed to aggressive environments. Consequently, softening of the FRP bar's polymeric resin is a mechanical damage that occurs due to bar swelling induced by moisture absorption, high temperature that causes surface microcracks, and interruption in the Van der Waals bond among the polymeric chains [76, 77]. These microcracks developed on the resin under the presence of aqueous solution and high temperature, which is the case in this study, allow the diffusion of aggressive solutions, containing chlorides, in the fibers and the interior matrix.

When the durability of interfacial bond between FRP rods and surrounding concrete is concerned, an increasing trend in the bond strength over exposure periods under aggressive environments can be expected due to the effects of FRP bar swelling which lead to an increased frictional bond with the surrounding concrete and/or slower than expected rate of degradation caused by the restricted access of aggressive solutions along the embedment length of FRP bar with concrete[78,79]. The presence of a chloride environment has a detrimental impact on the interfacial shear between the fiber and the surrounding matrix which is the governing bond failure mechanism observed in this study. Liu et al.[80] studied the performance of vinyl ester and epoxy BFRP composites toward saline water immersion, tap water immersion, and cycles of moisture and temperature for 240 days of aging. It was found that vinyl ester and epoxy FRP composites showed comparable results with no considerable decrease in the shear strength due to tap water immersion and cycles of moisture and temperature, however when immersing BFRP composites in saline water under high temperature (40 ^{o}C), a significant reduction in the shear strength of BFRP composites was observed. Another

study was done by [81] aiming at understanding the behavior of carbon fiber/resin interface under the effect of saline water exposure. The study indicated that saline solution had the most aggressive impact in the loss of the fiber/epoxy interfacial adhesion which was observed in the reduction of the resin density close to the interface as well as the decreased interfacial stress compared to dry and moisture case. Furthermore, beside the influence of temperature on the interlaminar shear between the fibers and the matrix, the increase in temperature accelerates the rate of moisture absorption of the polymeric resin [82,83]. Another factor that has a detrimental influence on the bond degradation of BFRP bars is the substantial difference between the coefficient of thermal expansion (CTE) of concrete (14.5×10^{-6} /K) and that of BFRP bars used (22×10^{-6} /K). Hence, the noticeably larger CTE of the BFRP bars compared to concrete causes them to exhibit different rates of expansion and contraction at the interface between the bar and surrounding concrete which is mainly dependent on the temperature of the surrounding aqueous solution [27,84]. This noticeable variation between the CTE of the BFRP bars and that of concrete allows the BFRP bar to expand at a much larger rate than concrete which causes the BFRP bar to exhibit radial bursting forces on the surrounding concrete, when these induced stresses are greater than the tensile strength of the used concrete, cracks start to form which tend to create voids along the embedment length that reduce the contact between the bar and surrounding concrete. Moreover, the immersion of the specimens in saline solution allow water molecules and chloride ions (Cl^-) to fill the formed voids and diffuse into the polymeric resin weakening the interfacial bond between the fibers and surrounding polymeric matrix and altering the mechanical properties of the bar as well, thus causing a higher rate of degradation in the bond at the interface between the BFRP bar and surrounding concrete. On the other hand, a counteracting effect results from the

increase in the compressive strength of concrete due to immersion which improves the bond strength of the BFRP bar with surrounding concrete [33,63,64].

Figures 45 and 46 show the column charts that represent the trend of the average bond strengths and bond retentions with exposure duration in saline environment under 35 ºC and 60 ºC which are the adopted temperatures in this study. It is worth to note that only one type of bar is used in this study, therefore the bond strength rate of degradation is mainly dependent on the type of concrete and its resistance to the surrounding environment and its ability to restrict the diffusion of aggressive solutions. Therefore, the detrimental influencing factors on the bond strength of HWBFRP bars with concrete are described as follows: (1) the effect of the significant variation in the CTE of concrete and that of the BFRP bars which was previously explained; (2) the effect of high temperature which accelerates the chloride diffusion in concrete [85] and chlorides rich moisture uptake by the composite bar; and (3) the reduction in the bonding between the added BMF to concrete due to the variation in CTE since bonding of the added fibers to concrete is what governs the performance of FRC. On the other hand, the counteracting effects that tend to increase the bond strength of the BFRP bars in concrete are: (1) the swelling of the bars induced by moisture absorption which tends to increase the bonding of the bars to concrete due to the increased friction and the additional confinement from surrounding concrete; (2) the increase in the compressive strength due to the increase in immersion periods and early stages of corrosion in case of steel FRC; and (3) the increase in the bonding of the macro fibers due to BMF swelling in case of basalt FRC and early stages of corrosion in case of SMF.

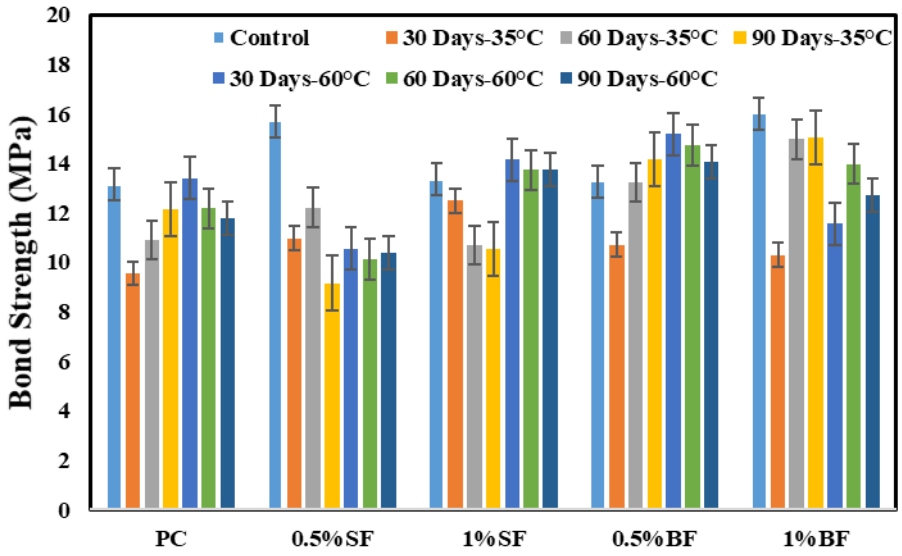

Figure 45:Effects of Exposure Time and Temperature on the Bond Strength.

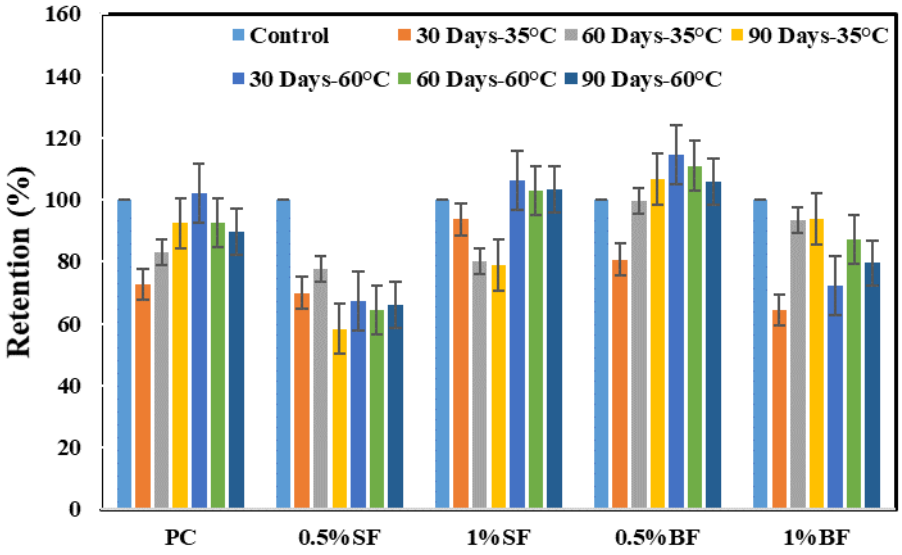

Figure 46:Effects of Exposure Time and Temperature on Bond Strength Retention.

4.3.1. Plain Concrete Specimens

For plain concrete specimens, as depicted in Figures 45 and 46, at 35 ^{o}C of immersion temperature in saline water, the bond strength results reveal an increasing trend with exposure duration whereas a decreasing trend was observed when increasing the immersion temperature to 60 ^{o}C. This is attributed to the lower temperature causing slower rate of moisture absorption, lower rates of expansions and contractions due to the variation in CTEs of the two materials causing a smaller number of cracks along the embedment length which limits the access of water molecules and chloride ions to diffuse in to the polymeric resin of the BFRP bar and causes less reductions in the contact between the bar and surrounding concrete. Moreover, the lower temperature slows down the rate of chloride diffusion in concrete. Therefore, this causes a slower rate of induced BFRP bar swelling and bond degradation. Another important factor that led to the increase in the bond strength with exposure duration is the increase in the compressive strength with the increased immersion. This indicates that along the exposure periods, the increasing rate of moisture induced bar swelling and the increase in compressive strength seem to have counteracted the effects of the slow rates of water molecules and chloride ions diffusion in the polymeric resin along the bonded length which led to the increasing trend in the bond strength with exposure time at 35 ^{o}C. Whereas at 60 ^{o}C, the higher rate of moisture induced bar swelling seemed to dominate the other effects and led to a dramatic increase compared to the control specimens at the early stages of exposure followed by a decrease in bond strength along the exposure time. The reductions in the bond strength of BFRP bars in plain concrete compared to control specimens at 35 ^{o}C and 60 ^{o}C are 8 and 10% respectively. Additionally, it can be observed that at 60 ^{o}C, the retention in the bond strength compared to the 30 days immersed specimens is 12% indicating the severity of the environmental conditioning

of seawater at high temperatures. It is worth to note that the increasing trend of the bond strength at the lower temperature along the exposure period of 90 days was not sufficient to retain the bond strength of the control specimens stored for 90 days in ideal environmental conditioning, indicating the severity of moisture and chloride ions existence in degrading the bond strength. The minimum bond strength of BFRP bars embedded in plain concrete after 90 days of exposure was found to be 11.77 MPa at 60 ^{o}C which meets the minimum requirement of the specifications provided by the CSA S807[70] (>8 MPa) and ACI 440.6 M [71] (>9.6 MPa) which reveals the suitability of using the adopted bars in plain concrete at marine structures.

4.3.2. Steel Fiber Reinforced Concrete Specimens

Regarding the bond durability performance of HWBFRP bars embedded in steel FRC in seawater under the effect of elevated temperatures, the effect of high temperature tended to improve the durability of the BFRP bars with steel FRC. Moreover, the increase in the steel fiber content significantly enhanced the bond strength of the conditioned specimens which contradicts with the observation for the unconditioned specimens regarding the effect of fiber volume fraction on the bond strength. That being said, BFRP bars embedded in 0.5% steel FRC exhibited bond strength reductions of 34% and 42% at 35 ^{o}C and 60 ^{o}C respectively, compared to their (unconditioned) control specimens which showed a significant improvement in the bond strength compared to plain concrete control under room temperature of (23 ^{o}C) and dry conditions revealing the suitability of using HWBFRP bars embedded in steel FRC with low content of steel fibers in offshore structures rather than in marine structures [86]. Whereas the performance of steel FRC with relatively high steel fibers content resulted in a significant enhancement in the bond durability when compared to

FRC with low steel fibers content. The BFRP bars embedded in steel FRC with 1% steel fiber volume fraction exhibited a reduction of 21% at 35 ^{o}C and an improvement of 3% at 60 ^{o}C when compared to the control specimens, which indicates more suitability of using BFRP embedded in steel FRC with 1% steel fiber volume fraction in marine structures than 0.5% steel fiber volume fraction. Possible reasons for the obtained results are as follows: (1) the permeability and chloride diffusivity tend to significantly increase with the addition of steel fibers when compared to plain concrete due to the high conductivity of steel fibers [87], allowing more water molecules and chloride ions to diffuse in the polymeric resin at lower temperatures, hence accelerating the bond degradation rate when compared to plain concrete; (2) The high temperature tends to accelerate the corrosion of steel fibers [88], and due to the early stages of corrosion, the compressive strength of steel FRC and bonding of steel fiber with surrounding concrete increase significantly [86,89-91], which in turn improves bond strength of BFRP bar with concrete due to the additional confinement and more effective crack bridging; (3) with increased time of immersion in aqueous solution, the increase in the content of steel fibers tend to significantly decrease the permeability of concrete due to the reduction of concrete shrinkage and the continuity destruction of porous channels by the fiber mechanism [92], limiting the access of water molecules and chloride ions to diffuse further in the polymeric resin; (4) and no noticeable changes were observed in the compressive strength of steel FRC at 35 ^{o}C after 30 days of exposure unlike the behavior of plain concrete and basalt FRC specimens. That being said, corrosion pits at the concrete surface were observed for steel FRC after 30 days of immersion at 60 ^{o}C indicating the early initiation of corrosion and more being obvious at the high content of steel fibers as shown in Figure 47, indicating the destruction of the oxide layer surrounding the steel fibers due to concrete carbonation

which led to significant improvement in compressive strength, less chloride ions diffusion, less water molecules uptake by the resin, and high bond between the steel fiber-concrete interface which led to the significant improvement in the bond strength over specimens exposed at lower temperature of 35 ^{o}C. The BFRP bars embedded in steel FRC at 60 ^{o}C experienced no reduction in the bond strength after 60 days of exposure regardless of the steel fiber volume fraction. Whereas at 35 ^{o}C, the different volume fractions exhibited different trends with a clear decreasing trend for 1 % steel fiber with a slight reduction after 60 days of exposure, unlike 0.5% steel fiber which caused the bond of the BFRP to increase until 60 days followed by a significant reduction afterward. This is attributed to the rate of chloride diffusion and the effect of increasing the fiber content with long periods of immersion on decreasing or limiting the concrete permeability. Additionally, it is worth to note that there was a noticeable increase in the bond strength after 30 days of immersion for 0.5% steel FRC conditioned at 35 ^{o}C. The minimum bond strength of BFRP bars embedded in 0.5% steel FRC after 90 days of exposure was found to be 9.16 MPa at 35 ^{o}C which meets the minimum requirement of the specifications provided by the CSA S807[70] (>8 MPa) but does not meet the requirement of the ACI 440.6 M [71] (>9.6 MPa) which reveals the unsuitability of using the adopted bars in steel FRC with steel fiber volume fraction of 0.5 % in marine structures if the ACI specifications are to be adopted.

Figure 47: Corrosion of Steel Fibers in Steel FRC.

4.3.4. Basal Fiber Reinforced Concrete

For HWBFRP bars embedded in basalt macro fiber reinforced concrete (BMFRC), at exposure of 35 ^{o}C in saline solution, it can be clearly seen that the bond strength at both volume fractions (0.5% and 1%) tend to increase with exposure time. Consequently, it can be observed that the increase in bond strength of BFRP bars at 1% BMF volume fraction was not sufficient to retain the bond strength of their counterpart unconditioned control specimens which showed the highest improvement in bond strength when compared to the control specimens of plain concrete. The reduction in the bond strength of 1% BMF at 35 ^{o}C after 90 days of exposure to saline water is 6% whereas the bond strength of BFRP bars in 0.5% BMF retained a higher value compared to their counterpart control specimens with an improvement of 7%. This indicates that the increased content of BMF in marine structures subjected to a temperature of 35 ^{o}C is beneficial in terms of durability due to the less reductions experienced compared to plain concrete, however it is not cost effective, since comparable bond strength values can be achieved with less BMF content particularly at 0.5% volume fraction. It is worth

that the BMF are a small prototype of the BFRP bars used. Therefore, possible explanations of the obtained trends at 35 ^{o}C are similar to those previously explained for plain concrete in addition to the following: (1) since the BMF are a small scale of the BFRP bars used, therefore the swelling of the BMF due to moisture absorption improved the bond between the BMF-concrete interface leading to an improved performance and confinement provided by BMF reinforced concrete on the BFRP bars; (2) the noticeable increase in the compressive strength due to the increased immersion; (3) the slower rate of chloride diffusion due to the addition of basalt fibers in the concrete mix [91] which tend to limit the access of aggressive solution to diffuse further in the polymeric resin along the embedment length. Moreover, at 60 ^{o}C, the low BMF content of 0.5% volume fraction revealed the optimum bond durability performance of BFRP bars among all fiber types and volume fractions used in this study retaining 106% of its counterpart control specimens with a reduction of 8% compared to the 30 days exposed specimens. It can be noticed that the increase in the content of basalt BMF indicates the high susceptibility of 1% basalt FRC to high temperatures which is attributed to the difference in the CTE of the BMF and surrounding concrete which could have possessed more voids which led to higher moisture and chloride diffusion into concrete and therefore more water molecules and chloride ions diffusion into the polymeric resin of the BFRP bar weakening the bond between the BFRP bars and surrounding concrete. Consequently, the increased amount of BMF in concrete led to a dramatic reduction in the bond strength after 30 days of immersion in saline water at 60 ^{o}C after that the BMF and BFRP bar swellings led to an improved bond with surrounding concrete leading an increase in the bond strength at 60 days followed by a significant reduction in the bond strength at 90 days to due to the high rate of degradation accelerated by the high temperature. The BFRP bars embedded in 1%

basalt FRC experience a reduction of 22% after 90 days of exposure at 60 ^{o}C indicating the severity of high temperature immersion with the presence of high BMF content in the concrete matrix. It is worthy to mention that the bond strength of BFRP bars embedded in 1 % BMFRC was lower than those embedded in 0.5% BMFRC along all exposure periods at 60 ^{o}C suggesting that low contents of basalt macro fibers are more suitable in marine structures. The bond strength of BFRP bars embedded in 1% BMFRC after 90 days of exposure was found to be 12.73 MPa at 60 ^{o}C which meets the minimum requirement of the specifications provided by the CSA S807[67] (>8 MPa) and ACI 440.6 M [68] (>9.6 MPa) which reveals the suitability of using the adopted bars in BMF reinforced concrete at volume fraction of 1% in marine structures.

4.3.5. Specimens Condition before and after Immersion

Figure 48 shows a comparison of the specimens before and after conditioning. All unconditioned specimens share similar grayish color, whereas after conditioning each type of concrete revealed a different outer surface color. For example: plain concrete specimens possessed a whitish color due to the diffusivity of NaCl in the concrete matrix. Consequently, basalt FRC specimens indicated a blackish outer surface color similar to the color of the basalt macro fibers used with less signs of NaCl presence compared to plain concrete. Finally, steel FRC specimens revealed a brownish color on the outer surface due to the corrosion of the fibers near the surface.

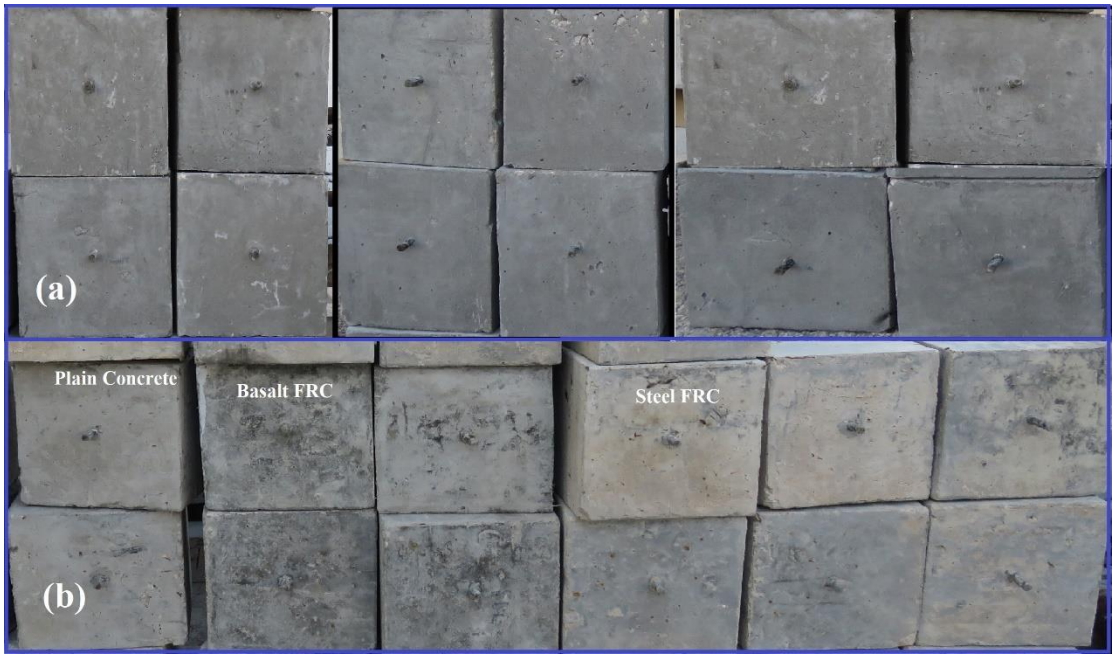

Figure 48: Pullout Specimens (a) before and (b) after conditioning.

4.4. Adhesion Stress:

Adhesion is a bond component that account for the bond of FRP bars with surrounding concrete in the initial stages of loading during the pullout test. In this study, the adhesion stress was determined as the value of stress at the first non-zero free end slippage reading obtained from the bond-slip curve. Figure 49 compares the average values of the adhesion stress at both temperatures along with exposure time. For unconditioned specimens, it can be observed that the addition of fibers regardless of the type caused a reduction in the adhesion stress and that the fiber content that caused less reduction in the adhesion stress are the optimum amounts of discrete fibers that showed the highest durability performance (1% volume fraction for steel fibers and 0.5% volume fraction for basalt fiber). In general, compared to the control specimens, the adhesion stress of BFRP bars at 60 ^{o}C seems to increase compared to 30 days conditioned specimens with immersion except for the bars embedded in 0.5% steel fiber, this might be attributed to the higher access of aggressive solutions to the

polymeric resin of the BFRP along the embedment length. Consequently, at 35 ^{o}C, the adhesion stress seems to increase for FRP bars embedded in basalt fibers regardless the volume fractions whereas, the adhesion seems to decrease for plain concrete and 1% steel fiber with immersion time. The increase and decrease in the adhesion stresses with immersion time are not of a particular trend due to the random deterioration of the specimens during immersion and the fact that all specimens had to be prestressed with an average of 0.1 MPa to avoid any measurement of the concrete relative movement to the loading plate by the top and bottom LVDTs which might have also interfered in the discrepancies of the obtained results. It is important to note that adhesion stress mainly depend on the surface treatment, the lack of sand coating in the bars used resulted in a low adhesion stress [94].

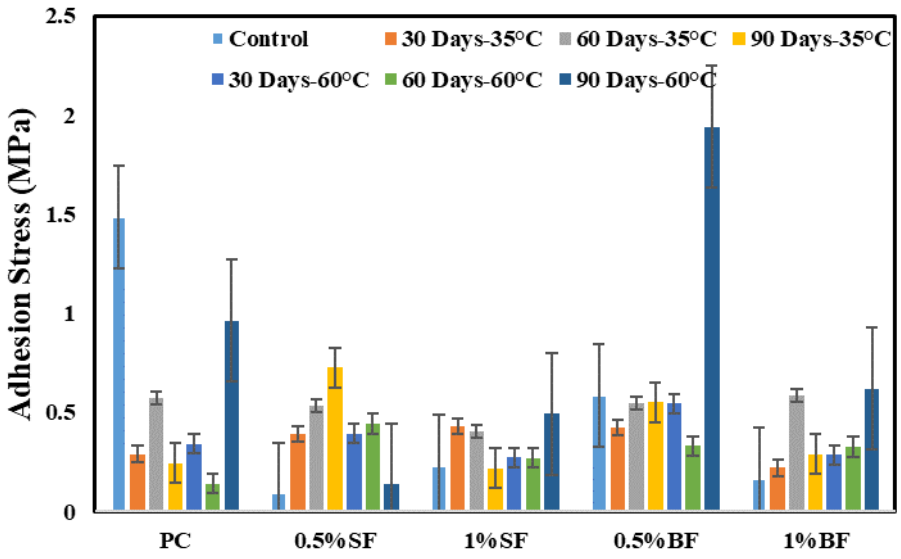

Figure 49:Effects of Exposure Time and Temperature on the Adhesion Stress.

4.5. Residual Bond Strength:

The residual bond strength, or post-peak strength, describes the bond behavior of the FRP bars after reaching the ultimate bond stress. The residual strength gives an indication about the resistance of bars to the applied loads which results in the gradual

drop in the bond stress along the descending branch of the bond slip curve. The residual stress was obtained at a large deformation of 12 mm on the loaded end slippage similar to the method used by Kim et al. [57] in obtaining the residual bond strength. Figure 50 shows the average residual bond strength obtained for all the specimens used in this study. The residual strength shows a similar trend to the bond strength with more obvious reduction with exposure time for 1% steel FRC. The only exception is 1% basalt FRC which shows a reduction at 60 days for specimens exposed to 60 ^{o}C unlike the bond strength trend where it showed an increase at 60 days, this can be explained by the failure modes of rebar fracturing for two of the three conditioned identical specimens which resulted in the loss of the residual strength. Consequently, it can be indicated that regardless the temperature, the residual strength shows a reduction after 90 days of exposure time compared to control specimens except for 0.5% basalt FRC at 35 ^{o}C which indicates the high post peak toughness provided by the addition of this optimum basalt fiber volume fraction. Moreover, Figure 51 shows the trend for the average bond strength index which is obtained by dividing the residual bond strength of each specimen by its ultimate bond strength as proposed by [57]. The bond strength index of 0.5% steel FRC seems to increase with exposure time at 35 ^{o}C. This is attributed to the huge reductions in the bond strength experienced by the BFRP bars embedded in 0.5% steel FRC at 35 ^{o}C. The results also indicate that the rate of degradation in the residual bond strengths is faster than that of the bond strength, the only exception is the 0.5 % steel FRC which indicates the high post peak toughness provided with the addition of steel fibers to the concrete mix. It is worth to note that the effect of immersion seems to be the predominant factor that controls the degradation rate of the residual strength rather than the temperature. The only exception is 1% basalt FRC which shows a higher reduction in the bond strength index with exposure time

which indicates the high susceptibility of residual bond strength of BFRP bars to high temperatures when high content of basalt BMF is added to the concrete mix. Another observation that is worth to note is that most of the plain concrete specimens at 90 days of immersion tend to show slip hardening where the bond strength drops after the ultimate bond stress then remains constant for large amount of slippage unlike control plain concrete specimens which showed a continuous reduction in the bond strength. This is attributed to the more pronounced delamination of the polymeric resin caused by immersion which created more polymeric residues in the embedment area that resulted in a higher friction with the surrounding concrete and led to the continuous resistance. Whereas, for BFRP bars embedded in FRC, this behavior was pronounced even for the control specimens indicating the effect of the addition of fibers in changing the bonding failure mechanism from partial debonding between the subsequent layers of the composite bar to more severe delamination or even complete peeling of resin.

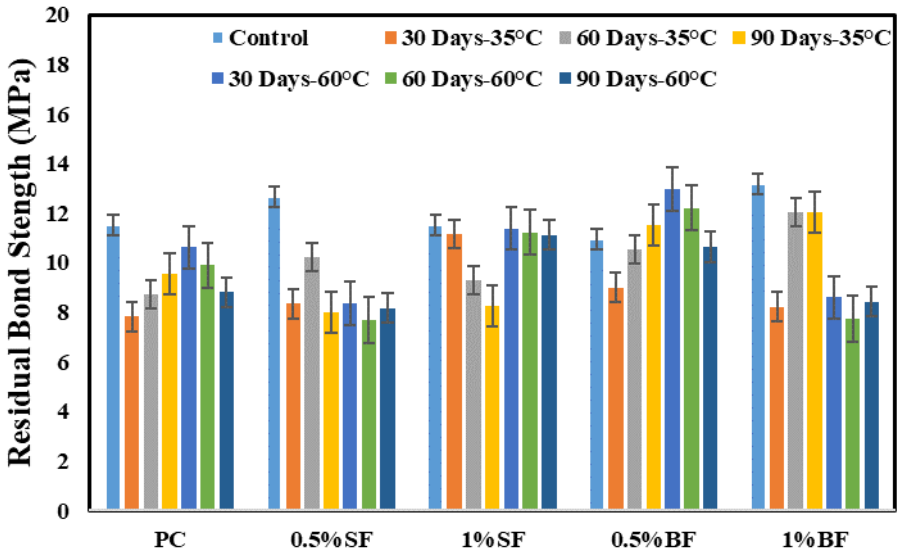

Figure 50:Effects of Exposure Time and Temperature on the Residual Bond Strength.

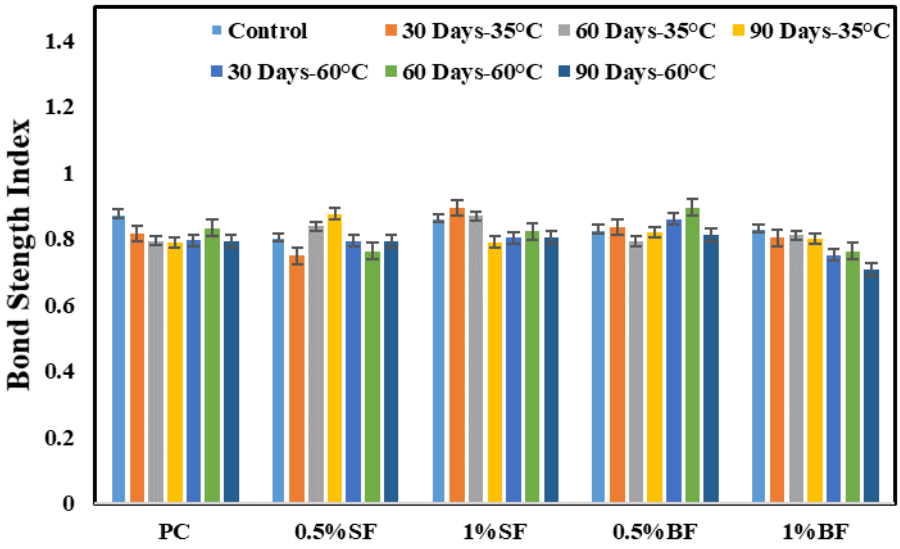

Figure 51:Effects of Exposure Time and Temperature on the Bond Strength Index.

CHAPTER FIVE: ANALYTICAL MODELLING OF BOND-SLIP BEHAVIOR.

In this chapter, analytical modelling for the bond-slip behavior of the Helically wrapped BFRP bars using two of the most successful analytical models for representing the ascending branch in the bond-slip curves of the actual experimental data. Numerous models have been formulated to represent the bond-slip behavior of steel reinforcement in concrete. Out of these models, the BPE model proposed by Eligehausen et al.[95] was found to be reliable in representing the ascending branch of the bond slip curve of FRP reinforcements. Furthermore, the CMR model proposed by Consenza et al.[49], was developed for a better representation of the ascending branch of the actual experimental data for FRP reinforcements. up to the author's knowledge, both the BPE and the CMR models have never been applied on modelling the bond behavior of the ascending branch for helically wrapped BFRP bars with no sand coating, therefore, for the serviceability state level, both model were used in this study to assess their reliability on simulating the experimental ascending branches of bond-slip curves for HWBFRP bars embedded in normal strength plain and fiber reinforced concrete taking into consideration the effect of type of fiber, fiber volume fraction, exposure duration, and exposure temperature.

5.1. Analytical Modelling for Bond Behavior of BFRP bars Using BPE and CMR Models

The BPE model was originally developed for describing the bond behavior of steel reinforcement to concrete. Since almost all structural problems are concerned with the serviceability state limits, therefore only the ascending branch of the bond-slip curve is modeled with the BPE model in this study. The BPE model defines the ascending branch that describes the bond behavior up to the ultimate stress in the following equation :

$$\frac{\tau}{\tau_b} = (\frac{s}{s_b})^{\alpha} \; for \; 0 \leq s \leq s_b, \qquad (8)$$

Where τ_b is the ultimate bond strength obtained from the experimental bond-slip curve, S_b is the slippage corresponding to the ultimate bond stress, and α is a parameter that should be less than 1 for it to be physically meaningful and is either obtained by curve fitting of the experimental data using the least square residuals or using the following equations:

$$A_{r1} = \int_0^{S_1} \tau(s).ds = \int_0^{S_1} \tau_1.\left(\frac{S}{S_1}\right)^{\alpha}.ds = \frac{\tau_1 . S_1}{1+\alpha} \qquad (9)$$

Where A_{r1} is the area underneath the ascending branch of the bond slip curve, τ_1 and S_1 are the ultimate bond stress and its corresponding slippage. Therefore, solving for α yields the following equation:

$$\alpha = \frac{\tau_m . S_m}{A_{r1}} - 1 \qquad (10)$$

It should be noted that the lower the value of α, the higher the stiffness and ultimate toughness (Area underneath the curve) In this study, all the 105 pullout specimens were modeled using the BPE model and average values of α were obtained for the free end slippage to calibrate the values taking into account the surface treatment, exposure duration, conditioning environment of seawater, FRC type, fiber volume fraction, and exposure temperature. It was noticed that for the BFRP bars used in this study, the value of α obtained using equations 9 and 10, seemed to be overestimating the actual experimental values for example the average value of α obtained for unconditioned specimens using the equations is 0.371 whereas the value of α obtained by curve fitting is 0.425, therefore, in order to be conservative and represent safe design values of α that represent the actual experimental data of this study, the method of curve fitting is adopted. The average values of α are tabulated in Table 8 along with the average design values for the bond strength and corresponding

free end slippage in case of absence of experimental data. The proposed values of α for unconditioned plain concrete, 0.5% basalt, 1% basalt, 0.5% steel, and 1% steel FRC are: 0.43, 0.49, 0.48, 0.41, and 0.46 respectively which are based on the average values of α obtained for the three identical specimens. The proposed values by Yan et al. [65] for α in the case of sand coated GFRP bars with helically wrapped surface treatment are 0.41, 0.40, and 0.40 for unconditioned plain concrete, 0.5%, and 1% steel FRC respectively. These differences are attributed to the type of bar used, the lack of sand coating on the bars used in this study, the differences in compressive strength in both studies, and the fact that proposed values of this study are based on the average values obtained in the three identical specimens whereas Yan et al. [65] proposed values based on one of the three identical specimens that showed the highest correlation with the analytical model.

On the other hand, the CMR model was proposed by Consenza et al.[49] for better representation of the ascending branch and is expressed in the form of:

$$\frac{\tau}{\tau_b} = (1 - \exp(-\frac{s}{s_r}))^{\beta} \qquad (11)$$

Where S_r and β are parameter obtained from curve fitting of experimental data, and τ_b is the maximum bond stress. This model was used in this study to model the 105 pullout specimens and average recommended design values of s_r and β are shown in Table 8 along with the maximum stress and corresponding slippage in case the experimental data are lacking. For unconditioned specimens, the proposed values of S_r and β are: 2.22 and 0.96 for plain concrete, 2.02 and 1.2 for 0.5 % steel FRC, 1.6 and 1.5 for 1% steel FRC, 1.61 and 1.15 for 0.5% basalt FRC, and 1.69 and 1.61 for 1% basalt FRC specimens. The proposed values of s_r and β by Yan et al. [65] are 0.4 and 1.16 for plain concrete, 0.36 and 1.04 for 0.5% steel FRC, and 0.55 and 0.63 for 1% steel FRC specimens. These differences observed between the values of this study and that of Yan

et al.[65] are attributed to the same reasons previously mentioned. It can be observed that in case of FRC the values of s_r and β tend to be closer to each other whereas for plain concrete, the value of s_r tend to be significantly higher than that of β which indicates the different behaviors exhibited by the BFRP bars when embedded in different types of concrete. Figures 52, 53, and 54 show representative modelling of the unconditioned (control), conditioned for 90 days at 35 ^{o}C, and conditioned for 90 days at 60 ^{o}C pullout specimens. It can be observed that the CMR model shows a better correlation with the experimental data than the BPE model. This is attributed to the fact that the BPE model was originally developed for steel reinforcement which possess no slippage up to high load levels close to the peak load indicating the high adhesion of steel reinforcements to concrete**.** Unlike conventional steel reinforcements, the used BFRP bars in this study consisting of helical wraps tend to exhibit low adhesion stresses which is attributed to the lack of sand coating, relatively low compressive strength, and the addition of discrete macro fibers to concrete which tend to reduce the chemical adhesion of the bar to surrounding concrete. This resulted in conservative values of the bond strength when the curve is approaching the ultimate stress and in an over estimated bond strength values at the initial loading stages of the ascending branch. In fact, the BPE model shows good correlation with pullout specimens that tend to exhibit high adhesion stresses such as plain concrete specimens. Moreover, the unique feature of the CMR model in exhibiting infinite slope in the initial stages of the ascending branch and the presence of the exponential term allows it to realistically model relatively low adhesion stresses and high ultimate bond stresses which is the case of the BFRP bars used in this study. Whereas, the BPE model with its feature to possess infinite slope in the initial stages of loading, however, it lacks the ability to effectively model bond behavior of FRP bars that exhibit low adhesion stresses and relatively high ultimate

stresses.

Table 8: Proposed Design Values for BPE and CMR Models' Parameters.

	BPE	CMR		Sm	τ_m
	α	Sr	β	(mm)	(MPa)
PC-Control	0.4254	2.218	0.9563	7.1	13.14
0.5%SF-Control	0.486	2.0154	1.1982	7.85	15.7
1%SF-Control	0.4802	1.6042	1.5012	6.87	13.34
0.5%BF-Control	0.4142	1.6096	1.1502	6.52	13.27
1%BF-Control	0.4588	1.6847	1.6056	7.9	16.01
30 Days Conditioned Specimens at 35 ºC					
PO-PC-30-35	0.5345	1.5824	1.4382	6.17	9.547
PO-0.5%SF-30-35	0.4653	1.4578	1.2512	5.6	10.97
PO-1%SF-30-35	0.4493	1.4866	1.5393	6.92	12.49
PO-0.5%BF-30-35	0.5403	1.467	1.4481	5.32	10.7
PO-1%BF-30-35	0.4754	1.563	1.6597	6.93	10.29
30 Days Conditioned Specimens at 60 ºC					
PO-PC-30-60	0.4933	1.5991	1.4536	6.37	13.4
PO-0.5%SF-30-60	0.4996	1.4073	1.3176	5.24	10.54
PO-1%SF-30-60	0.4753	1.4133	1.5789	6.31	14.15
PO-0.5%BF-30-60	0.4685	1.4862	1.3524	5.99	15.18
PO-1%BF-30-60	0.492	1.4406	1.4887	5.87	11.55
60 Days Conditioned Specimens at 35 ºC					
PO-PC-60-35	0.4481	1.6977	0.9702	5.56	10.9
PO-0.5%SF-60-35	0.4342	1.8365	1.2565	7.69	12.21
PO-1%SF-60-35	0.4002	1.5664	1.3017	7.34	10.69
PO-0.5%BF-60-35	0.4322	1.6153	1.0421	5.94	13.22
PO-1%BF-60-35	0.4975	1.7653	1.1623	5.98	14.97
60 Days Conditioned Specimens at 60 ºC					
PO-PC-60-60	0.4834	1.4548	1.3355	5.51	12.17
PO-0.5%SF-60-60	0.4361	1.6341	1.0395	5.83	10.12
PO-1%SF-60-60	0.5407	1.254	1.6434	5.14	13.72
PO-0.5%BF-60-60	0.5575	1.6925	1.6917	6.88	14.72
PO-1%BF-60-60	0.5416	1.6637	1.6508	6.7	13.97
90 Days Conditioned Specimens at 35 ºC					
PO-PC-90-35	0.5219	1.346	1.6498	5.44	12.14
PO-0.5%SF-90-35	0.4264	1.9568	1.0697	6.92	9.157
PO-1%SF-90-35	0.5755	1.3115	1.7301	4.84	10.53
PO-0.5%BF-90-35	0.4301	1.7543	1.2339	7.35	14.16
PO-1%BF-90-35	0.4335	1.8794	1.2282	7.21	15.03
60 Days Conditioned Specimens at 60 ºC					
PO-PC-90-60	0.4272	1.8311	0.9619	6.23	11.77
PO-0.5%SF-90-60	0.5342	1.8672	1.4496	6.84	10.37
PO-1%SF-90-60	0.5259	1.7398	1.3143	4.29	13.76
PO-0.5%BF-90-60	0.2636	2.0133	0.5696	5.05	14.03
PO-1%BF-90-60	0.4732	0.9367	1.3416	3.79	12.73

**τ_m and S_m are mean design values for bond strength and free end slippage

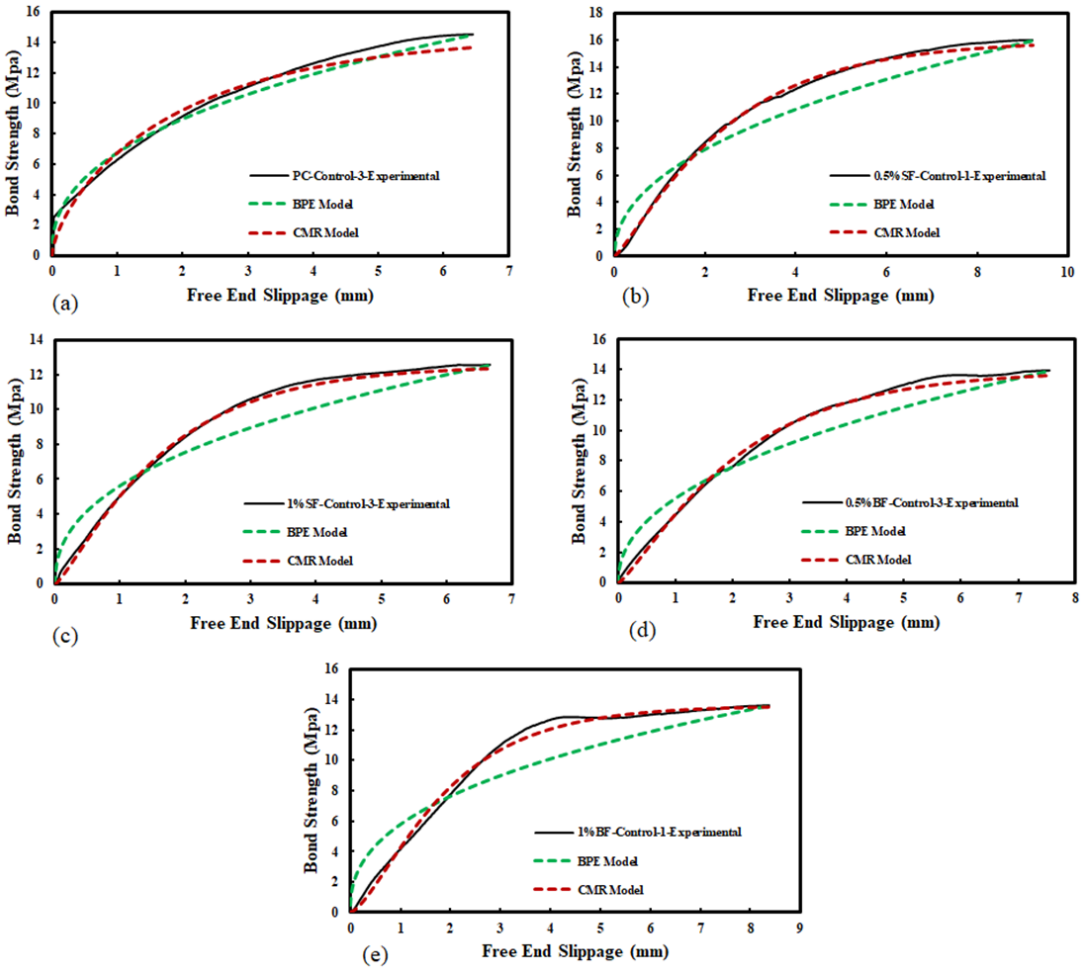

Figure 52: Experimental Data Vs. BPE and CMR Models for Control Specimens of (a) Plain Concrete; (b) 0.5% Steel FRC; (c) 1% Steel FRC; (d) 0.5% Basalt FRC; (e) 1% Basalt FRC.

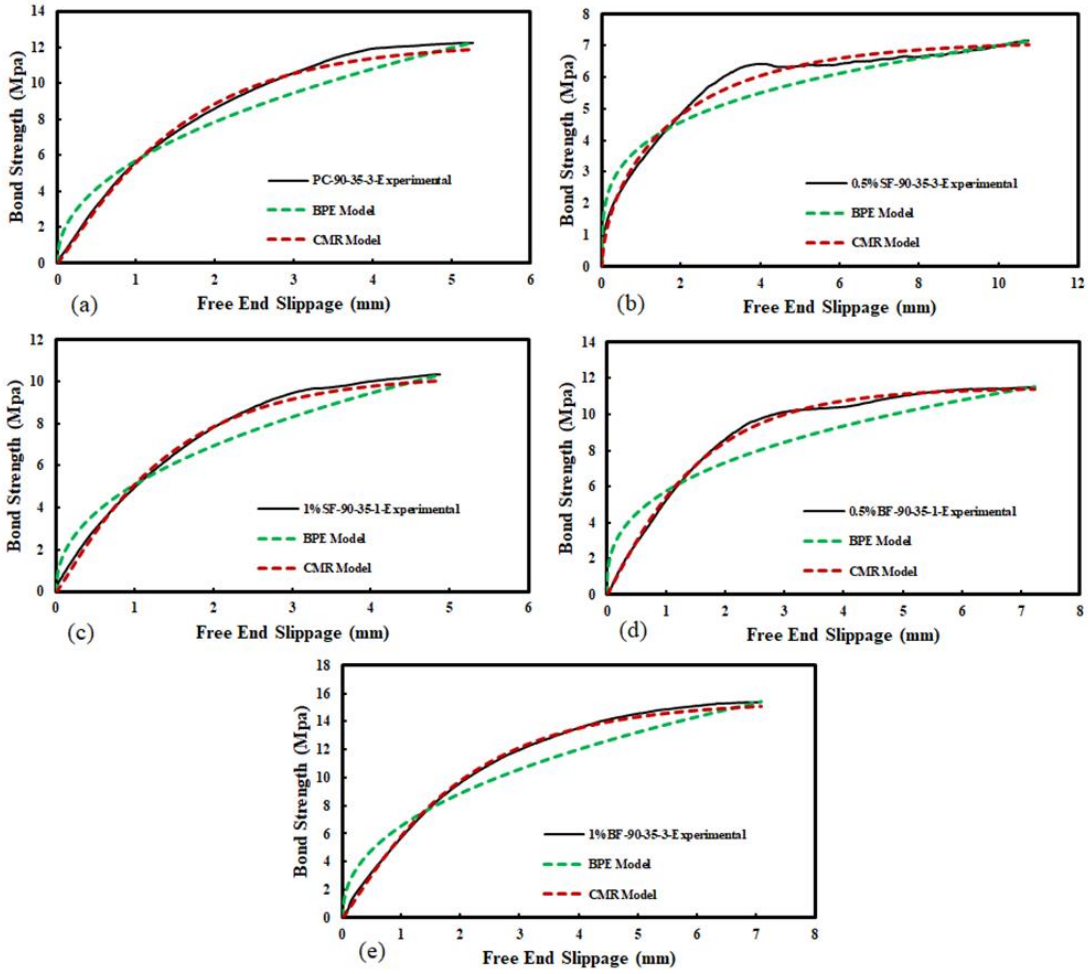

Figure 53: Experimental Data Vs. BPE and CMR Models for Conditioned Specimens to Saline Solution after 90 Days at 35 ºC of (a) Plain Concrete; (b) 0.5% Steel FRC; (c) 1% Steel FRC; (d) 0.5% Basalt FRC; (e) 1% Basalt FRC.

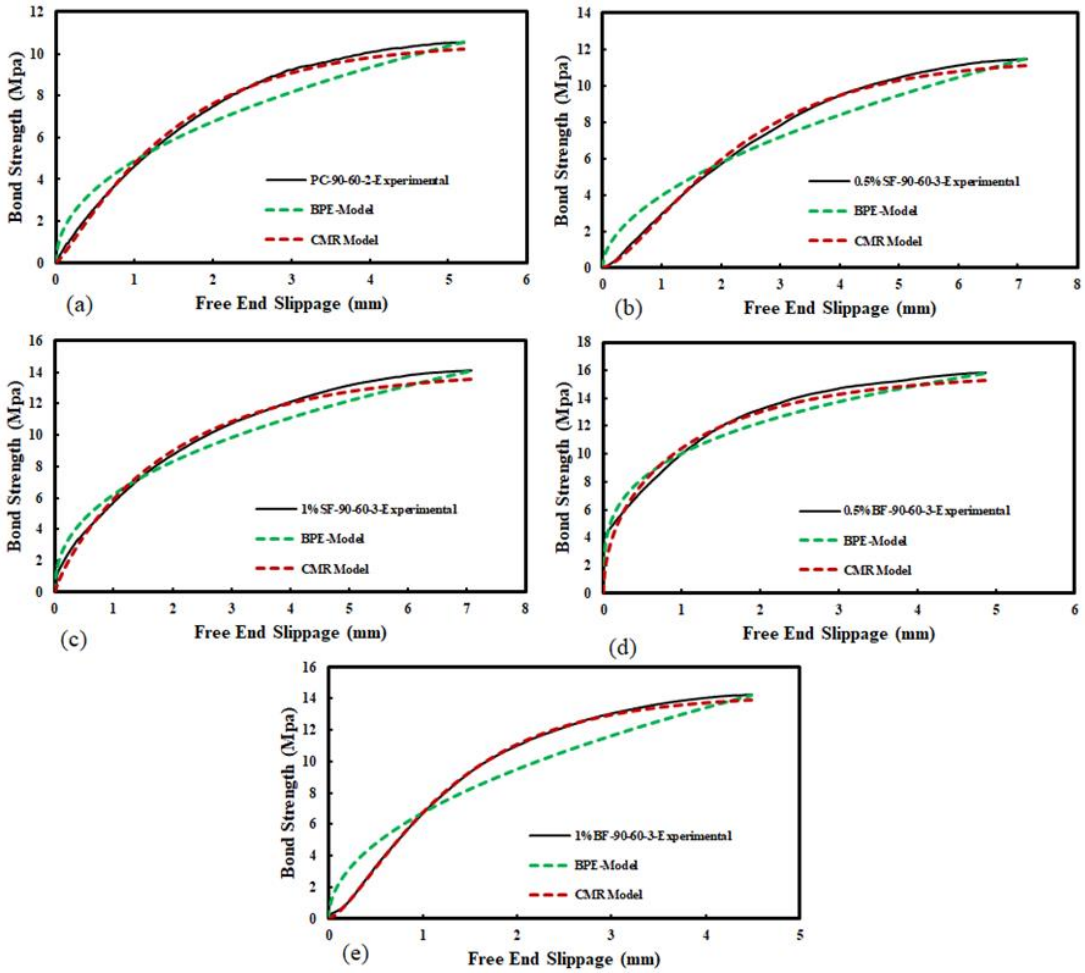

Figure 54: Experimental Data Vs. BPE and CMR Models for Conditioned Specimens to Saline Solution after 90 Days at 60 ºC of (a) Plain Concrete; (b) 0.5% Steel FRC; (c) 1% Steel FRC; (d) 0.5% Basalt FRC; (e) 1% Basalt FRC.

CHAPTER SIX: SERVICE LIFE PREDICTION

In this chapter, the service life predications on the long-term bond strength retentions of the HWBFRP bars were performed based on the method mentioned in the fib Bulletin 40 [96]. This method takes into consideration a factor of safety for the bond strength deterioration with time. The bond strength of HWBFRP bars must be reduced by $\eta_{env,b}$ obtained from the following equations:

$$\eta_{env,b} = 1/[(100-R_{10})/100]^{n} \quad (12)$$

$$n = n_{mo} + n_T + n_{SL} \quad (13)$$

where n_{mo}, n_T, n_{SL} are parameters that take into consideration the effects of humidity condition, conditioning temperature, and required service life; R_{10} is the standard reduction value of the bond strength in percent per decade obtained from the slope of the individual degradation line fitted in a double logarithmic scale. The points of the degradation line are the bond strength retentions at 30, 60, and 90 days. For this study, the service life predications are only performed on BFRP bars embedded in plain concrete, and in FRC at fiber volume fractions that showed the least reductions in the bond strength after 90 days of exposure which are 1% in the case of steel FRC and 0.5% in the case of basalt FRC. For this method to be valid, R-square of the fitted line in a double logarithmic scale must be greater than 0.8. Therefore, this method is only applicable on the degradation lines of the plain concrete and 0.5% basalt FRC specimens conditioned at 60 °C, whereas for steel FRC specimens, a modification in the method proposed by Serbesco [97] can be applied to take into account both conditioning temperatures. The service life adopted in this study is 50 years which leads to a value of n_{SL} equals to 2.7 according to [96] assuming moisture-saturated conditions. n_T equals to 1 at 35 °C according to [96] and to 2.5 at 60 °C in accordance to [97]. The increasing trends of the BFRP bars immersed at 35 °C for plain concrete and 0.5%

basalt FRC specimens are ignored in order not to overestimate the bond durability of the bars by assuming a negative R_{10} value because longer periods are required to evaluate the bond performance at 35 °C for these types of specimens if the modification in method [97] is to be used. Whereas, for steel FRC specimens, the retentions at both temperatures are considered in order to simulate the temperature changes during the year in the Arabian Gulf and not to over predict the bond durability performance of BFRP bars embedded in steel FRC by considering the temperature of 60 °C only, therefore method modification in [97] is used to predict the bond strength retention after 50 years of service life for BFRP bars embedded in steel FRC. As shown in Figure 55, for plain concrete specimens, the retention values at 30, 60, and 90 days are 102, 93, and 90% at 60 °C respectively leading to an R_{10} value of 11.6%. The bond strength retention for plain concrete specimens after 50 years of service life is predicted to be 48%. Consequently, as shown in Figure 56, for 0.5% basalt FRC specimens, the bond strength retentions at 30,60, and 90 days are 114,111, and 106% at 60 °C respectively. The predicted bond strength retention after 50 years of service life is 77% with an enhancement of 60% in the tolerance to extreme environmental conditioning over plain concrete. Figure 57 shows the predicted bond strength retentions at 35 °C and 60 °C for steel FRC specimens, the average slope of the two degradation lines can be adopted based on the method modification proposed by [97] to simulate their bond degradation assuming similar degradation rates, this yields an R_{10} value of 12.35% resulting in bond retentions of 80% and 26% at 35 and 60 °C after 50 years of service life, whereas if the method in the fib Bulliten 40[96] is used, the value of R_{10} is 2.8% resulting in a bond retention of 88% at 60 °C after 50 years of service life. These significant differences in the R_{10} values obtained by the two methods are attributed to the early stages of corrosion of the steel fibers which resulted in an increase in the bond of the steel fibers with the

surrounding concrete, noticeable increase in the compressive strength, and a reduction in the diffusion rates of moisture and chloride ions (Cl^-) in the polymeric resin. These effects are not taken into consideration in equation (12).

Table 9 summarizes the bond strength retentions in dry, moist, and moisture saturated environmental conditions obtained from equation 12 and mean annual temperatures (MATs) for a service life of 50 years. The bond strength retentions after 50 years varied from 56% to 86% in case of BFRP bars embedded in plain concrete. Whereas the bond strength retentions of BFRP bars embedded in 0.5% basalt FRC varied from 74% to 92% indicating an enhancement of 7% to 32 % compared to plain concrete after 50 years of service life. On the other hand, the bond strength retentions of BFRP bars embedded in 1% steel FRC showed a slight reduction in the bond durability that varied from 1% to 4% in cases of dry, moist, and moisture saturated conditions compared to plain concrete, indicating the more suitability of using BFRP bars embedded in steel FRC in offshore applications rather than in marine structures. Furthermore, more investigations are needed to validate the proposed model taking into consideration longer periods of exposure time, different fiber volume fractions suggested to be higher than 1% in case of steel FRC and slightly above or less than 0.5% in case of basalt FRC, different temperatures of exposure such as 30,50, and 70 °C , and higher concrete compressive strengths.

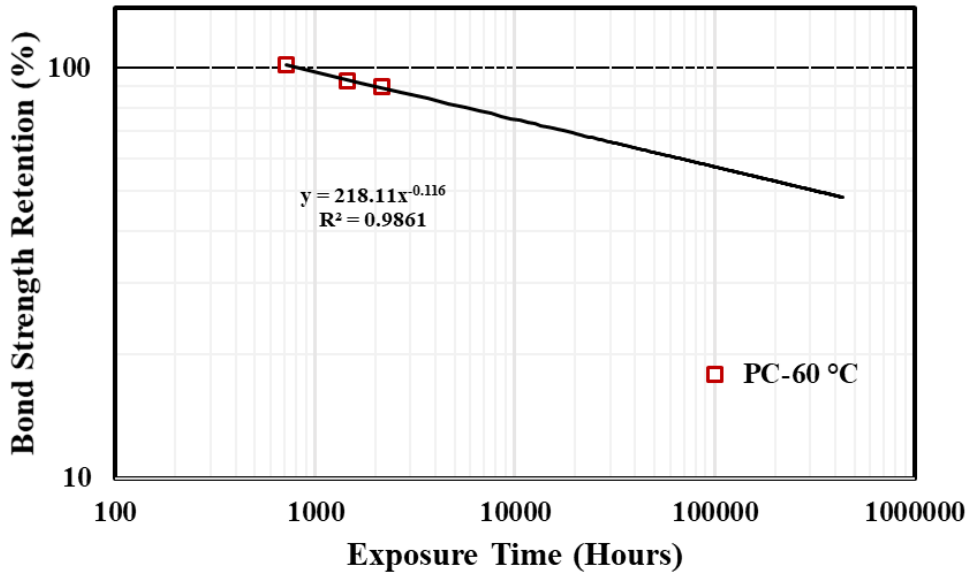

Figure 55: Bond Strength Retention Curve of HWBFRP Bars Embedded in Plain Concrete at 60 °C

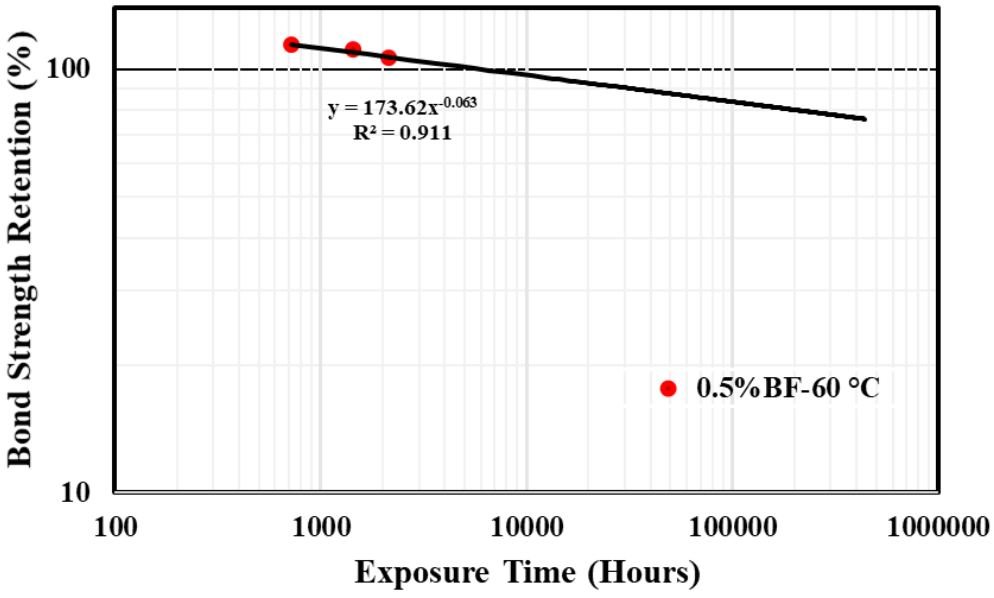

Figure 56:Bond Strength Retention Curve of HWBFRP Bars Embedded in 0.5% BMF Reinforced Concrete at 60 °C

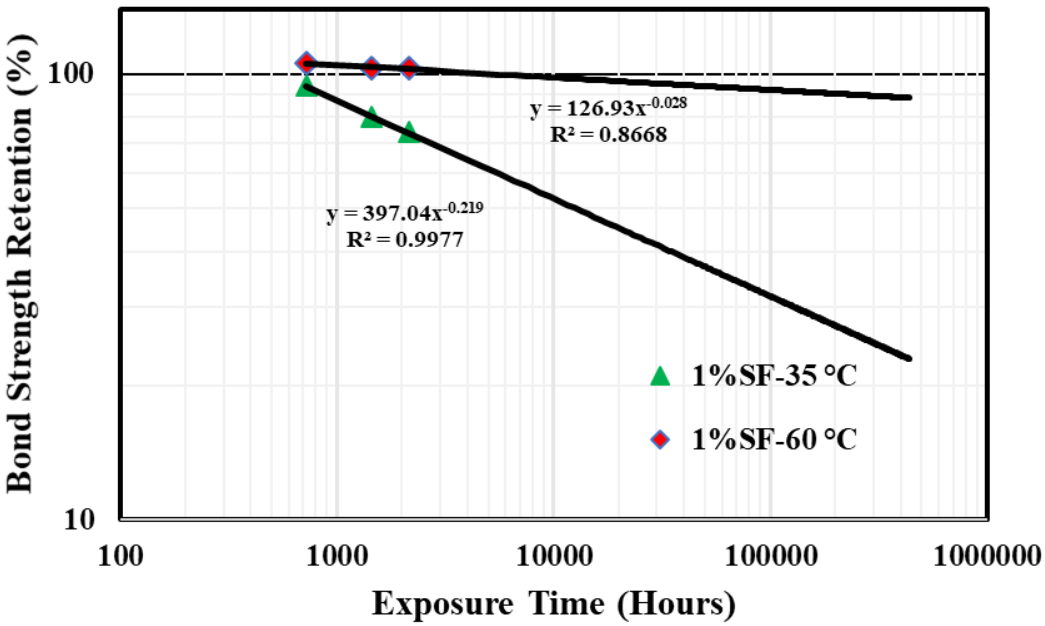

Figure 57: Bond Strength Retention Curve of HWBFRP Bars Embedded in 1% Steel FRC at 35°C and 60 °C.

Table 9 : Predicted Bond Strength Retention Values Based on Method [96] after 50 Years of Service Life.

					Plain Concrete		**Basalt FRC**		**Steel FRC**	
n_{SL}	n_{mo}	MAT (°C)	n_T	n	$\eta_{env,b}$	$1/\eta_{env,b}$ (%)	$\eta_{env,b}$	$1/\eta_{env,b}$ (%)	$\eta_{env,b}$	$1/\eta_{env,b}$ (%)
2.7 (50 years of service life)	-1 (Dry)	<5	-0.5	1.2	1.16	86	1.08	92	1.17	85
		(5-15)	0	1.7	1.23	81	1.12	90	1.25	80
		(15-25)	0.5	2.2	1.31	76	1.15	87	1.34	75
		(25-35)	1	2.7	1.4	72	1.19	84	1.43	70
	0 (Moist)	<5	-0.5	2.2	1.31	76	1.15	87	1.34	75
		(5-15)	0	2.7	1.4	72	1.19	84	1.43	70
		(15-25)	0.5	3.2	1.48	67	1.23	81	1.52	66
		(25-35)	1	3.7	1.58	63	1.27	79	1.63	61
	1 (Moisture Saturated)	<5	-0.5	3.2	1.48	67	1.23	81	1.52	66
		(5-15)	0	3.7	1.58	63	1.27	79	1.63	61
		(15-25)	0.5	4.2	1.68	60	1.31	76	1.74	57
		(25-35)	1	4.7	1.79	56	1.36	74	1.86	54

CHAPTER SEVEN: SCANNED ELECTRON MICROSCOPY (SEM) ANALYSIS

Scanning electron microscopy (SEM) was performed on the cross-section of the BFRP bars after the pullout test. The cross sections of the BFRP bars were of 1 cm in length and were obtained by cutting the bar at the embedment length of the BFRP bar in concrete. The obtained bar specimens were then polished and coated by a thin coating layer of gold. Three bar specimens were obtained and studied. The SEM analysis was conducted to observe the effect of saline environmental conditioning at elevated temperature on the bond degradation between the fibers and the surrounding polymeric resin. For that, one bar specimen was obtained from unconditioned plain concrete specimen and the other two specimens were obtained from plain concrete specimens subjected to 35 ^{o}C and 60 ^{o}C immersion temperatures after 90 days of exposure duration. The SEM analysis were focused on the part of the bar's cross-section close to the bar's edge to examine the bar's most pronounced degradation due to the surrounding environment.

Figure 58 shows the SEM images with different magnifications for the three specimens investigated in the SEM analysis of this study. For unconditioned specimen, the SEM images show partial delamination of the polymeric resin concentrated in a region of 130 to 286 μm from the edge of the cross-section towards its center as shown in Figure 58(a). Whereas, for the conditioned specimen at 35 ^{o}C, the affected region is much larger than that observed in the unconditioned specimen with an affected region of 1 to 1.2 mm from the edge of the cross-section toward its center as shown in Figure 58(b). Consequently, the effect of 60 ^{o}C immersion temperature clearly reveals the highest detrimental impact on the interlaminar shear between the fiber and surrounding polymeric matrix as depicted in Figure 58 (c) which shows an affected area greater than 1.3 mm with severe loose fibers. These findings support what has been reported in

the literature about the effect of high temperature in accelerating the diffusion of aggressive solutions inside the polymeric resin, thus disturbing the fibers and weakening the interlaminar shear between the fiber and the polymeric matrix. Moreover, the observations noted in this study supports what has been mentioned earlier about the temperature being the main factor in changing the governing mode of failure from partial debonding to rebar fracture rather than the addition of the macro fibers to concrete.

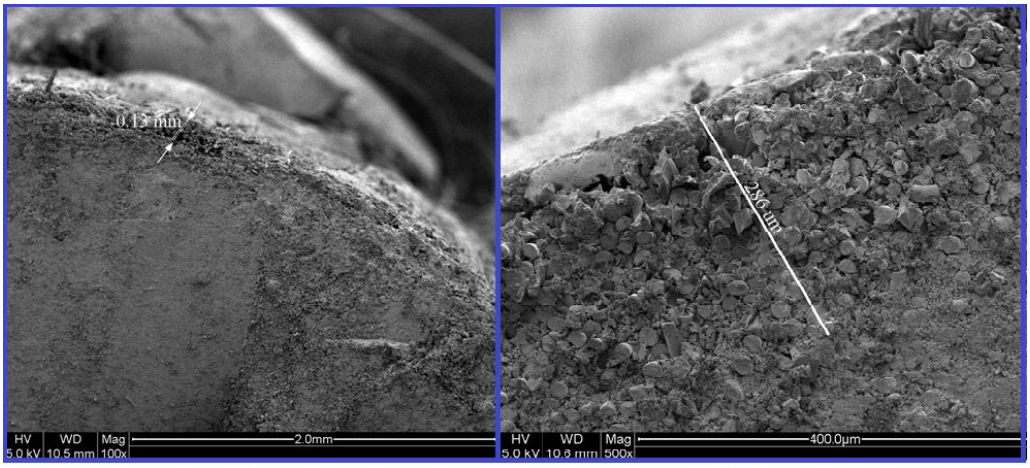

(a) 100x 500x

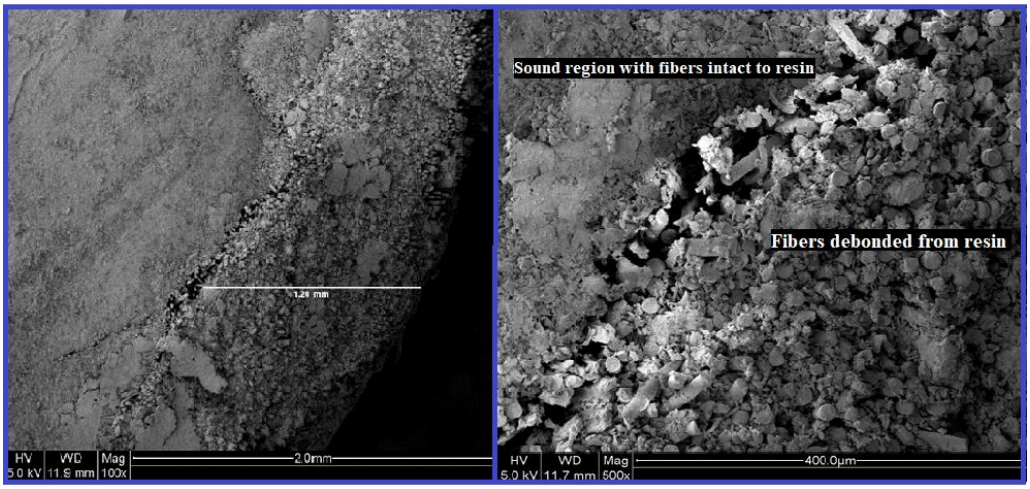

(b) 100x 500x

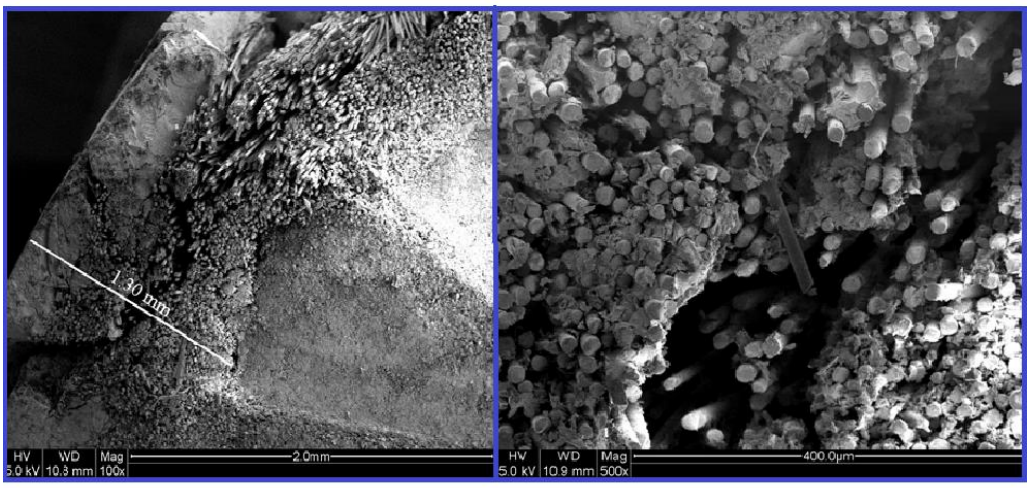

(c) 100x 500x

Figure 58: SEM Images plain concrete : (a) Control; (b) 90 Days -35 ºC; (c) 90 Days-60 ºC

CHAPTER EIGHT: SUMMARY, CONCLUSIONS, AND RECOMMENDATIONS

8.1. Summary

In this study, 105 pullout specimens, consisting of 15 control specimens and 90 conditioned specimens, were tested in an attempt to study the effect of fiber reinforced concrete on the bond strength and bond durability of HWBFRP bars subjected to aggressive environmental conditions. Four parameters were investigated: (1) the saline immersion temperature of (35 ^{o}C and 60 ^{o}C); (2) the exposure duration of (30, 60, and 90 days); (3) the FRC type (steel FRC and basalt FRC); and (4) the fiber volume fraction (0.5% and 1%). The study began with a general overview about the conducted study followed by an extensive literature review that covers numerous related studies concerning the bond durability of FRP bars in general and BFRP bars in particular. Correspondingly, the thesis presented a detailed experimental program that describes the methods, materials, and procedures followed in the research program. Moreover, a detailed discussion was presented concerning the effect of the investigated parameters on the: (1) the failure mechanism of HWBFRP bars (2) the bond-slip behavior; (3) the bond strength degradation; (4) the adhesion stress; and (5) residual bond strength. Consequently, two of the most successful models in presenting the ascending branch of the bond slip curves, the BPE and CMR models, were utilized to assess their validity and were calibrated to effectively represent the actual experimental data obtained from the pullout tests taking into account the parameters investigated in this study. Moreover, a prediction model was proposed that predicts the bond strength reductions after 50 years of service life for plain concrete and optimum fiber volume fractions for each fiber type. Finally scanned electron microscopy (SEM) analysis were performed to investigate the effect of temperature, after 90 days of conditioning in saline environment, on the interlaminar shear of the fibers and surrounding resin.

8.2 Conclusions

Based on this study, the following conclusions can be drawn

1. The addition of steel and basalt macro-fibers improve the bond strength of HWBFRP in ideal environmental conditions to a certain limit. However, for unconditioned specimens, the effect of fiber volume fraction is insignificant in improving the bond strength in case of steel FRC, whereas the basalt FRC tend to show significance in terms of fiber volume fraction. The highest enhancement in the bond strength compared to plain concrete was in 1% basalt FRC with an improvement of 22% followed by 0.5% steel FRC with an enhancement of 20%. Whereas negligible improvements of 1% and 2% were observed for 0.5% basalt FRC and 1% steel FRC respectively.

2. Pullout failure and rebar fracturing were the failure types observed in this study. The effect of immersion temperature is the predominant factor in changing the governing mode of failure from partial debonding to a more severe interlaminar shear failure between the successive layers of the BFRP bars, followed by the effect of fiber type, particularly BMF.

3. Based on this study, the increase in immersion temperature results in less slippage corresponding to the ultimate bond stress regardless of the fiber type. Similarly, the increase in fiber volume fraction resulted in less slippage at failure for conditioned specimens.

4. Plain concrete and basalt FRC showed similar behaviors with higher reductions in bond strength at 60 ^{o}C than that obtained at 35 ^{o}C. Unlike steel FRC specimens which seemed to be uninfluenced by the increase in immersion temperature but rather affected by the presence of the corrosive solution containing high concentrations of NaCl.

5. At 35 ^{o}C, steel FRC specimens showed the highest degradation compared to their counterpart unconditioned specimens with a reduction of 42% and 21% for 0.5 % and

1% steel fiber volume fractions. Conversely, at 60 ^{o}C, steel FRC specimens possessed a reduction of 34% in case of 0.5% steel FRC and an improvement of 3 % in case of 1% steel FRC compared to their counterpart control specimens. This indicates that steel FRC at 0.5% volume fraction is not complementary to HWBFRP when utilized in marine structures but is rather suitable for offshore applications. Even though, the addition of high content of steel fibers resulted in an enhanced durability performance but this addition may not be cost effective, since comparable or even better performance can be achieved with plain concrete. However, in actual applications of BFRP bars, the BFRP bars are subjected to tensile loads which may cause higher degradation rates in which the effect of the steel fibers come to action therefore further investigations are required in this matter.

6. The addition of BMFs resulted in higher a bond strength than that of plain concrete after 90 days of exposure regardless of the immersion temperature and volume fraction retaining 14.2 MPa and 14 MPa at 35 ^{o}C and 60 ^{o}C in case of 0.5% basalt FRC ,and 15 and 12.7 Mpa at 35 ^{o}C and 60 ^{o}C in case of 1% basalt FRC. Differing from plain concrete which retained 12.1 MPa and 11.8 MPa at 35 ^{o}C and 60 ^{o}C. Clearly, plain and basalt FRC meet the minimum requirement of the specifications provided by the CSA S807[70] (>8 MPa) and ACI 440.6 M [71] (>9.6 MPa) which reveals the suitability of using the adopted bars in plain concrete and basalt FRC at marine structures.

7. In terms of bond strength retention, the optimum fiber volume fractions are 0.5% in case of BMFs, and 1% in case of steel fibers.

8. The addition of the fibers tends to reduce the adhesion stress of the BFRP bars to concrete at ideal conditions regardless the fiber type, however after 90 days of conditioning, the adhesion stress tend to increase with increasing temperature except for 0.5%steel FRC which showed the highest bond degradation. It is important to note

that the adhesion stress of BFRP to 0.5 % basalt FRC was higher than that of plain concrete after 90 days of exposure regardless of the conditioning temperature.

9. The residual bond strength seems to exhibit a similar trend to that of the bond strength, the only exception is 1% basalt FRC after 60 days of exposure at 60 ^{o}C due to the failure type of rebar fracturing obtained for two of the three identical specimens that showed the highest bond stresses which caused a loss in the residual bond strength.

10. Both the BPE and CMR models showed a good correlation with experimental data of HWBFRP bars embedded in plain concrete. However, when modelling the effect of FRC and conditioning environment, the CMR model showed much better agreement with the experimental data.

11. Based on the model proposed for the service life prediction after 50 years of service life, the lowest retention values are 72% ,63%, and 56% for plain concrete subjected to dry, moist, and moisture saturated conditions respectively. The lowest bond strength retentions in case of 0.5% basalt FRC are 84%, 79%, and 74% subjected to dry, moist, and moisture saturated conditions with an enhancement of 7% to 32% compared to plain concrete. On the other hand, the lowest bond strength retentions in the case of 1% steel FRC are 70%, 61%, and 54% in dry, moist, and moisture saturated indicating a slight reduction of 1% to 4% compared to plain concrete. This is attributed to the significant reduction exhibited by 1% steel FRC subjected to 35 ^{o}C.

12. The SEM analysis revealed the severe effect of high temperature immersion in saline solution in degrading the interlaminar shear strength between the basalt fibers and surrounding polymeric matrix.

8.3. Recommendations:

Finally, the results of this study are promising for the wider implementation of non-corrosive structural discrete macro fibers, such as basalt macro fibers, in marine structures due to its effect in providing significant resistance to aggressive environments for the BFRP bars. However, the obtained are limited to the types of fibers, bars, and concrete used and that further investigations are required to tackle other parameters that have not been mentioned in this study. The following are some recommendations for future work:

1) Testing the BMFs along with the BFRP bars in different environmental conditioning is mandatory to evaluate their tolerance to different aggressive solutions such as: acidic and alkaline solutions for wider implementations in different applications.

2) Consider other types of fibers such as polypropylene, polyvinyl alcohol, and stainless-steel fibers and their effect on BFRP bars.

3) Consider the effects of surface treatment of the BFRP bars: such as ribbed and sand coated BFRP bars on the performance of the discrete fibers.

4) Study the effect of different compressive strengths of the bond durability of BFRP bars embedded in fiber reinforced concrete.

5) Investigate the bond durability for longer periods of exposure, particularly when steel fibers are considered. Recommended temperatures of immersion are 25^{o}C, 40 ^{o}C, and 55 ^{o}C.

6) Focus on durability tests with high humidity due to its noticeable effect on degrading the bond strength.

7) Examine the permeability and chloride diffusivity of BMFRC and concrete with different non-corrosive fibers for enriching the literature.

8) Develop standard tests and procedures for conducting the bond durability test of FRP

bars in aggressive environments.

REFERENCES

[1]Augenti N., Nanni A., Parisi F. Construction Failures and Innovative Retrofitting. Buildings. 2013;3(1):100-21.

[2] Mohamedien M.A., Hosny A.-H., Abdelrahman A. Use of FRP in Egypt, Research Overview and Applications. Procedia Engineering. 2013;54:2-21.

[3] Newhook J., Svecova D. Reinforcing Concrete Structures with Fibre Reinforced Polymers. 2 ed: ISIS Canada Research Network; 2007. 151 p.

[4] Sarker P., Begum M., Nasrin S. Fiber reinforced polymers for structural retrofitting: A review. Journal of Civil Engineering (IEB). 2011;39(1):57.

[5] Lieser M. Glass fibre reinforcement type significantly impacts FRP corrosion performance. Technology & Innovations. 2011(69):51.

[6] Sonnenschein R., Gajdosova K., Holly I. FRP Composites and their Using in the Construction of Bridges. Procedia Engineering. 2016;161:477-82.

[7] Mallick P.K. Fiber Reinforced Composites. 3 ed. United States of America: Taylor & Francis Group; 2008. 616 p.

[8] Ueda T. FRP for Construction in Japan. 2016:54-68.

[9] B. Wan, M.F. Petrou, K.A. Harries, M.A. Sutton, B. Yang, Experimental investigation of bond between FRP and concrete, in: 3rd Int. Conf. on Composites in Infrastructures ICCI'02, 2002.

[10] M. Molina, J.J. Cruz, S. Oller, A.H. Barbat, L. Gil, Behaviour of the interface between concrete and FRP using serial/parallel mixing theory, Ingeniería e Investigación 31 (3) (2011) 26–39.

[11] J.G. Dai, Y. Saito, T. Ueda, Y. Sato, Static and fatigue bond characteristics of interfaces between CFRP sheets and frost damage experienced concrete, Spec. Publ. 230 (2005) 1515–1530.

[12] Y.J. Kim, P.J. Heffernan, Fatigue behavior of externally strengthened concrete beams with fiber-reinforced polymers: state of the art, J. Compos. Constr. 12 (3) (2008) 246–256.

[13] C. Carloni, K.V. Subramaniam, M. Savoia, C. Mazzotti, Experimental determination of FRP–concrete cohesive interface properties under fatigue loading, Compos. Struct. 94 (4) (2012) 1288–1296.

[14] I. Iovinella, A. Prota, C. Mazzotti, Influence of surface roughness on the bond of FRP laminates to concrete, Constr. Build. Mater. 40 (2013) 533–542.

[15] J.C. López-González, J. Fernández-Gómez, E. González-Valle, Effect of adhesive thickness and concrete strength on FRP-concrete bonds, J. Compos. Constr. 16 (6) (2012) 705–711.

[16] P. DohnAlek, Environmental durability of FRP bond to concrete subjected to freeze-thaw action (Doctoral dissertation), Massachusetts Institute of Technology, USA, 2006.

[17] J. Shrestha, T. Ueda, D. Zhang, Durability of FRP concrete bonds and its constituent properties under the influence of moisture conditions, J. Mater. Civ. Eng. 27 (2) (2014) A4014009

[18] Mukhtar, F.M., Faysal, R.M. A review of test methods for studying the FRP-concrete interfacial bond behavior (2018) Construction and Building Materials, 169, pp. 877-887.

[19] J. Pan, C.K. Leung, Effect of concrete composition on FRP/concrete bond capacity, J. Compos. Constr. 11 (6) (2007) 611–618.

[20] P.M. Santos, E.N. Júlio, A state-of-the-art review on roughness quantification methods for concrete surfaces, Constr. Build. Mater. 38 (2013) 912–923.

[26] Chen Y, Davalos JF, Ray I, Kim H-Y. Accelerated aging tests for evaluations of

durability performance of FRP reinforcing bars for concrete structures. Compos Struct 2007;78(1):101e11.

[27] Belarbi A, Wang H. Bond durability of FRP bars embedded in fiber-reinforced concrete. J Compos Constr 2011;16(4):371e80.

[28] Mijovic J. Interplay of physical and chemical aging in graphite/epoxy composites. J Compos Mater 1985;19(2):178e91.

[29] Tuttle M. A framework for long-term durability predictions of polymeric composites. Rotterdam: Progress in Durability Analysis of Composite Systems; 1996. p. 196e176.

[30] Micelli F, Nanni A. Durability of FRP rods for concrete structures. Constr Build Mater 2004;18(7):491e503.

[31] Charles R. The strength of silicate glasses and some crystalline oxides. In: ICF0, Swampscott-MA (USA) 1959; 2012.

[32] Gonenc O. Durability and service life prediction of concrete reinforcing materials. UNIVERSITY OF WISCONSIN-MADISON; 2003.

[33] Abbasi A, Hogg PJ. Temperature and environmental effects on glass fibre rebar: modulus, strength and interfacial bond strength with concrete. Compos Part B Eng 2005;36(5):394e404.

[34] Koller R, Chang S, Xi Y. Fiber-reinforced polymer bars under freeze-thaw cycles and different loading rates. J Compos Mater 2007;41(1):5e25.

[35] Alves J, El-Ragaby A, El-Salakawy E. Durability of GFRP bars' bond to concrete under different loading and environmental conditions. J Compos Constr 2010;15(3):249e62.

[36] Won J-P, Park C-G, Lee S-J, Hong B-T. Durability of hybrid FRP reinforcing bars in concrete structures exposed to marine environments. Int J Struct Eng

2013;4(1e2):63e74.

[37] ASTM. (2014). “Standard Test Method for Bond Strength of Fiber-Reinforced Polymer Matrix Composite Bars to Concrete by Pullout Testing” D7913/D7913M − 14, West Conshohocken, PA.

[38] ASTM. (2011). “Standard test method for tensile properties of fiber reinforced polymer matrix composite bars.” ASTM D7205/D7205M-06, West Conshohocken, PA.

[39] CSA (Canadian Standards Association). (2012). “Design and construction of building structures with fibre-reinforced polymers.” CAN/CSA S806-12, Rexdale, ON, Canada.

[40] T. Mohammadi, B. Wan, K.A. Harries, Bond–slip behavior of fiber-reinforced polymer/concrete interface in single shear pull-out and beam tests, J. Reinf. Plast. Compos. 35 (5) (2016) 375–386.

[41] Committee, A. Bond and Development of Straight Reinforcing Bars in Tension (ACI 408R-03). Detroit, Michigan, US: American Concrete Institute; 2003.

[42] S.Y. Seo, L. Feo, D. Hui, Bond strength of near surface-mounted FRP plate for retrofit of concrete structures, Compos. Struct. 95 (2013) 719–727.

[43] Achillides Z, Pilakoutas K. Bond behavior of fiber reinforced polymer bars under direct pullout conditions. J Compos Constr 2004;8(2):173e81.

[44] Pepe M, Mazaheripour H, Barros J, Sena-Cruz J, Martinelli E. Numerical calibration of bond law for GFRP bars embedded in steel fibre-reinforced self-compacting concrete. Compos Part B Eng 2013;50:403-12

[45] Antonietta Aiello M, Leone M, Pecce M. Bond performances of FRP rebarsreinforced concrete. J Mater Civ Eng 2007;19(3):205-13.

[46] Benmokrane B, Tighiouart B. Bond strength and load distribution of composite

GFRP reinforcing bars in concrete. ACI Mater J 1996;93(3).

[47] Masmoudi A, Masmoudi R, Ouezdou MB. Thermal effects on GFRP rebars:experimental study and analytical analysis. Mater Struct 2010;43(6):775e88

[48]Won J-P, Park C-G, Lee S-J, Hong B-T. Durability of hybrid FRP reinforcingbars in concrete structures exposed to marine environments. Int J Struct Eng 2013;4(1e2):63-74.

[49] Cosenza E, Manfredi G, Realfonzo R. 20 analytical modelling of bond betweenFRP reinforcing bars and concrete. In: Non-metallic (FRP) Reinforcement forConcrete Structures: Proceedings of the Second International RILEM Symposium. CRC Press; 1995.

[50] Rolland, A., Quiertant, M., Khadour, A., Chataigner, S., Benzarti, K., Argoul, P. Experimental investigations on the bond behavior between concrete and FRP reinforcing bars (2018) Construction and Building Materials, 173, pp. 136-148.

[51] Baena, M., Torres, L., Turon, A., Barris, C. Experimental study of bond behaviour between concrete and FRP bars using a pull-out test (2009) Composites Part B: Engineering, 40 (8), pp. 784-797.

[52] El Refai, Ahmed & Ammar, Mohamed-Amine & Masmoudi, Radhouane. (2014). Bond Performance of Basalt Fiber-Reinforced Polymer Bars to Concrete. Journal of Composites for Construction. 10.1061/(ASCE)CC.1943-5614.0000487.

[53] Ding, Y., Ning, X., Zhang, Y., Pacheco-Torgal, F., Aguiar, J.B. Fibres for enhancing of the bond capacity between GFRP rebar and concrete (2014) Construction and Building Materials, 51, pp. 303-312.

[54] Bi, Qiaowei & Wang, Hui. (2011). Bond Strength of BFRP Bars to Basalt Fiber Reinforced High-Strength Concrete. 576-580. 10.1007/978-3-642-17487-2_125.

[55] Sólyom, Sándor & Balázs, György. (2016). Influence of FRC on bond

characteristics of FRP reinforcement.

[56] Liu, H., Yang, J., Wang, X. Bond behavior between BFRP bar and recycled aggregate concrete reinforced with basalt fiber (2017) Construction and Building Materials, 135, pp. 477-483.

[57] Kim B, Doh J-H, Yi C-K, Lee J-Y. Effects of structural fibers on bonding mechanism changes in interface between GFRP bar and concrete. Compos Part B Eng 2013;45(1):768e79.

[58] Abdeldjelil Belarbi, H. W. (2004) 'Bond-slip response of FRP reinforcing bars in fiber reinforced concrete under direct pullout', International Conference on Fiber, pp. 1–10. doi: 10.1111/evo.12826.This.

[59] Chenchen Li, Danying Gao, Yinglai Wang, Jiyu Tang, Effect of high temperature on the bond performance between basalt fibre reinforced polymer (BFRP) bars and concrete, Construction and Building Materials, Volume 141, 2017, Pages 44-51.

[60] Altalmas, A., El Refai, A., Abed, F. Bond degradation of basalt fiber-reinforced polymer (BFRP) bars exposed to accelerated aging conditions (2015) Construction and Building Materials, 81, pp. 162-171.

[61] Dong, Z., Wu, G., Xu, B., Wang, X., & Taerwe, L. (2016). Bond durability of BFRP bars embedded in concrete under seawater conditions and the long-term bond strength prediction. MATERIALS & DESIGN, 92, 552–562.

[62] El Refai, A. El, Abed, F. and Altalmas, A. (2015) 'Bond Durability of Basalt Fiber – Reinforced Polymer Bars Embedded in Concrete under Direct Pullout Conditions', 19(5), pp. 1–11. doi: 10.1061/(ASCE)CC.1943-5614.0000544.

[63] Zhou, J., Chen, X., and Chen, S. (2011). "Durability and service life prediction of GFRP bars embedded in concrete under acid environment." J. Nucl. Eng. Des., 241(10), 4095–4102.

[64] El Hassan, Mohamed, Brahim Benmokrane, Adel Elsafty, and Amir Fam. 2016. “Bond Durability of Basalt- Fi Ber-Reinforced-Polymer (BFRP) Bars Embedded in Concrete in Aggressive Environments.” 106: 262–72.

[65] Yan, F., Lin, Z. Bond durability assessment and long-term degradation prediction for GFRP bars to fiber-reinforced concrete under saline solutions (2017) Composite Structures, 161, pp. 393-406.

[66] Kanstad, T. et al., 2011. Forslag til retningslinjer for dimensjonering, utførelse og kontroll av fiberarmerte betongkonstruksjoner, COIN Project report 29 -2011. Trondheim; SINTEF Building and Infrastructure.

[67] Abbas, U. (2013) ‘Materials Development of Steel-and Basalt Fiber-Reinforced Concretes’, (November).

[68] Bentur A, Mindess S. Fibre reinforced cementitious composites. London: Taylor & Francis; 2007. XX, 601 s. : ill. p.

[69] Okelo, R. and Yuan, R. L. (2005) ‘Bond Strength of Fiber Reinforced Polymer Rebars in Normal Strength Concrete’, Journal of Composites for Construction, 9(3), pp. 203–213. doi: 10.1061/(asce)1090-0268(2005)9:3(203).

[70] Canadian Standards Association (CSA). Specification for fibre reinforced polymers (CAN/CSA S807e10 (R2015). Rexdale. Ontario. Canada. 2015. p. 27.

[71] ACI Committee 440. Specification for carbon and glass fiber-reinforced polymer bar materials for concrete reinforcement (ACI 440.6M-08). Farmington Hills, MI: American Concrete Institute; 2008. p. 6.

[72] Schultheisz, C. R., Schutte, C. L., McDonough, W. G., Macturk, K. S., McAuliffe, M., Kondagunta, S.,and Hunston, D. L., (1996), “Effect of Temperature and Fiber Coating on the Strength of E-Glass Fibers and the E-Glass/Epoxy Interface for Single Fiber Fragmentation Samples Immersed in Water,” Fiber, Matrix, and Interface

Properties, ASTM STP 1290, C. J. Spragg and L. T. Drzal, Eds., American Soc. Testing and Materials, West Conshohoken, PA, pp. 103–131.

[73] Tannous, F. E., and Saadatmanesh, H., (1999), "Durability of AR Glass Fiber Reinforced Plastic Bars," Journal of Composites for Construction, Vol. 3, No. 1, pp. 12–19.

[74] Bakis, C. E., Freimanis, A. J., Gremel, D. and Nanni, A., (1998), "Effect of Resin Material on Bond andTensile Properties of Unconditioned and Conditioned FRP Reinforcement Rods," First Intl. Conf. onDurability of Composites for Construction, B. Benmokrane, and H. Rahman, Eds., Sherbrooke, Quebec,Canada, pp. 525–535.

[75] Gentry, T. R., Bank, L. C., Barkatt, A., and Prian, L., (1998), "Accelerated Test Methods to Determine the Long-Term Behavior of Composite Highway Structures Subject to Environmental Loading," J. Composites Technology & Research, Vol. 20, pp. 38–50.

[76] Wolff, E.G., (1993), "Moisture Effects on Polymer Matrix Composites," SAMPE Journal, Vol. 29, No.3, pp. 11–19.

[77] Bank, L. C., and Puterman, M., (1997), "Microscopic Study of Surface Degradation of Glass-Fiber-Reinforced Polymer Rods Embedded in Concrete Castings Subjected to Environmental Conditioning," High Temperature and Environmental Effects on Polymeric Composites: 2nd Vol.,ASTM STP 1302, T. S. Gates and A.-H., Zureick, Eds., American Society for Testing and Materials, pp. 191–205.

[78] Porter, M. L., and Barnes, B. A., (1998), "Accelerated Aging Degradation of Glass Fiber Composites," 2nd Intl. Conf. on Composites in Infrastructure, Vol. 2, H. Saadatmanesh and M.R. Ehsani, Eds., Univ. Arizona, Tucson, pp. 446–459.

[79] Sen, R., Shahawy, M., Sukumar, S., and Rosas, J., (1998), "Effect of Tidal Exposure on Bond of CFRP Rods," 2nd Intl. Conf. on Composites in Infrastructure,

Vol. 2, H. Saadatmanesh and M.R. Ehsani, Eds., Univ. Arizona, Tucson, pp. 512–523.

[80] Liu, Qiang, Montgomery T. Shaw, Richard S. Parnas, and Anne Marie McDonnell. "Investigation of basalt fiber composite aging behavior for applications in transportation." Polymer Composites 27 (5) (2006): 475-483.

[81] Lik-ho Tam, Li He & Chao Wu (2019) Molecular dynamics study on the effect of salt environment on interfacial structure, stress, and adhesion of carbon fiber/epoxy interface, Composite Interfaces, 26:5, 431-447, DOI: 10.1080/09276440.2018.1506901.

[82]Grammatikos, Sotirios & Zafari, Behrouz & Mark, Evernden & Mottram, James & Mitchels, John. (2015). S Grammatikos Moisture uptake characteristics of a pultruded fibre reinforced.

[83] Li, Mei. 2000. "Temperature and Moisture Effects on Composite Materials for Wind Turbine Blades." THESIS at MONTANA STATE UNIVERSITY-BOZEMAN (March): 128.

[84] Ceroni, F., Cosenza, E., Manfredi, G., and Pecce, M. (2006). "Durability issues of FRP rebars in reinforced concrete members." Cement Concrete Compos., 28(10), 857–868.

[85] Touil, B., Ghomari, F., Bezzar, A., Khelidj, A., & Bonnet, S. (2017). Effect of temperature on chloride diffusion in saturated concrete. ACI Materials Journal, 114(5), 713-721. doi:http://0-dx.doi.org.mylibrary.qu.edu.qa/10.14359/51688929.

[86] Frazão, Cristina, Aires Camões, Joaquim Barros, and Delfina Gonçalves. 2015. "Durability of Steel Fiber Reinforced Self-Compacting Concrete." Construction and Building Materials 80: 155–66.

[87] Afroughsabet, V., Biolzi, L. and Monteiro, P. J. M. (2018) 'The effect of steel and polypropylene fibers on the chloride diffusivity and drying shrinkage of high-strength

concrete', Composites Part B: Engineering. Elsevier, 139(November 2017), pp. 84–96. doi: 10.1016/j.compositesb.2017.11.047.

[88] Khalil W. Influence of high temperature on steel fiber reinforced concrete. J Eng Develop 2006;10(2).

[89] Zabihi, Samad & Alizade, Elham & Alaee, Farshid. (2016). Effect of Steel Fiber Corrosion on Mechanical properties of Steel Fiber Reinforced Concrete. Asian Journal of Civil Engineering. 17. 147-158.

[90] Alwan J, Naaman AE, Hansen W. Pull-out work of steel fibers from cementitious composites: analytical investigation, Cement and Concrete Composites, No. 4, 13(1991) 247-55.

[91] Frazão, C. et al. (2016) 'Corrosion effects on pullout behavior of hooked steel fibers in self-compacting concrete', Cement and Concrete Research. Elsevier Ltd, 79, pp. 112–122. doi: 10.1016/j.cemconres.2015.09.005.

[92] Singh A, Singhal D. Permeability of steel fibre reinforced concrete influence of fibre parameters. Proc Eng 2011;14:2823–9.

[93]] Mohamed, O. A. and Al Hawat, W. (2016) 'Influence of Fly Ash and Basalt Fibers on Strength and Chloride Penetration Resistance of Self-Consolidating Concrete', Materials Science Forum, 866(November 2017), pp. 3–8. doi: 10.4028/www.scientific.net/msf.866.3.

[94] Sayed Ahmad F, Foret G, Le Roy R. Bond between carbon fiber-reinforced polymer (CFRP) bars and ultra high performance fiber reinforced concrete (UHPFRC): experimental study. Constr Build Mater 2011;25(2):479–85.

[95] Eligehausen, R., Popov. E. P., and Bertero, V. V. (1983). "Local bond stress-slip relationships of deformed bars under generalized excitations." Rep. No. 83/23, Earthquake Engrg. Res. Ctr. (EERC), Univ. of California, Berkeley, Calif.

[96] [1]Fib Bulletin 40. FRP reinforcement in concrete structures. In: International federation for structural concrete, Lausanne, Switzerland; 2007.

[97] Serbescu A, Guadagnini M, Pilakoutas K. Mechanical characterization of basalt FRP rebars and long-term strength predictive model. J Compos Constr 2014;19(2):04014037. http://dx.doi.org/10.1061/(ASCE)CC.1943- 5614.0000497.